CHARACTERIZATION AND INVESTIGATION OF SUBMARINE GROUNDWATER DISCHARGE FROM A COASTAL AQUIFER INTO THE NEARSHORE ENVIRONMENT

BY

JOSHUA LEE CAULKINS

B.Sc., University of California, Santa Cruz, 1998

A THESIS SUBMITTED IN PARTIAL FULFILLMENT OF
THE REQUIREMENTS FOR THE DEGREE OF

MASTER OF SCIENCE

in

THE FACULTY OF GRADUATE STUDIES

Department of Earth and Ocean Sciences

We accept this thesis as conforming
to the required standard

THE UNIVERSITY OF BRITISH COLUMBIA

April 2004

Library Authorization

In presenting this thesis in partial fulfillment of the requirements for an advanced degree at the University of British Columbia, I agree that the Library shall make it freely available for reference and study. I further agree that permission for extensive copying of this thesis for scholarly purposes may be granted by the head of my department or by his or her representatives. It is understood that copying or publication of this thesis for financial gain shall not be allowed without my written permission.

Joshua Lee Caulkins
Name of Author *(please print)*

22/04/2004
Date (dd/mm/yyyy)

Title of Thesis: CHARACTERIZATION AND INVESTIGATION OF SUBMARINE GROUNDWATER DISCHARGE FROM A COASTAL AQUIFER INTO THE NEARSHORE ENVIRONMENT

Degree: Master's of Science Year: 2004

Department of Earth and Ocean Sciences
The University of British Columbia
Vancouver, BC Canada

ABSTRACT

The current trend of global populations moving increasingly to high density, coastal cities places a greater emphasis upon the water quality of aquifers supplying those cities. Problems that affect coastal aquifers (e.g. saltwater intrusion, non-point source pollution) will be amplified as this trend increases. The goal of this research project is to understand the processes that control freshwater/saltwater interactions in the coastal zone, specifically in areas of high submarine groundwater discharge (SGD). A site in NW Florida along the Gulf Coast is a well-documented SGD locale and provides an excellent opportunity to examine how tidal fluctuations, differential pressure in the seabed and groundwater seepage rates are interrelated. Experiments at the site focus on characterization of the nearshore aquifer, submarine groundwater discharge at the seabed and numerical modeling of the system. New onshore wells at the field site show that hydraulic conductivities in onshore region are similar to those in the offshore region. Slug tests and water level monitoring of the onshore wells are used to measure a seaward, horizontal hydraulic gradient. Direct measurements of discharge are conducted with an automated seepage meter, which shows that peak discharge rates tend to occur at the transition between high and low tides. A new apparatus called a differential piezometer system (DPS) is designed and used to measure differential hydraulic head in the seabed created by seepage and tidal interactions. This system failed to accurately portray differential head fluctuations in the seabed as a result of calibration error. Salinity samples are collected from on and offshore wells and from a newly installed multi-level well, the data of which are made into salinity profiles. These profiles define the

boundaries of a saline wedge and mixing zone in the nearshore region. FRAC3DVS is a flow and transport groundwater model that is used to design and run a 1-dimensional numerical model. The model results confirm the temporal effects of tidal elevation on discharge rates observed in the seepage meter.

Table of Contents

Table of Tables

Table of Figures

Note: Figures are found at the end of each chapter.

ACKNOWLEDGEMENTS

This project was funded from a Natural Science and Engineering Research Council grant.

Special thanks are extended to the staff of Florida State University Marine Lab in St. Teresa for their flexibility and assistance in field experiments: Bobby Henderson, Dr. John Hitron, Nelson Wheeler, Patricia Jackson, Dennis Tinsley and Butch.

Additionally, thanks go to the Florida State University Department of Oceanography graduate students and professors who were generous in their equipment loans, advice and assistance: Harmon Harden, Henrieta Dulaiova, Christina Springer, Dr. Bill Burnett and Dr. Jeffrey Chanton.

I am grateful to Craig Thompson for his assistance during fieldwork. His insight during the computer simulations was also invaluable. I would like to thank my parents, my sister and brother for their words of encouragement. My deepest gratitude goes to my partner, Regina, for her constant encouragement and support. Without her commitment to my endeavor, this thesis would not have been possible.

Finally, thanks to my supervisor, Dr. Leslie Smith, and the members of my committee, Dr. Roger Beckie and Dr. Ulrich Mayer for their teaching and guidance.

1. Problem Background

The definition of submarine groundwater discharge (SGD) has been refined over the last two decades as the driving processes controlling discharge have become more widely understood. Zekster et al. (1983), in exploring SGD from a global water budget perspective, equated SGD to the net groundwater discharge to the ocean. Church (1996) defined SGD as the direct groundwater outflow across the ocean-land interface into the ocean. Li et al. (1999) provided a more complete description, defining SGD as the combination of net groundwater discharge, the outflow due to wave-setup-induced groundwater circulation, and that due to tidally driven oscillating flow. They present a conceptual model as follows,

$$D_{SGD} = D_n + D_w + D_t$$

where D_{SGD} is the total combined discharge across the seabed, D_n is the net groundwater component, D_w is the wave-induced groundwater circulation component, and D_t is the tidally driven component of flow (**Figure 1-1**). The current research will focus on the net groundwater discharge and the tidally driven components of the model presented above.

Historically, submarine groundwater seeps and springs have been viewed as hydrologic "curiosities" rather than as a phenomenon worthy of scientific research (Kohout 1966). The number of publications produced over the last two decades investigating submarine groundwater discharge into the nearshore environment shows that this is no longer the case (Bokuniewicz 1980; Taniguchi and Fukuo 1993; Moore 1996; Cable et al. 1996; Burnett et al. 2001; Taniguchi 2002; Langevin 2003). A few recent examples of SGD quantification studies are listed in **Table 1-1**. SGD has been recognized as a potentially significant driver of nutrients to the coastal oceans, likely

impacting nearshore coastal ecosystems (Oberdorfer et al. 1990; Giblin and Gaines 1990; Moore 1996). The initiation of SGD is freshwater (D_n) flowing through unconfined or confined aquifers that extend into the nearshore coastal zone. The processes driving SGD in the coastal zone are not well understood and current research seeks to expose how onshore hydraulic gradients, tidal pumping of coastal aquifers and leakage across confining units at depth interrelate to produce SGD at the seabed.

Table 1-1. Estimates of SGD from Recent Studies

Study Area	Methods	Estimated Discharge (cm/day)	Reference
Cape Cod, MA	Manual Seepage Meters	2.4 to 7.2	Giblin and Gaines, 1990
Lake Biwa, Japan	Automated and Manual Seepage Meters	0 to 24 (manual) 3 to 23 (automated)	Taniguchi and Fukuo, 1993
NE coastal Gulf of Mexico, FL	Tracers: ^{222}Rn	2 to 10	Cable, et al. 1996
NE coastal Gulf of Mexico, FL	Manual Seepage Meters	3 to 22	Cable, et al. 1997a
NE coastal Gulf of Mexico, FL	Manual Seepage Meters	0.1 to 1	Rasmussen, 1998
Osaka Bay, Japan	Automated Seepage Meter	0.9 to 43*	Taniguchi, 2002
NE coastal Gulf of Mexico, FL	Tracers: ^{222}Rn	8.6 to 13	Lambert and Burnett, 2003
NE coastal Gulf of Mexico, FL	Tracers: ^{226}Ra	10.8	Moore, 2003
NE coastal Gulf of Mexico, FL	Automated and Manual Seepage Meters	2 to 50* (manual) 1 to 77* (automated)	Taniguchi, et al. 2003
Waquoit Bay, Cape Cod, MA	Manual Seepage Meters	3 to 37*	Michael, et al. 2003
Shelter Island, Long Island, NY	Ultrasonic Seepage Meter	40 to 200*	Paulsen, et al. in press

* Estimated from figures in paper

Despite significant advancements in the field of submarine groundwater discharge, quantifying SGD and determining its effects on the nearshore environment is

proving to be a serious challenge for hydrogeologists, oceanographers and coastal zone managers. Direct methods of quantifying groundwater discharge remain subject to large errors and current best practices involve using multiple approaches. These approaches have most recently focused on direct measurement with manual or automated seepage meters, natural tracer concentrations (Ra and Rn) of onshore and offshore samples and applications of numerical modeling (Burnett et al. 2002). Moore and Church (1996) challenged hydrologists to develop SGD models that will include tidal pumping due to diurnal, monthly, seasonal or longer changes of sea level; saltwater intrusion and changes in GW usage; and mixing and chemical reactions within coastal aquifers.

One aspect of this research seeks to expand the current knowledge of SGD by examining onshore groundwater flow in a coastal aquifer through the measurement of nearshore water table elevations in onshore wells and through the creation of salinity profiles from samples of onshore and offshore wells. One hypothesis is that by determining aquifer parameters from onshore wells, a rough estimate of the discharge at the shoreline can be obtained. This estimate is equivalent to the net groundwater discharge, or D_n from the conceptual model above, which can be used to obtain a clearer understanding of freshwater input to the system. Salinity data from both on and offshore wells should provide a general location of the saltwater/freshwater contact, giving a spatial understanding of the nearshore mixing zone.

Recent investigations have shown that there is a need for further exploration into pressure fluctuations within the seabed, which would expose the nature of vertical hydraulic gradient changes (Smith and Zawadzki 2003). Exploring how vertical hydraulic gradients fluctuate with discharge and tides should provide insight into how the mixing of

groundwater and seawater occur within the seabed. Work of this nature has been attempted with some success in streams (Kelly and Murdoch 2002) yet these systems are in pseudo-steady-state and are not subject to the diurnal and semi-diurnal head fluctuations affecting coastal aquifers. Fang et al. (1993) looked at pore pressure fluctuations in abyssal plain sediments near the Atlantic mid-oceanic ridge but their differential pressure transducer system (PUPPI) was designed for deep sea work and is not necessarily applicable to the present study. No study to date has attempted to investigate nearshore vertical hydraulic head fluctuations by coupling direct measurements of discharge with pressure measurements in the seabed in a tidally dominated setting. Thus, it was not known prior to this study how tides affected fluctuations of differential head in shallow, nearshore sediments or how those fluctuations related to SGD. The hypothesis is that if correlations can be made between temporal fluctuations of differential head in shallow sediments and submarine groundwater discharge rates, a greater understanding of the nature of SGD will emerge. To test this hypothesis, two dual-port piezometers hydraulically connected to differential pressure transducers were inserted parallel to shore, one on each side of an automated seepage meter. Successful calibration and deployment of a dual-port system should increase the ability of scientists and coastal zone managers to understand rates and variations in discharge across the seabed.

Numerical models capable of resolving density-dependent flow have been used to understand the groundwater/seawater interactions in numerous recent publications (Smith and Zawadzki 2003; Langevin 2003; Uchiyama et al. 2000; Li et al. 1999; Ataie-Ashtiani et al. 1999). A 1-dimensional, non-density-dependent flow model was created to predict

SGD rates and the vertical hydraulic gradients within the nearshore shallow seabed. Tide data from the field experiments were used as input for the model and the temporal effects of tides on discharge rates and differential pressure in the seabed were examined. The hypothesis is that accurate model predictions, when compared with field measurements of SGD and differential pressure within the seabed, would indicate that the model has correctly portrayed the system. Failure to accurately portray the system should point to areas where increased field or lab work is required.

The current study seeks to characterize the nature of processes affecting the discharge of groundwater to the nearshore environment. The experimental focus is on tidal and onshore hydraulic properties and does not explore wave induced re-circulation as proposed in the conceptual model. The following three chapters explore these questions in detail. Chapter 2 presents the hydrogeologic setting of the field area and describes the scope of the research conducted. Chapter 3 is an investigation of the nearshore aquifer characterization work and submarine groundwater discharge experiments conducted at the site, where each experiment is outlined and the results discussed. Chapter 4 demonstrates the construction of a 1-dimensional flow model designed to predict seepage rates and seabed pressure fluctuations observed in the field.

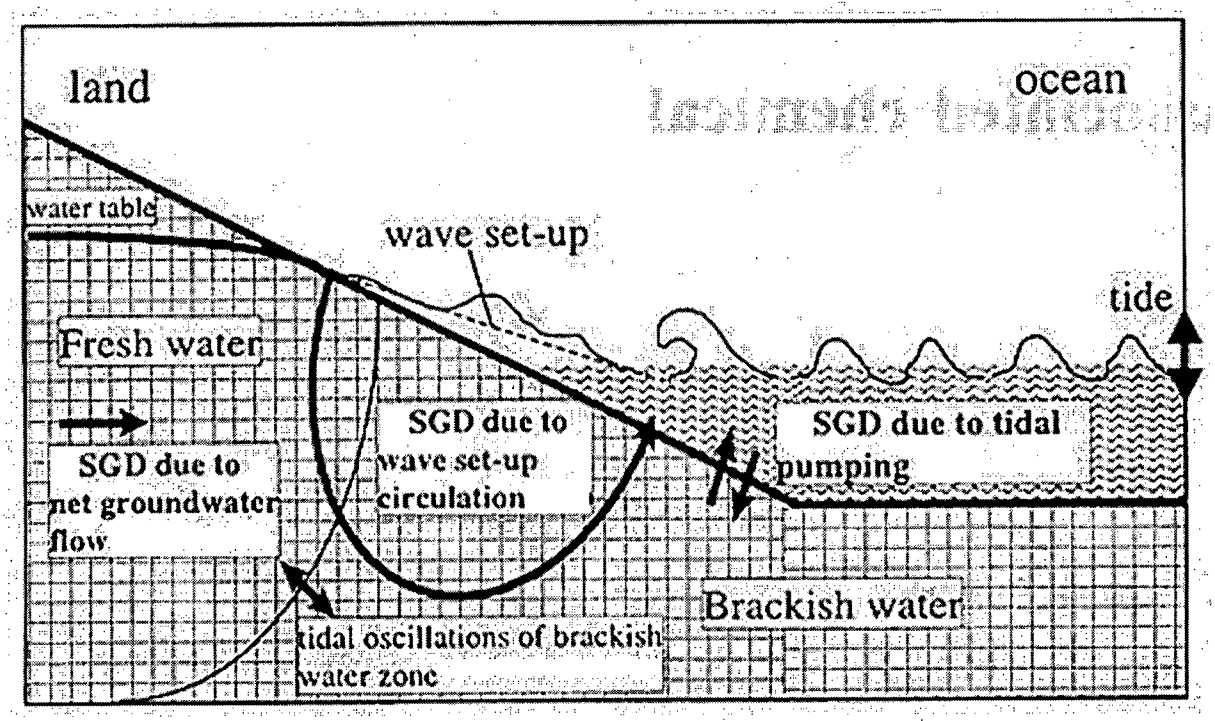

Figure 1-1. Processes affecting submarine groundwater discharge (adapted from Li et al. 1999).

2. Hydrogeologic Setting and Scope of Research

2.1 Hydrogeologic Setting

The field area is situated in the NE Gulf of Mexico, along the Florida coast (**Figure 2-1**). Three major geologic units occur in the region immediately surrounding the field site. The Bruce Creek Limestone, a porous aquifer, is the uppermost unit of the Floridan Aquifer System. Overlying the Bruce Creek Limestone is the Intracoastal Formation, a very sandy, highly microfossiliferous, poorly consolidated, argillaceous, calcarenitic limestone (Schmidt 1984). The Intracoastal Formation produces artesian conditions in the Bruce Creek Limestone and is estimated to be 1 to 5 meters thick in the region immediately surrounding FSUML. Overlying the Intracoastal Formation are the Pleistocene-to-recent sands that make up the Surficial Aquifer System. These sediments are between 6 and 7 meters thick in the nearshore region, based on Waterloo Profiler data collected in 2002 (discussed below).

The Intracoastal Formation and Bruce Creek Limestone dip locally to the south and regionally to the southwestward at angles generally less than 0.05°. The Intracoastal Formation is exposed north and east of the field site. The Floridan Aquifer becomes unconfined near where the Intracoastal Formation is exposed.

The current research focuses on flow within the Surficial Aquifer yet recognizes that leakage from the Floridan Aquifer across the Intracoastal Formation may contribute to submarine groundwater discharge in the field area (Rasmussen 1998; Smith and Zawadzki 2003).

2.2 Prior Submarine Groundwater Discharge Studies at FSUML

A number of previous studies have explored processes that affect SGD at the study site. Rasmussen (1998) conducted extensive fieldwork at the site between 1995 and 1997 where groundwater discharge was measured directly via manual seepage meters and a groundwater flow model was used to simulate the hydrologic system. Five piezometer nests with a total of 18 wells were installed in the Surficial Aquifer and used to measure salinity and hydraulic head. Each nest has 2 to 4 wells, inserted to various depths. One nest (A-nest) is located onshore, another nest (AB-nest) is located in the intertidal zone and the remaining nests (B, BC, C and D) are located offshore (**Figure 2-2**).

In 1997, the Scientific Committee on Oceanic Research (SCOR) created Working Group 112 (SCOR webpage, 2003), whose mandate was to investigate the "Magnitude of Submarine Groundwater Discharge and its Influence on Coastal Oceanographic Processes." In August of 2000, WG112 conducted an "Intercomparison Experiment," where different methods of quantifying SGD were implemented and evaluated. The team of researchers estimated SGD using automated and manual seepage meters, groundwater and seawater chemistry and water level measurements in the offshore and onshore wells. The aim of that study was to compare SGD measurement techniques (**Figure 2-3**). Water level measurements were not used because of the coarse temporal resolution of the data. Additionally, surface seawater and pore water chemistry analyses were conducted using radioactive isotopes (Ra and Rn). Three of the research groups involved in that study, Lambert/Burnett; Taniguchi et al. and Moore, produced independent estimates of SGD rates using Radium isotopes, seepage meters and Radon isotopes, respectively. Lambert and Burnett, using Radium isotope ratios, estimated a SGD rate of 8.6 to 13 cm/day while

Moore predicted a rate of 10.8 cm/day using the Radon isotope ratios. Taniguchi et al. measured seepage rates that ranged from 2 to 50 cm/day for manual seepage meters and 1 to 77 cm/day for automated seepage meters. All intercomparison experiment results have been published in a special edition of *Biogeochemistry* (**66**, 2003).

A project that was part of the August 2000 intercomparison experiment was an attempt to numerically model the hydrologic regime of the field site. Smith and Zawadzki (2003) used FEFLOW, a commercially available density-dependent flow model, to produce a two-dimensional flow and transport model based on data collected at the site. Their research was an attempt to build a hydrogeologic model for the site from which estimations of SGD could be made. Offshore flow and recirculation within the saltwater wedge were included in their model. This model under predicted the field measurements of SGD at the site, producing a number approximately 1 to 2 orders of magnitude lower than those observed in the field.

Findlater (2001) discusses the hydraulic conductivity of sediments at the site and an adapted MODFLOW simulation where her model produces the same low discharge values that were observed by Smith and Zawadzki (2003).

2.3 Research Overview

A main thrust of this study is to investigate how discharge at the seabed is affected by tides and differential pressure in the seabed. All fieldwork for this research was completed over a 1-month period from August 9th to September 9th, 2002 at the FSUML site. Equipment calibrations were conducted between May and August of 2002,

at the University of British Columbia, Vancouver, Canada. A 1-dimensional, density-independent flow model is constructed and used to predict discharge rates at the site.

2.3.1 Nearshore Aquifer Characterization

In order to properly identify the magnitude of groundwater flow to the nearshore area, a number of parameters required definition, including horizontal hydraulic gradients toward the ocean, hydraulic conductivity of the system and depth of geologic units.

Prior to the current field work, five new onshore wells were installed in two nests, one with three wells ~80m inland of A-nest and the other with two wells ~20m from A-nest (**Figure 2-2**). These nests are labeled "P-nest" and "N-nest," respectively. The wells were surveyed by Roddenberry & Assoc., Inc. for latitude, longitude and elevation relative to North American Vertical Datum, 1988 (NAVD88).

An average onshore horizontal hydraulic gradient was calculated from continuous measurements made by pressure transducers in wells P1 and N1, the deepest wells of each nest noted above. This data can be used to estimate a volumetric flow of groundwater within the Surficial Aquifer that is delivered to the nearshore. An accurate horizontal hydraulic gradient also allows for appropriate boundary conditions to be applied in computer simulations.

In order to constrain the hydraulic conductivity of the system slug tests were used to assess of sediments surrounding new onshore wells. Slug tests were attempted on all new wells and successful in wells P1, P2 and N1. The screened intervals of wells P3 and N2 did not extend below the water table and were not tested.

Salinity data was collected at the site in order to identify how salinity is distributed with depth in the Surficial Aquifer. Salinity samples were collected from existing on and offshore wells and using a Waterloo Profiler™ (WP), which samples porewater at any depth in the same borehole. The WP was also used to insert a multilevel well at offshore site 1 (labeled "ML" on **Figure 2-2**), approximately 26m offshore of the low tide line. This method is advantageous because vertical profiles with numerous, discrete sampling points can be made with relative ease. Two such profiles were conducted during the course of the field study, one onshore and one offshore. One reason for using the Waterloo Profiler was to determine if penetration of the Intracoastal Formation was possible. As stated previously, the Intracoastal Formation is "poorly consolidated" and thus may have been accessible with the WP, which is designed for use only in saturated sediments. The combined sampling points (wells and waterloo profiles) were plotted onto a vertical cross-section (**Figure 2-4**).

2.3.2 Submarine Groundwater Discharge Experiments

Two sites were located offshore at which simultaneous measurements of seepage and differential pressure in the seabed were made. Differential pressure (ΔP) is defined as the difference in pressure between two ports separated by a known vertical distance, Δz. ΔP is measured by a differential pressure transducer, which produces an electrical output representing that differential pressure. The differential pressure is directly related to differential hydraulic head (Δh) with a standing manometer which was used to calibrate the output. Calibration experiments were conducted both before and after the fieldwork in order to ensure accurate data processing. Differential hydraulic head, defined by the

equation $\Delta h = (\Delta P/\rho g) + \Delta z$ is directly proportional to differential pressure because all other variables are known. The density of water in the seabed is assumed to be constant to a depth of at least 1m, the maximum depth of the DPS piezometers, based on salinity profiles of wells immediately adjacent to the sites chosen and from samples collected from sediments at depths of 0.7m below the seabed. How differential pressure changes are affected by tidal oscillations and how they relate to discharge rates has not yet been explored by any of the current literature investigating submarine groundwater discharge.

A differential piezometer system (DPS) was used to measure pressure fluctuations in the seabed. Two ports in a single piezometer are hydraulically connected to a differential pressure transducer located in a secure box above the high tide line. Two, dual-port piezometers were inserted on each side of the automated seepage meter. A diagram of a DPS/Seepage meter experiment is shown in **Figure 2-5**.

Tidal pumping of a coastal aquifer is defined as the oscillating flow in the aquifer induced by tidal fluctuations, contributing to the water exchange between the seabed and the ocean (Li et al. 1999). Li et al. (1999) predict that the majority of discharge across the seabed may be caused in large part by these tidal forcings and wave setup, as presented in their conceptual model that was inspired by Moore (1996). Direct seepage measurements, described below, are used to investigate how seepage rates are influenced through time by tidal oscillations. A Taniguchi-style automated seepage meter was used to directly measure groundwater discharge (D_{SGD}) across the seabed. Seepage rates are measured with a heat pulse/thermistor system, described in detail in Chapter 2, which attach directly to a drum similar to those used for manual seepage meters. Discrete measurements were made at 5 minute intervals.

Tidal data was collected so as to determine the magnitude of tidal influence on SGD at the site. A tide meter was attached to a piling on the FSUML dock, used to record the tidal fluctuations near the field site. A pressure sensor at the base of a 2m long PVC pipe measured the height of water. Later, this station was surveyed by the surveying company mentioned previously. This elevation data was corrected to NAVD88. The location of the tide meter was approximately 370m west of A-nest.

Two experiment runs were conducted at each site, producing 4 sets of seepage and DPS data of varying quality. These data sets were then superimposed over tidal data collected with the tide meter. Results are discussed in chapter 3.

2.3.3 Numerical modeling of the Flow Regime at FSUML

A one-dimensional model was created using FRAC3DVS, a groundwater flow model produced by researchers at the University of Waterloo, Ontario. With this model, the author has attempted to simulate the DPS and seepage meter data. This was done by assigning estimated hydraulic conductivities to the Surficial Aquifer and the Intracoastal Formation and applying the observed tidal fluctuations to the seabed upper boundary of the model. Non-density dependent flows were used in multiple runs of the model.

Rainfall rates were estimated from NEXRAD radar data because no weather station has been established at the site and none were installed during the course of the experiments. The closest operating weather station was in Apalachicola (~30 miles to the west). In order to account for rain events at FSUML, NEXRAD data was used to estimate the amount of precipitation at the site. Precipitation data was provided by the US National Oceanographic and Atmospheric Agency and Jim Smith of Princeton

University, who processed the data for this project. Nine, 1km^2 cells containing 15 minute averaged rainfall data were determined from Doppler radar data collected at a station in Tallahassee, FL. The center cell, which contained the field area, served as a proxy for a weather gauge. Unfortunately, a number of periods exist where no data was collected over the site. These periods are concentrated between August 31st and September 6th, and are given a value of "-1" in **Figure 2-6** and in all subsequent plot containing the rainfall data. From conversations with the night security staff and from field notes, the only rainfall to occur during this period occurred on August 31st, in the form of light rain in the early morning (3:00 to 6:00am) and light rain sporadically throughout that day, clearing by late afternoon.

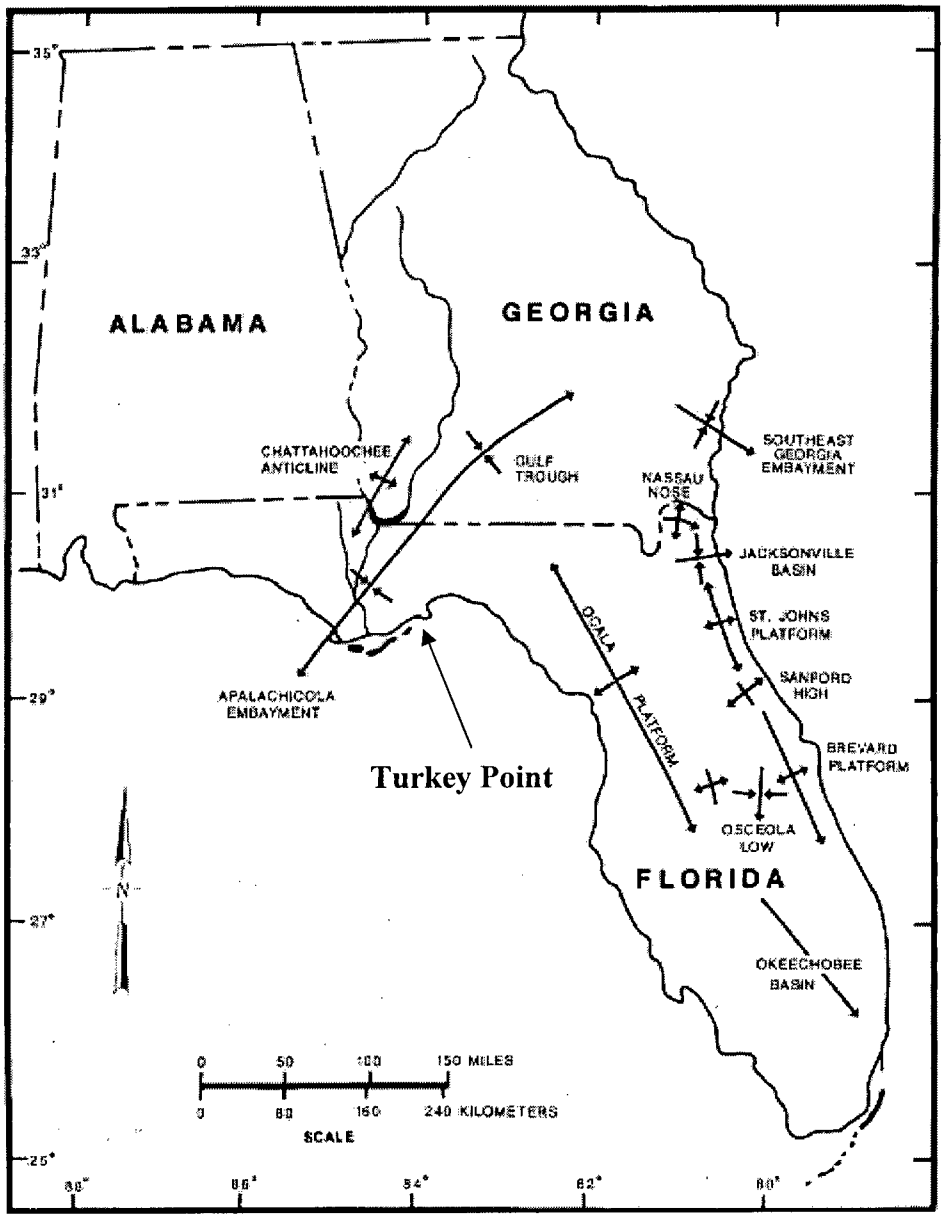

Figure 2-1. Map of structural features of Florida with location of Turkey Point field site as well as the Apalachicola Embayment (Scott, 1992).

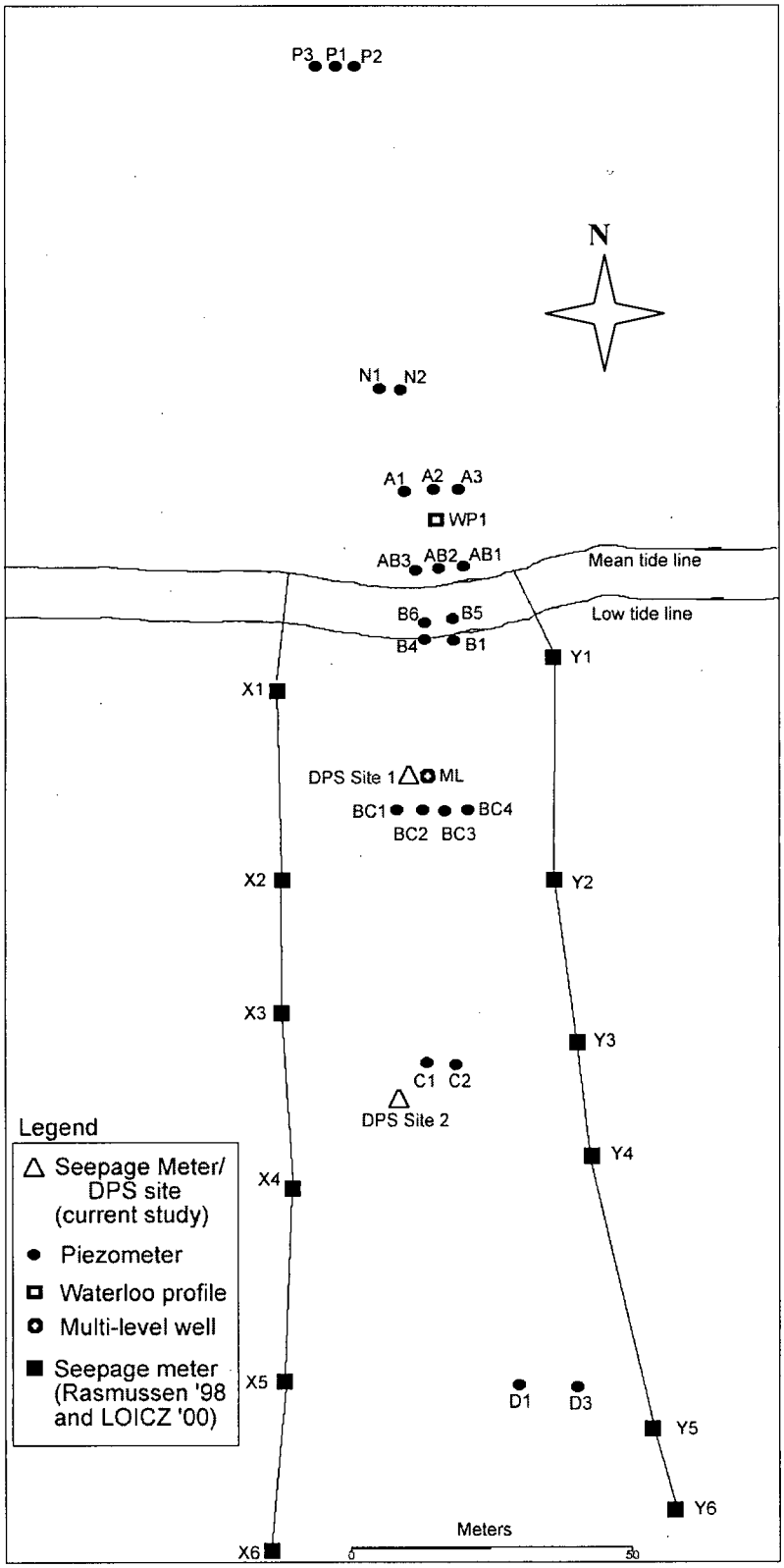

Figure 2-2. Site Map

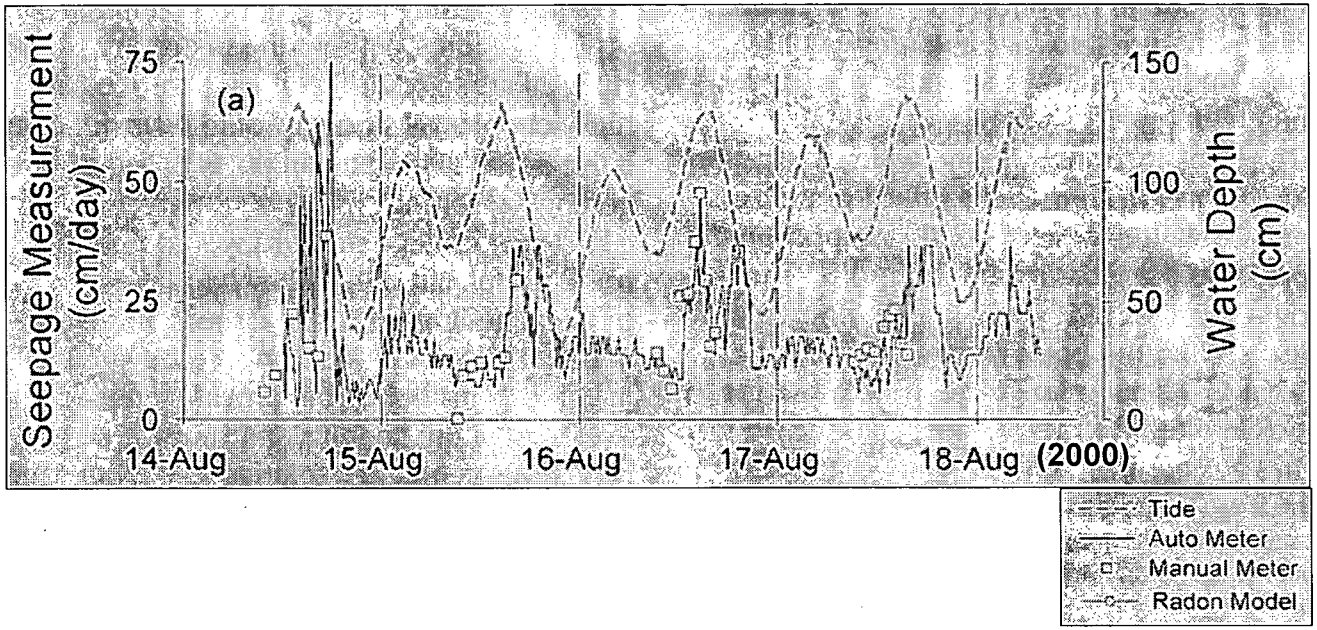

Figure 2-3. Results from Burnett et al. 2002. Note that highest discharge rates are observed between high and low tides.

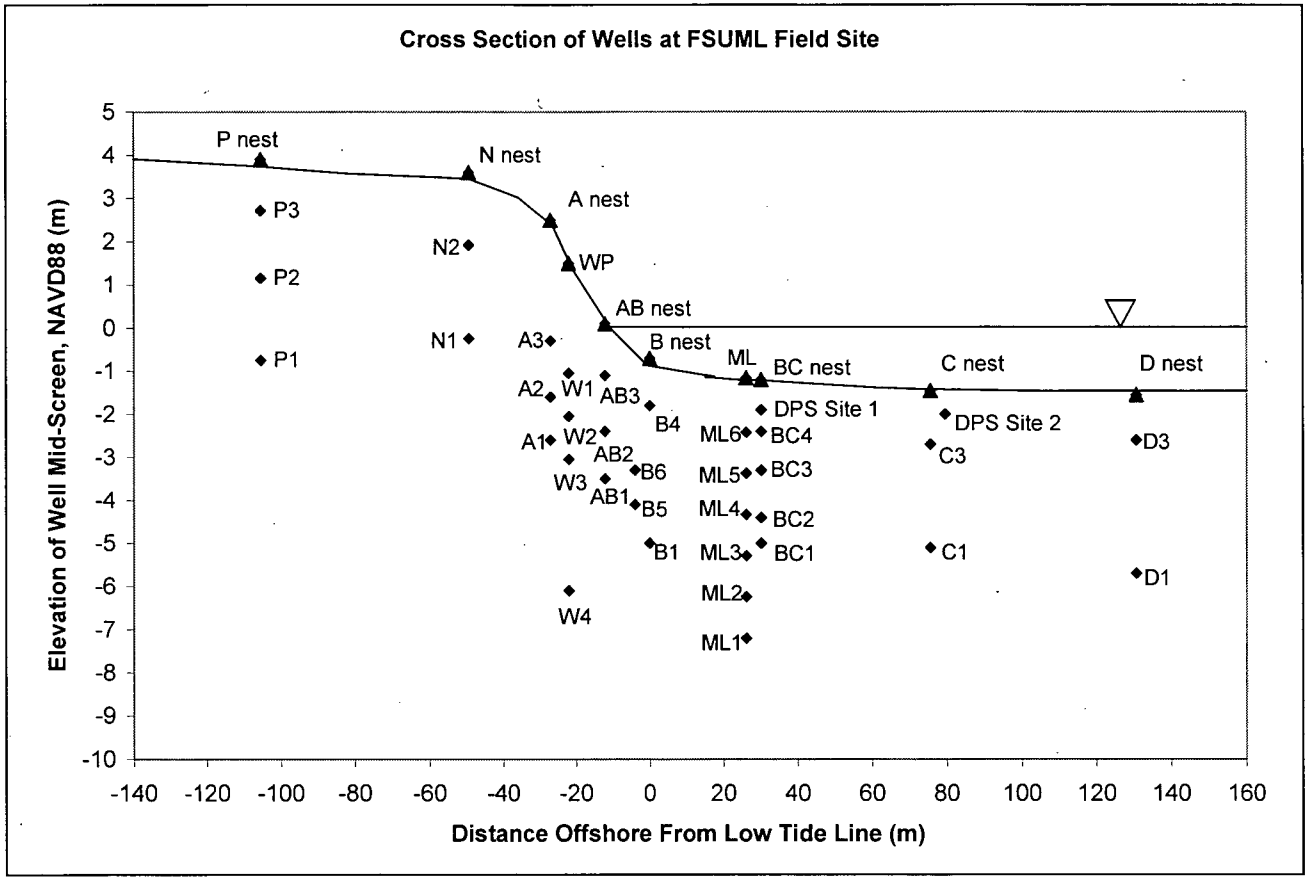

Figure 2-4. Cross-section of Monitoring Well Sampling Depths

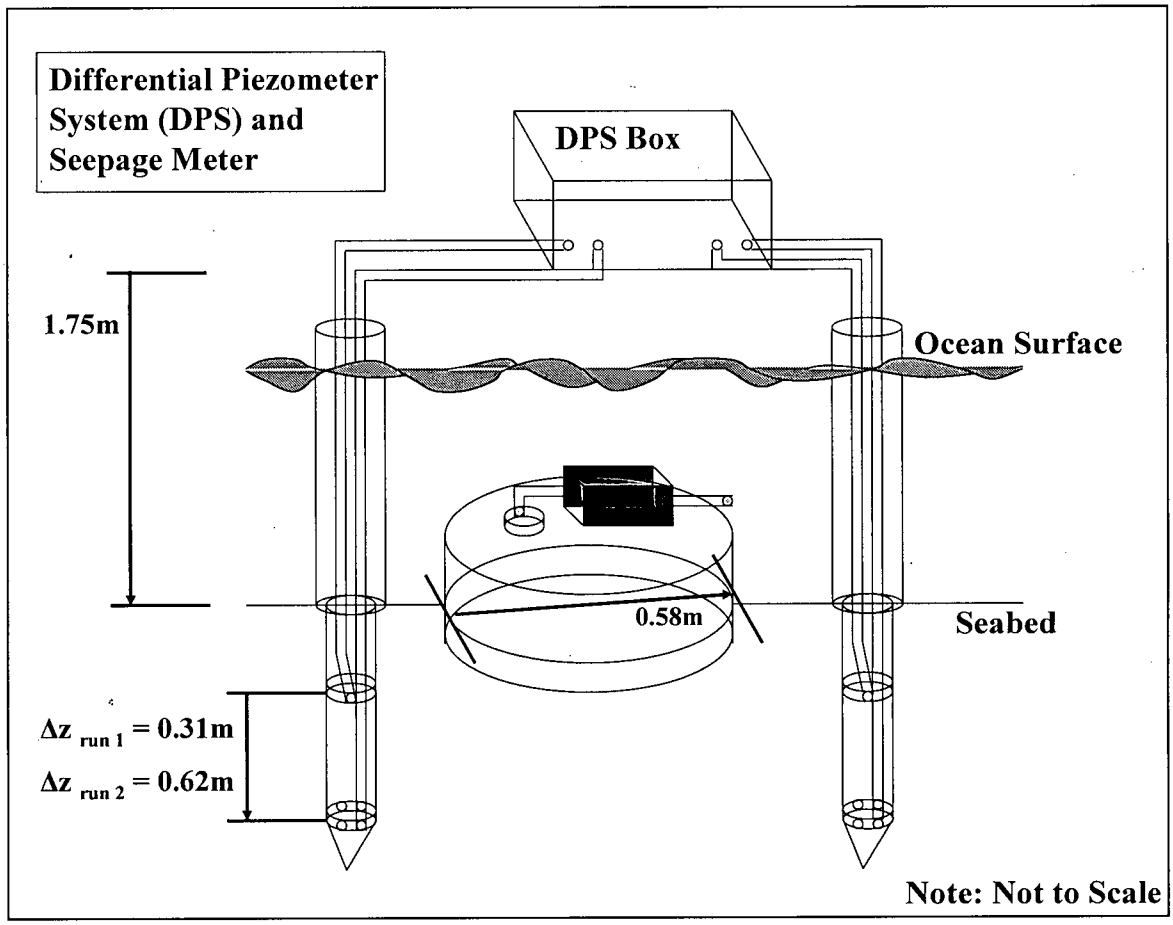

Figure 2-5. Diagram of Differential Piezometer System with Seepage meter

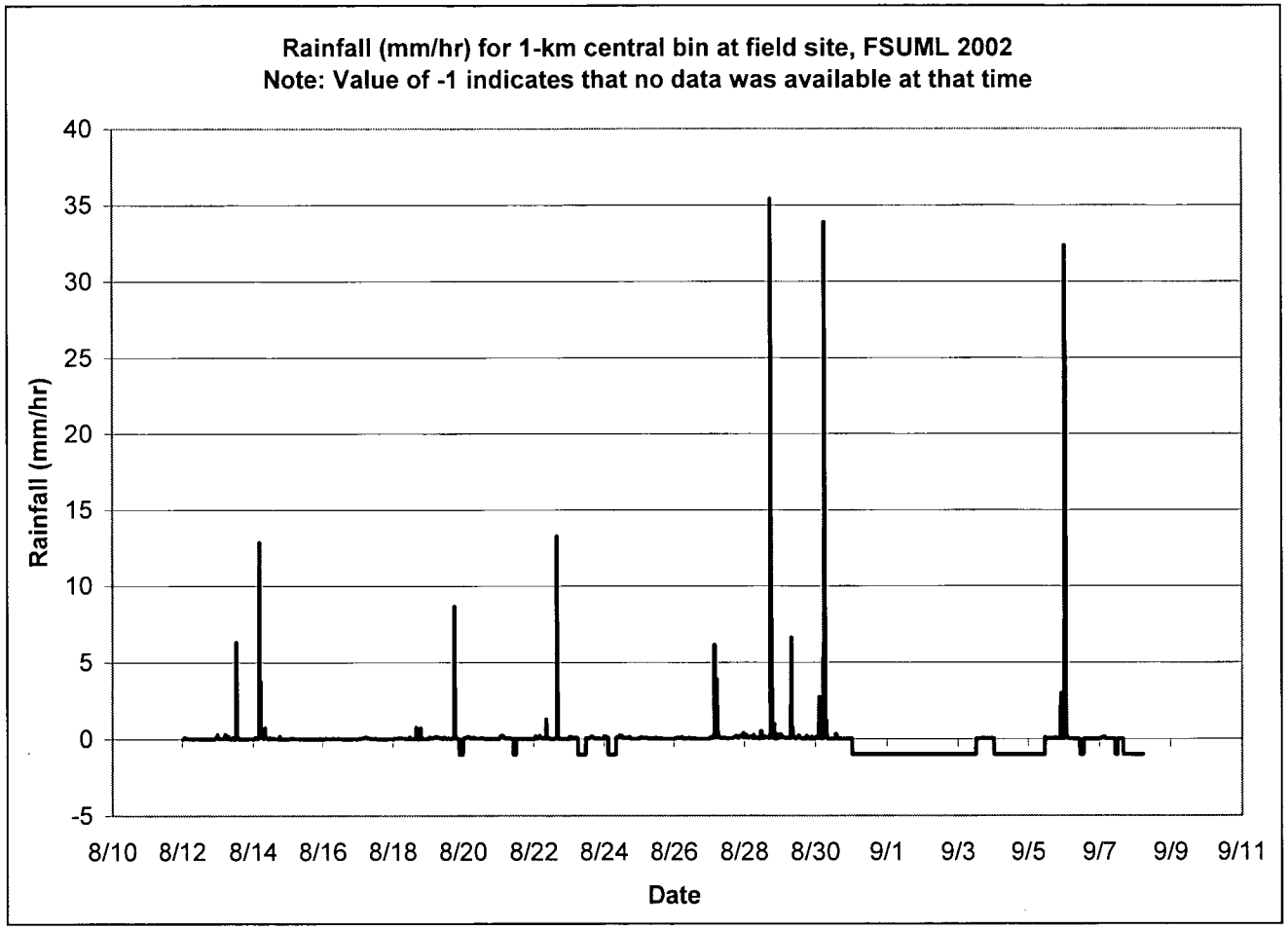

Figure 2-6. NEXRAD Precipitation data

3. Field Measurements of the Coastal Aquifer, SGD and Pressure Changes in the Seabed

3.1 Nearshore Aquifer Characterization

3.1.1 Determination of Geologic Contacts at Depth

The Waterloo Profiler was pushed to refusal at two locations at the FSUML field site. The Profiler, a pneumatic hammer powered by compressed air, was used to drive the steel rods into the Surficial Aquifer with a heat-treated steel tip. The depth of termination was assumed to be the top of the Intracoastal Formation as the Profiler is designed to penetrate only non-lithified strata. A competent rock unit, as the Intracoastal Formation appears to be, would not be penetrated by the Profiler. Rasmussen (1998) had assumed that the water jet used to insert the offshore wells stopped at the top of the Intracoastal Formation but the Waterloo Profiler was able to extend that estimate by 2-3 meters in both sampling locations. It should be noted, however, that a dense sediment or shell layer ~0.1 to 0.2 m thick was encountered at Rasmussen's terminal depth. Using the depth of termination of the profiler, the top of the Intracoastal Formation near A-nest is estimated to have an elevation of -5.5m (NAVD88) and an elevation of -6.8m (NAVD88) near BC-nest. This is deeper than Rasmussen's wells by 3.5m and 2.2m respectively.

3.1.2 Onshore Horizontal Hydraulic Gradient and Tidal Signal in Onshore Wells

The horizontal hydraulic gradient in the onshore area was estimated in order to constrain the estimate of the flux of freshwater to the nearshore and provide the location of the water table. Water levels in wells P1 and N1 were monitored continuously between August 14th and September 7th, 2002. A North-South cross-section with the locations and

depths of the onshore well nests is shown in **Figure 3-1**. In this figure, a snapshot of the water table was captured in wells A1, N1 and P1 on August 25th at 12:10pm because at that time an independent measurement of the water table depth was made at well A1. All distances in this study are made relative to the low tide line, estimated for this study at the location of the B-nest. It should be noted at this point that well A1 had been damaged in a fire sometime between 1998 and 2002. The standpipe had been melted to the ground surface and was sitting deformed and open. The well was repaired with a new standpipe and cap. As there is some discrepancy between the depth of the well measured in 2002 and the depth referenced in the thesis by Rasmussen (1998), it is likely that wind and storms had forced sand into the opening, decreasing the total depth of that well. Solinst Leveloggers™ were placed immediately above the screens in each of wells P1 and N1. The Levelogger pressure transducers were used to measure the height of the water column above the sensor and can detect changes in water level to an accuracy of +/- 1mm and to a maximum water depth of 5m. Readings were taken every 10 minutes and plotted against time. The depth of each Levelogger below the top of casing is 4.5m for well P1 and 4.4m for well N1. All measurements were converted from height of water above sensor to elevation relative to NAVD88 based on survey data collected at each well. Each logger was calibrated for 40 minutes at atmospheric pressure before being submerged in a bucket containing 0.3m of water for 90 minutes. These measurements were used during data processing to calibrate the water levels in each well. A Solinst Barologger™ was placed at ground level near well N1 and used to correct for atmospheric pressure fluctuations. Precipitation data is plotted with the onshore water table data because it shows distinctly how the water table responds to large rainfall events (**Figures 3-2**).

Figure 3-3 is similar to **Figure 3-2** but the plot is of water table depth below ground surface, not water table elevation as in **Figure 3-2**. Note that well P1 has a ground surface elevation about 0.3m higher than that of well N1. Depth and elevation data for all new onshore wells is presented in **Table 3-1**.

Table 3-1. Characterization of New Onshore Wells

Well	Top of Casing Elevation (m)	Ground Surface Elevation (m)	Mid-Screen Elevation (m)	Screen Length (m)
P1	5.311	3.871	-0.75	0.45
P2	4.685	3.950	1.16	0.91
P3	5.003	3.953	2.716	0.45
N1	4.452	3.612	-0.245	0.41
N2	4.100	3.700	1.917	0.91

Notable in the data collected at each well are tidal signals and intense rainfall events that caused significant rising of the water table at each well. Tidal signals are stronger in well P1 (amplitudes of 1 to 1.5cm) than in well N1 (amplitudes of 0.5 to 1cm) despite the fact that this well is 56m further onshore (**Figures 3-4 and 3-5**). This is discussed in greater detail in Section 3-3.

Two significant storm events (>30 mm/hr of rainfall) occur two-thirds of the way through the data collection period on the evening of August 28th and the morning of August 30th, raising the water table at both wells (total increase of 0.28m at P1, 0.16m at N1). These events effectively bisect the data set, leaving two periods of uniform water table decline in each well which are used to determine the hydraulic gradient. There is one long period of 11 days preceding the events and one shorter period of 2 days following the events in the Levelogger data. Three small rainfall events occurred during the first sequence but did not significantly affect the water table elevation in either well. It should be noted that the raising of the water table at well N1 was much slower than in

well P1 (**Figures 3-4 and 3-5**). This is due to the fact that the gradient can only be realistically calculated when the water table in each well is dropping (or rising) at approximately the same rate. The determination of the hydraulic gradient is presented later in this chapter.

The two other wells in P-nest and one other well in N-nest were also investigated and characterized although water table information was not gathered outside of a few isolated measurements. Well P2 is the second deepest well at the P-nest with a depth below ground surface of 2.8m (ground surface to mid-screen). Well P3 is the shallowest well in the nest with a depth below ground surface of 1.24m (ground surface to mid-screen). The water table never fully rose above the screen of this well and was muddy whenever it was dipped with the water level. See **Figure 3-6** for an East-West cross-sectional diagram of P-nest. Well N2 had been affected by a brushfire and was bent over 90 degrees, pointing eastward. **Figure 3-6** also has an East-West cross-section of N-nest. The water table never reached higher than 0.2m above the base of well N2.

3.1.3 Slug Testing

Wells located at P-nest and N-nest were tested to determine the hydraulic conductivity of the sediments surrounding the well screen of each well. These were the only wells in the field area that had not been evaluated in previous studies. The slug was composed of a sand-filled, PVC pipe 0.52 meters long and 0.032 meters in diameter, producing a volume displacement of 418 cm^3. Wells N1, P1 and P2 were successfully tested while water levels in wells N2 and P3 were too low for effective measurement with

the slug. Three tests were conducted in each well on September 6th and 7th, 2003 using the Solinst Leveloggers described previously.

As hydraulic conductivity estimates were not available for the onshore sediments a priori, equilibration time for the slug tests had to be estimated. The time allotted for each test was set to 5-7 minutes. This proved to be inadequate for complete recovery of well P1 after test 1 and thus data from tests 2 and 3 for this well were not used in the analysis. All other tests recovered completely within this time interval in wells P2 and N1. The Hvorslev method (1951) was used to calculate the hydraulic conductivities. In this method, an initial water level measurement is taken before the slug is lowered into the well with an electronic interface meter (a well "dipper"). The slug is then instantaneously inserted into the well and the decline in the elevation of the water table is measured with time. Slug test recovery plots are presented in **Appendix A**, hydraulic conductivity calculations from slug tests are presented in **Appendix B** and normalized displacement vs. time figures are presented in **Appendix C**.

3.1.4 Salinity profiling

Another aim of the FSUML research was to constrain estimates of upward flux of fresh water from the Intracoastal Formation and to examine the mixing zone in the Surficial Aquifer. By determining the spatial variation of salinity with depth, an estimate can be made as to the location and extent of the saltwater/freshwater mixing zone. With these estimates, a flow model can be designed and run in an attempt to simulate SGD data observed in the field. A 1-dimensional flow model of offshore site 1 was successfully designed and run, which is discussed in detail in Chapter 4.

Salinity profiling of the Surficial Aquifer was conducted by sampling all existing on and offshore wells using a peristaltic pump, and with a direct-push sampling method in two additional locations. All existing wells were purged and sampled once over the course of the field study except for wells P2 and P3 due to time constraints. These wells are expected to have similar salinity values to well P1. Wells were purged of 3 well volumes before a 50mL sample was collected for analysis. The Waterloo Profiler^{tm} is a direct-push sampling method that uses a pneumatic hammer to push steel AW rod into the surface sediments (see **Figure 3-7**).

Two sites in the field area were profiled with the Waterloo Profiler, one onshore approximately 5m seaward of well nest A (labeled WP1 in **Figure 2-3**) and one offshore at site 1, approximately 4m shoreward of well nest BC (labeled ML in **Figure 2-3**). The offshore site is a permanent multilevel well installed with 6 ports spaced approximately 1m apart, spanning the entire depth of the Surficial Aquifer. Porewater samples were analyzed for salinity, which were then mapped in vertical cross-sections to produce salinity profiles (**Figure 3-8**) and percent freshwater profiles of the site (**Figure 3-9**). Percent freshwater is defined relative to seawater sampled from the water column above site 1.

Technicians at Florida State University analyzed the samples. The salinity values were determined using refractometry while chloride concentrations were determined via ion chromatography. Tables containing salinity and chloride data are available in **Appendix D**.

The 2002 salinity profiling produced a similar salinity cross-section plot as the 2000 study (**Figure 3-10**). Both salinity profiles of the field site collected during the

current research (**Figure 3-8**) and for the Intercomparison Experiment in August 2000 (Smith and Zawadzki 2003) show distinct freshening of the porewater with depth in the offshore region. A relatively diffuse area defines the mixing zone in 2002, bounded roughly between the onshore WP site and the B-nest data points. The salinity of seawater collected in the water column above site 1 was 31.5 ppt. The multilevel well was sampled three times in September 2002 and a fourth time in September 2003 to determine if salinities at depth had changed. Two of the six ports had ceased to function properly and were not sampled. The 2003 samples had salinity values that were within 1ppt of the samples acquired one year earlier, indicating that the subsurface salinity profile had not changed at that location. There appears to be a rather sharp freshwater/brackish water contact between the WP1 profile and the AB-nest, a horizontal distance of 12m. Moore (2003) recognized two isotopically distinct sources in his radium measurements of the field area (and up to 28km offshore), likely indicating discharge from both the Surficial Aquifer and the Upper Floridan Aquifer. The idea of two sources is discussed briefly in the next section.

As mentioned in the previous chapter, depths between 1 and 2m below the seabed have salinity values similar to that of seawater, except those wells very close to shore. It is apparent from the salinity profiles that complex interactions occur at depth within the freshwater/brackish water mixing zone, indicated by lower salinity values at some nearshore, mid-depth wells. Additional variability may be caused by the fact that all wells have been projected onto a cross-section for presentation when in reality they are separated in three dimensions.

3.2 Submarine Groundwater Discharge Experiments

3.2.1 Tidal Measurements

Tidal oscillations and waves cause pressure changes at the seabed, applying or removing pressure on the fluids in the sediment pores, influencing the rate of submarine groundwater discharge.

Wave and wind action at the field site usually follows a set daily pattern. The nearshore water surface is generally calm in the morning, with wind increasing steadily into the afternoon. Wave action also increases, reaching a peak in mid-afternoon, usually with mild, choppy waves. Calm water returns to the nearshore region in the late afternoon to evening as the wind and waves recede. The number of major storms (>5cm of rainfall per day) affecting the marine lab ranges between 2 and 6, annually. Seasonally, storms tend to occur in late summer and early fall but they can occur at any time during the year. No major storms were recorded during the experiment period but two significant events, described above, did occur.

Tidal oscillations were measured using a submerged pressure transducer protected by a 2in. diameter, 2m long PVC pipe. The pipe was attached to a piling along an auxiliary wooden dock, running parallel to and immediately north of the main concrete dock at FSUML. The piling is approximately 350m east of well A1. A photograph of the apparatus is shown in **Figure 3-11**. Tape was applied at measured intervals along the PVC pipe so that independent measurements of tidal elevation could be made and used to calibrate the sensor data.

The transducer measured tidal fluctuations from August 14th to September 7th, 2002, at a rate of one measurement every 10 minutes until August 27th when the rate was

increased to every 5 minutes. The sensor measures the height of water above it instantaneously, occasionally capturing "noise" in the form of anomalously high or low water level measurements. The PVC standpipe is not sensitive to wave and wind action and noise is introduced from wakes or large waves. The data was corrected to North American Vertical Datum 1988 (NAVD88) after the elevation of the piling was determined from the survey conducted.

The maximum tidal range measured at the dock of FSUML over the period indicated above was 1.26m (**Figure 3-12**). The elevation ranged from -0.47m to 0.79m, NAVD88, averaging 0.21m. The tidal sequence over the experiment period began with a spring tide (August 14th), transitioned to neap tide (essentially equal tides on August 28th) and back to spring tide again at the end (September 7th). The tides can be characterized as follows: higher high tides (HHT) ranged from 0.472m to 0.793m, lower high tides (LHT) ranged from 0.298m to 0.683m, higher low tides (HLT) ranged from -0.169m to 0.353m and lower low tides (LLT) ranged from -0.466m to -0.098m. The data presented in this graph has been smoothed with a 5-point running average. This data is used as input for the numerical models and for statistical correlation analyses with seepage and DPS data.

3.2.2 Seepage Measurements

An automated seepage meter system is preferred over a manual seepage meter due to the increased efficiency in data collection in temporal measurements and the ability of an automated system to continuously collect data. While both systems are challenging to install, manual seepage meters have been noted for being difficult to monitor and show significant aliasing effects if bags are not pre-filled (Taniguchi and Fukuo, 1993; Cable et

al. 1997). In light of these drawbacks, automated seepage meters are becoming more popular in coastal zone studies.

Characterization of seepage across the seabed was made using a Taniguchi-type automated seepage meter (Taniguchi and Fukuo, 1993) and a differential piezometer system (DPS). The automated seepage meter employs a nichrome wire heater and a series of thermistors to determine the rate of groundwater discharge through the seabed over a certain area. Water passing into the drum from the sediments travels through a hose and past an electric heater. The temperature of the water increases as it passes the heater. A series of thermistors downstream of the heater measure the temperature of the water by its ability to conduct electricity, which is output as a voltage. Background temperatures are removed when the voltage measured at an upstream thermistor is subtracted from the downstream thermistors. The voltages are analyzed to back-out the seepage flow rate. Discharge rates as low as 1×10^{-7} m/sec (0.864 cm/day) can be detected by the Taniguchi-type automated seepage meter (M. Taniguchi, 2004, personal communication).

The seepage meter was set to collect an instantaneous reading once every 5 minutes during the time it was installed. The data collected can only be examined after the system has been disconnected and removed from the seabed. This can become a significant issue because problems with the seepage data will not be discovered until the end of the collection period. This occurred during the final run at site 2 and is discussed in Section 3.3.

The seepage meter was installed four times at two locations within the field area in conjunction with the differential piezometer system, which is described in the next section. Site 1 is located approximately 25m offshore of the low tide line (4m shoreward

of BC-nest) and site 2 is located approximately 80m offshore of the low tide line (4m seaward of C-nest). Two separate "runs" were conducted at each site, referred to here after as site 1, run 1 (S1R1); site 1, run 2 (S1R2); site 2, run 1 (S2R1); and site 2, run 2 (S2R2). Temporary scaffolding was constructed at each site, providing a platform for equipment and where direct measurements of seepage and differential pressure were made. Taniguchi et al. (2003) determined that submarine groundwater discharge rates varied significantly, both spatially and temporally, at certain locations at the field site. The locations mentioned above were chosen to help constrain this variability discovered in the intercomparison experiments of 2000. Seepage output is presented in **Figures 3-13, 3-14 and 3-15**. Three of the four runs conducted at FSUML had values that appeared to be realistic but the final run at site 2 (S2R2) outputted values that were well below the minimum detection limit for the seepage meter and are not presented.

A drawback of this system is that it can only measure discharge out of the seabed. The system is not currently designed to capture both discharge and recharge as some seepage meters are (Paulsen, et al., 2003). The seepage meter was not calibrated immediately prior to the 2002 study and thus, a reading of zero seepage is not exactly known nor is it known what voltage will be output for recharge at the site, should it occur. The calibration curve used to determine discharge rate was provided by researchers at Florida State University, Department of Oceanography. While recharge is unlikely and has not been measured at the site before, it is possible that it does occur. This idea is explored in Chapter 4. A diagram of the seepage meter is shown with the differential piezometer system in **Figure 2-5**.

3.2.3 Differential Piezometer System

The differential piezometer system (DPS) is designed to measure the vertical difference in pressure between two points in the seabed. Two piezometers installed parallel to shore on each side of an automated seepage meter are used to evaluate how pressure changes in the seabed relate to seepage and tidal fluctuations. Each piezometer is constructed of three to four, 31cm-long, 4cm-outside diameter, steel, female-threaded AW rods attached with steel, male-threaded AW connectors. Two ports in each piezometer (one located at the tip, another located in an AW connector 0.31m or 0.62m above the tip) connect to plastic tubing which runs up the inside of the AW rod, attaching to each side of a differential pressure transducer. The differential pressure transducer is thus hydraulically connected to the points located in the seabed. Also, as mentioned previously and shown in **Figure 2-4**, the density of porewater was nearly equivalent to seawater to depths of 1.5 to 2m. If waters of different densities exist at the two ports, the equation presented in Chapter 2 ($\Delta h = (\Delta P/\rho g) + \Delta z$) will not be valid as it assumes constant density.

A vertical distance of 0.31m was chosen initially for port separation (lower port at a depth of 0.7m below the seabed) based on work done by Findlater (2001). Her thesis presented cross-sections through time of average freshwater heads measured in the various wells in the offshore region. Her cross-sections showed that vertical hydraulic head differences did not exceed 0.8m between any of the wells and were usually within the range of 0.05 to 0.3m over vertical distances of 1 to 3m. Based on the fact that the piezometers were to be shallow and to have a vertical distance of only 0.31m, two Setra M230, bi-directional differential pressure transducers were acquired that are sensitive to

pressure fluctuations within the +/- 0.5psi range (+/- 3.45 x 10^3 Pa). This equates to a range approximately equal to +/- 0.34m of head difference (maximum measurable head difference would be 0.68m) and accurate to within +/- 0.0017m (or +/- 1.7mm). Thus, a positive reading on the differential transducer would indicate discharge and a negative reading would indicate recharge. The initial port separation of 0.31m proved to be inadequate as measured output during S1R1 and S2R1 indicated that recharge was occurring (negative differential heads), an observation not supported by the automated seepage meter. A photograph of the external components of the system can be found in **Figure 3-16**. Internal components are illustrated in **Figure 3-17**.

Stilling tubes filled with sand were used to minimize noise caused by wave action in the water column between the seabed and the water surface. Flexible plastic tubing (4in. diameter) was used to minimize noise caused by wind between the stilling tubes at the water surface and the differential pressure transducers located in a plastic box above the high tide surface. These tubes may not have been adequately stiff to dampen out the significant onshore winds occurring in the late afternoons at the field site as observed in noisy sections of the data and discussed in the next section. The box houses the electronic components of the system, which includes the two Setra differential pressure transducers, one temperature probe to collect temperatures inside the DPS box, one 12V battery used to power the system and one CR-10X Campbell data logger used to control the transducers and the temperature probe and record measurements from these devices. The two piezometers are independent of each other and collect separate data sets. This allows for comparison between data sets and verification of data quality.

Installation of the differential piezometer system is an involved process and takes 5 to 6 hours on average, outside of prep-work. One fundamental preparation was the process of making de-aired water. This process is important because dissolved atmospheric gases, which were present in the tap water used for the DPS, tend to come out of solution, forming bubbles on the inside of the plastic tubing. Bubbles act as tiny cushions when subjected to pressure changes and are much more compressible than the water that surrounds them. This means that the accuracy of the pressure transducer readings may be thrown off by air bubbles trapped in the tubing of the DPS. De-aired water is made by boiling tap water for 15 minutes, which strips out the dissolved air, poured into glass jars, sealed and allowed to cool. This water is then pumped through the tubing of the system and out the ports during installation to keep the ports from getting clogged with sediment.

Deployment began immediately after high tide, maximizing the time spent working in low water. Piezometers and the seepage meter are assembled onshore. The piezometers are driven into the seabed with a sledgehammer with water being pumped through the system and out the ports. The rate of pumping is important because if pumping is too slow, the ports can clog with sediment. If the ports become clogged, the process is aborted until they can be cleaned. Unlike the seepage meter setup, however, the DPS data can be downloaded periodically during the experiment. It should be noted that on one occasion, high tides forced the removal of the system before a full tidal cycle of 24 hours could be recorded for fear of the DPS box being submerged in seawater. This event occurred at site 2, run 2, where the highest tides during the field study were

observed. The combination of the high tide and 0.25m waves led to the removal of the sensors and recording equipment at lower high tide (12noon) on September 7th.

At the end of each DPS run, independent measurements of differential head were made by observing the water levels in each tube after they had been disconnected from the DPS box. In the case of S2R2, the measurements were made prior to the run, on September 6th. The measurements were made as close to shutdown as possible so that transducer measurements could be compared with the independent measurements. Both tubes from each piezometer were pulled taut out of the water and allowed to equilibrate for a few minutes before being held together against a ruler. The height of the water level in each tube was then measured relative to the sea surface and these numbers subtracted to give the head differential. If waves were present during the measurement, the sea surface was estimated and the heights of the water inside the tubes measured against this temporary datum. This data is presented in **Table 3-2**. Multiple measurements were made of the observed head difference in the tubing and thus an averaged value was used. This was compared to the last 30 seconds of data from the transducers, which was averaged.

Table 3-2. Independent Differential Head Measurements

Site	Run	Sensor	Average Observed Head Difference (cm)	Differential Piezometer System Output (cm) (last 30 seconds averaged)
1	1	1	0.9	-0.1
1	1	2	0.7	0.5
2	1	1	0.9	0.8
2	1	2[1]	-1.0[2]	0.9
1	2	1	3.2	3.1
1	2	2	5.3	5.3
2	2	1	Not available	20.2
2	2	2[3]	6.3	1.6

[1]Sensor 2 tubing was observed to be constricted, may have been clogged.
[2] May have observed incorrect tube.
[3]Sensor 2 tubing was observed to be slightly constricted, may have been clogged.

This data indicates that there is good agreement between measured and outputted differential head data. This is problematic, as discussed below, because large errors are associated with the calibrations of the differential pressure sensors. Despite these errors, the observed differential heads in **Table 3-2** show that if the calibration was performed more carefully, perhaps the output of the DPS would be usable for analysis.

Prior to field work, and again after returning from Florida, calibration experiments were conducted with the differential pressure transducers using a standing manometer capable of producing head differentials of up to 1m. De-aired water was pumped into a manifold and through the pressure transducers. Bleed valves were used to ensure that no air bubbles would be present, which might act as cushions to any pressure fluctuations, reducing the data accuracy. Once the manometer tubes were filled, a syringe was used to add or remove water from the columns. The differential heads were varied to obtain the widest possible range of output in millivolts from the pressure transducers. The relationships determined from these experiments were used to produce calibration equations to process the raw DPS data.

3.3 Results and Discussion

3.3.1 Nearshore Aquifer Characterization

Onshore Horizontal Hydraulic Gradient

In order to estimate groundwater flow to the nearshore marine environment, an onshore horizontal hydraulic gradient is calculated. A hydraulic gradient is calculated is based on the Levelogger data collected at wells P1 and N1 as described above. The horizontal distance between P1 and N1 is 56.1m. The fluctuations caused by the tidal

signals in each well did not significantly affect the hydraulic gradient calculation because the elevation difference remained nearly constant during these times, ranging on average between 4 and 5cm. In that the storm events on the 28th and 30th of August created two periods of steady water table rise and decline, each period was examined separately. The first period will likely produce a more accurate portrayal of the average hydraulic gradient because it is over a longer time interval although both the first and second periods were used to calculate a gradient. For the first period, the vertical water table difference between wells P1 and N1 ranged between 1.36 and 1.40m, averaging 1.38m. An average gradient of 0.025 was determined. The second period produced a hydraulic gradient very close to that of the first, determined to be 0.026. While the Leveloggers are actually recording the pressure head in the onshore wells, the elevation recorded is used as a proxy for the water table elevation. An interesting observation mentioned previously is that the August 28th event caused a 6cm rise in the water table at well P1 while only a 1cm rise is noted in well N1. This observation is further discussed later in the chapter.

It should be noted that independent measurements of the water level in wells N1 and P1 placed the water table 0.5 to 3.7cm higher in well N1 and 4.9 to 5.1cm higher in well P1 than measured with the Leveloggers. One possible explanation is that the coiled wire used to suspend the Leveloggers in the wells had not been straightened enough prior to insertion and that the slight helical shape of the wire produced friction against the inside of the wells. The Leveloggers would thus not extend to their expected full depth. The Leveloggers were removed and reinserted two to three times over the course of the field study (for slug testing, water sampling) and each reinsertion would produce a possibility for error. An independent measure was made at each removal, giving the

opportunity to correct for such errors. If a maximum difference between the well elevations for each period is used to calculate the hydraulic gradient, the same gradients reported above are produced. Thus, the difference between the independent measurements and the sensor measured data does not affect the calculated hydraulic gradient of 0.025. Average water table depth below the ground surface is -2.086m for well P1 and -0.934m for well N1.

Slug Test Results

Slug testing of wells N1, P1 and P2 produced hydraulic conductivity estimates of 1.02×10^{-4} m/s, 9×10^{-6} m/s and 2.79×10^{-4} m/s, respectively, suggesting medium grained sand. These conductivities seem reasonable and are similar to those found in other onshore wells from previous studies (Findlatter, 2001). A comparison is displayed on **Table 3-3** (adapted from Findlatter, 2001).

Table 3-3. Hydraulic Conductivity of Wells at FSUML

Monitoring Well	Mid-screen depth below sediment interface (m)	Elevation of mid-screen (m, NAVD88)	Hydraulic Conductivity (m/s)
P1	4.62	-0.75	$9.0x10^{-6}$
P2	2.79	1.16	$2.8x10^{-4}$
N1	3.86	-0.245	$1.0x10^{-4}$
A1	3.13 [a]	-2.61	$3.1x10^{-6}$
A2	2.87	-	$9.1x10^{-6}$ [b]
A3	1.73	-	Very permeable [c]
AB1	3.63	-	$2.2x10^{-4}$
AB3	1.28	-	$1.4x10^{-4}$
B1	4.29	-	$5.8x10^{-6}$
B4	1.07	-	$2.0x10^{-5}$
B5	3.67	-	$3.5x10^{-6}$
B6	2.78	-	$5.1x10^{-6}$
BC1	3.87	-	$1.1x10^{-5}$
BC4	1.23	-	$1.4x10^{-5}$
C1	3.75	-	$2.3x10^{-6}$
C3	1.38	-	$5.6x10^{-6}$
D1	4.38	-	$4.9x10^{-5}$ [b]
D3	1.32	-	$1.9x10^{-6}$

[a] The mid-screen depth has changed since reported in Rasmussen, 1998 (initially recorded as 3.93m). This is likely due in part by infilling of sediment after the standpipe was opened at ground level during a fire.
[b] For wells where more than 1 test was performed, the arithmetic mean of the K values was reported (see Findlater, 2001).
[c] The rate of recovery during the testing was too rapid to be accurately measured.

A significant decrease in hydraulic conductivity with depth is noted between wells P2 and P1, the value of K decreasing by a factor of 31. This implies a change in vertical structure between these two wells. This local vertical difference is not consistent throughout the field area. Findlater (2001) recognized that the rest of the wells at the field site do not have an obvious trend of hydraulic conductivity values with depth. Despite this, Smith and Zawadzki (2003) adopted a vertical layer model to see if that would explain the rate of SGD observed at the site. Hydraulic conductivities determined from the 2002 slug tests established that values were within one order of magnitude of those found by Rasmussen (1998) and Findlater (2001).

Approximate Discharge Rate at the Shoreline

From the onshore hydraulic gradient estimate and slug test data of onshore wells, an approximate discharge rate at the shoreline can be determined. An arithmetic mean of the hydraulic conductivities calculated at wells P1, P2 and N1 produced an average conductivity of $1.3x10^{-4}$ m/s. A geometric mean gives an average hydraulic conductivity value of $6.4x10^{-5}$ m/s. Both are used to calculate an approximate range of submarine groundwater discharge values expected at the site. The unit length of shoreline (below) was chosen to match the width of the field area used by the 2000 intercomparison study researchers. This area extends 200m offshore of the mean tide line. The result of this calculation will then be comparable to their summary results, published in Burnett et al. (2002) and the results of the models produced by Smith and Zawadzki (2003) whose numerical model was based on this study area. The following values were used in the calculation:

Hydraulic Conductivity (K_{mean}):	$1.3x10^{-4}$ m/s = $7.8x10^{-3}$ m/min
Hydraulic Conductivity ($K_{geomean}$):	$6.4x10^{-5}$ m/s = $3.8x10^{-3}$ m/min
Hydraulic Gradient (dh/dx):	0.025
Unit Length of Shoreline:	100m
Thickness of Surficial Aquifer:	7m

Using these variables, total discharge rate (Q) at the site is estimated to be:

$$Q = K_{mean} A \frac{dh}{dl} = (7.8x10^{-3} m/\min)(0.025)(100m)(7m) = 0.14m^3/\min$$

$$Q = K_{geomean} A \frac{dh}{dl} = (3.8x10^{-3} m/\min)(0.025)(100m)(7m) = 0.07m^3/\min$$

These results indicate that another source of freshwater is required to maintain the SGD rates measured by Burnett et al. (2002). They report discharge rates ranging from 1.6 to 2.5 m^3/min over the same region indicated above based on measurements from chemical tracers and manual and automated seepage meters. Alternatively, Smith and Zawadzki (2003) predicted seepage rates between 0.005 and 0.15 m^3/min from their first model, which incorporated input only from the Surficial Aquifer. Their higher value of 0.15 m^3/min, is based on a modeled vertical structure where hydraulic conductivity decreases with depth. The second calculation above (with $K_{geomean}$) produces an estimated discharge rate similar to their model. It seems likely then, that leakage across the Intracoastal formation, as proposed by Moore (2003) and modeled by Smith and Zawadzki (2003), is one potential source for additional freshwater input to the system.

The hydraulic conductivity values determined for the onshore wells are not necessarily representative of the rest of the onshore region. The hydraulic conductivity varies by two orders of magnitude between wells P1 ($9x10^{-6}$ m/s) and P2 ($2.8x10^{-4}$ m/s) over a vertical distance of 1.9 m. Additionally, the well-screen of well A1 has an elevation ~2 m lower than well P1 (**Figure 3-1**) and a similar hydraulic conductivity ($3.1x10^{-6}$ m/s). Well N1 is relatively deep, screened at a point 0.5 m higher than P1 and with a hydraulic conductivity estimated at $1.02x10^{-4}$ m/s, which is closer to that of well P2. If we assume that wells A1 and P1 are part of the same sediment unit, a sloping "contact" might run between the two wells. Unfortunately, it is unknown whether the heterogeneity of the onshore Surficial Aquifer is laterally extensive or if there are discontinuous pockets of high and low conductivity. The tidal signal analysis section

explains one hypothesis for why the site may have zones of high and low hydraulic conductivity.

While the offshore Surficial Aquifer wells also range in hydraulic conductivity, no apparent vertical structure with depth was found by Findlater (2001). Smith and Zawadzki (2003) do suggest a structure in their numerical model, as mentioned previously. Again, the $K_{geomean}$ calculation above matches well with their simulated discharge across the seabed from the Surficial Aquifer. This lends credence to the hypothesis of vertical structure in the onshore region.

Tidal signal analysis

As described previously, tidal signals are present in both well P1 and well N1. The signal at P1 is noticeably stronger (signal amplitude of 1 to 1.5 cm) than at N1 (signal amplitude of 0.75 to 1 cm) despite P1 being farther onshore. Well data from P1 and N1 are presented with tidal elevation data in **Figures 3-18 and 3-19**. The storm events inhibit a continuous assessment of the relationship but there are enough clear signals in the well data before and after the rain events to explore how the water table onshore is influenced by the tides. The rain events occur during a period of transition between neap and spring tides. Semi-diurnal tides are difficult to identify in the well data but 12.5 hour signals are present in the data, as will be discussed in the Power Spectrum Density section of this chapter.

An analytical solution is attempted to predict the tidal amplitude damping expected at wells P1 and N1. The equation, $H(x) = h_o \exp\left(-x\sqrt{\pi S_s / t_p T}\right)$, calculates the

amplitude of the tidal signal ($H(x)$) at a well x meters from the mean tide line, with parameters of the tidal amplitude (h_o), specific storage (S_s), tidal period (t_p) and aquifer transmissivity (T), which is Kb or hydraulic conductivity multiplied by the aquifer thickness (Yim and Mohsen 1992). This tidal analysis is a transient boundary value problem equation that assumes a semi-infinite aquifer, which is perfectly confined. The Surficial Aquifer is not confined and thus, this assumption is violated. A correction is made, however, in that the specific yield (S_y) is used instead of the specific storage (Ss) because S_y is defined for calculations involving an unconfined aquifer. The following values are used in the equation:

Distance from Shoreline, P1 (x):	92 m
Distance from Shoreline, N1 (x):	36 m
Tidal amplitude (h_o):	0.5 m
Specific Yield (S_y):	0.20
Tidal period (t_p):	12.67 hours = 45612 seconds
Transmissivity, P1 ($T=Kb$):	$(9\text{x}10^{-6}$ m/s)(7m) = $6.3\text{x}10^{-5}$ m^2/s
Transmissivity, N1 ($T=Kb$):	$(1\text{x}10^{-4}$ m/s)(7m) = $9.1\text{x}10^{-4}$ m^2/s

With these parameters, tidal signal amplitudes of $1\text{x}10^{-17}$ cm and 0.6cm are estimated for wells P1 and N1, respectively. The value calculated for well P1 is essentially equal to zero, an estimation that is not reflected in the observed well data where amplitudes of up to 1.5 cm are observed. The value calculated at well N1 is approximately correct, being very close to the observed 0.75 cm amplitudes. As an experiment, the hydraulic conductivity in the equation was changed to see what value would produce a tidal signal amplitude equivalent to that seen in the field. A tidal signal of 1.5 cm observed at a well

92 m inland from the shoreline would require an aquifer hydraulic conductivity of $1.3x10^{-3}$ m/s, a value 144 times higher than the value estimated at well P1. A conductivity of $1.4x10^{-4}$ m/s produces the amplitude that is seen in the field at well N1, amplitude of approximately 0.75cm. This value for N1 is approximately the same as the estimated value.

It is not entirely clear why the tidal signals at N1 are damped relative to P1. Tidal signals are not as evident during the water table decline at N1 prior to the storm events yet the signals are very evident in the data after the storm events, perhaps in response to the large spring tide observed September 4^{th} to 7^{th}. As mentioned above, the hydraulic conductivity of the sediment immediately surrounding well N1 is ~31 times higher than that of the sediment surrounding well P1 (**Table 3-3**), implying that greater attenuation, and thus smaller signals, should be seen at P1, as reflected in the calculations. This, however, does not appear to be the case at the field site. One possible explanation is that well N1 is immediately shoreward of a low conductivity unit, which would dampen pressure signals from the tides at the shoreline. It is apparent from **Table 3-3** that wells A1 and A2, the deepest wells in the A-nest, have conductivities in the range of 10^{-6} m/s. This represents a low hydraulic conductivity zone between the shoreline and well N1 that may act to inhibit tidal influences. Adding weight to this argument is the fact that when the first large storm (Aug 28^{th}) infiltrated into the Surficial Aquifer, it caused a notable increase in the water table in well P1 (6 cm) while only a minor increase was noted in well N1 (2 cm), despite well N1 being 31 times more conductive than P1 (**Figures 3-4 and 3-5**). This implies that well N1 is near some kind of low hydraulic conductivity unit. It is also possible that some kind of high conductivity unit exists at depth, transmitting the

tidal signal deep onshore while leaving hydraulically-insulated, nearshore wells like well N1 mostly unaffected. This hypothesis is unlikely and would require further fieldwork before being rejected. The best assumption that can be made is that well N1 is adjacent to a low conductivity unit that could be part of the A-nest low K zone.

3.3.2 Submarine Groundwater Discharge

As mentioned previously, two sites in the offshore region were chosen for discharge experiments; site 1 located 26m offshore from the low tide line and site 2 located 78m offshore from the low tide line. The results of the automated seepage meter and the differential piezometer system are presented separately and then examined for dominant frequencies via power spectrum density analyses, discussed later in the chapter.

Direct Seepage Measurement Results

The rate of submarine groundwater discharge at the FSUML field site varied extensively over the course of the field examination. Tidal signals are apparent in the seepage data both visually and in the power spectrum analyses. Statistically significant relationships also exist between some of the seepage data and the sea surface elevation although most relationships are quite weak. The following discussion is broken down by individual runs at each site.

The data set collected during run 1 of site 1 (S1R1) is continuous between August 16th and August 23rd and displays discharge rates in the range of 10 to 80 cm/day, steadily increasing with time (**Figure 3-13**). It is not understood why the discharge would be

increasing over this interval, namely because no significant rainfall events occurred that might increase overall seepage rates. Early seepage results do not exhibit strong tidal influences until approximately August 19th. Data collected between August 17th and August 23rd is plotted in **Figure 3-20**. From visual examination of the data, peak discharge occurs after the high tide has passed but before the low tide is reached. This observation is explored and reproduced with the numerical model in Chapter 4. Paulsen et al. (2003) found a strong inverse relationship at West Neck Bay, Long Island, New York, by directly plotting tidal stage against discharge. This behavior seems to be site specific, however, as an inverse, linear relationship is not observed in the data from FSUML.

Groundwater discharge during the second run at site 1 (S1R2), collected between September 3rd and September 5th, is difficult to characterize (**Figure 3-15**). Initial rates during the first 24 hours are 10 to 20 cm/day (with a few higher spikes) but taper off to less than 10 cm/day. Prior to 18:20 on the 4th, the data has one recognizable peak early on, corresponding to a drop in the tide (**Figure 3-21**). At 18:20 on September 4th, the meter started recording seepage rates 3 times higher than before. During the second half (after 18:20, Sep 4th), there are two peaks that correspond to dropping or low tides but visible correlation is difficult. It is not clear why there is a sudden increase in the discharge rate part way through the run.

Tide/seepage interactions during run 1 at site 2 (S2R1) are easier to explore than other data sets because the interval of collection was over a relatively long period (8 days). The seepage data (**Figure 3-14**) has obvious tidal influences from the beginning of the run, August 24th until about August 31st, with the seepage rate ranging in magnitude

from 6 to 49 cm/day. From this point until the end of the run on September 2nd, the seepage rate dropped and remained steady at about 15 cm/day. It should be noted that this drop in seepage coincides with the two major storm events on August 28th and 30th (**Figure 3-22**). It is not clear why seepage would drop off immediately after these rain events. It is logical to assume that the opposite would occur, with discharge increasing after rain events of this magnitude. From the field observations, it can be seen that seepage follows a cyclic pattern that follows the tidal cycle. At the tidal extremes, discharge rates are at a minimum and near zero. During the transition of high to low tide, seepage rate reaches a maximum. Conversely, when the tide is transitioning from low to high tide, seepage is at a minimum. Hence, with only discharge occurring (no recharge), a plot of seepage rate against tidal height should give a non-linear relationship that is convex down, highest seepage at mid-tides, and low seepage at the extremes. This process is illustrated extremely well in the 1D model results of Chapter 4.

The seepage data collected during second run at site 2 (S2R2) was not used in an analysis because the output produced is below the detection limit of the meter (1 cm/day). This situation highlights one of the design problems with the Taniguchi-type automated seepage meters. The seepage measurements can be examined only after the system has been removed from the seabed, which in this case meant the loss of the entire data set. If there was a way to remotely check the output without disassembling the apparatus, these problems could be avoided.

Notable in **Figures 3-14 and 3-15** are extended periods of near constant discharge rates of 10 to 20cm/day that extend from 10 to 72 hours at a time. Discharge is recorded

by the automated seepage meter but these periods do not display the effects of tidal fluctuations. This is unusual and it is not known why this behavior is observed.

In general, the seepage data sets collected for this project are similar to the seepage data collected for the 2000 intercomparison project. The main similarity between the seepage results is that the range of discharge rates (averaging about 20-40 cm/day) is similar and the temporal variations in the data with tidal fluctuations is similar. In this regard, the discharge is observed to be greatest during the transition between high and low tides.

Seepage and Rainfall

An investigation of seepage response to storm events was conducted on the seepage data. Five significant rainfall events occurred over the course of the experiment. A significant rainfall event was considered to be any storm that produced 8 mm/hr of rainfall within a 15 minute period or more over the field area.

A peak discharge in the seepage meter data after the two rain fall events of August 28th and August 30th was expected but a significant increase in discharge was not observed. On the contrary, seepage dropped to less than 20cm/day and stayed relatively constant after the Aug. 30th event. In the Levelogger data, these events were captured as a rapid and significant rise (0.28m over 3.5 days) in the water table at well P1 and a slightly more gradual and moderate rise (0.16m over 4 days) in well N1. The heightened water table at well P1 reached its peak on August 31st/September 1st. It is not clear why offshore seepage rates would decline after such significant infiltration has occurred.

On August 19th and 22nd, during run 1 at site 1, smaller events occurred (8.6mm/hr and 13mm/hr) than those listed above yet an increased seepage rate is notable in the seepage meter output for both events (**Figure 3-20**). The peaks in seepage are caused by the tidal influences but may be enhanced by the storms.

Differential Piezometer System

The Differential Piezometer System did not successfully resolve pressure differences in the seabed during the period of observation at FSUML. The reason for the difficulty arises from two key issues: the vertical distance (Δz) between the two ports on the piezometers and the calibrations used to process the data.

Four calibration tests were conducted on the differential pressure transducers under laboratory conditions, two before the fieldwork and two after the fieldwork. A standing manometer was used to vary the heads, the output plotted and a regression line fit to each line. The calibrations were not designed to mimic the environment of the Florida field area but were intended to measure the output of the pressure sensors in a controlled setting. It became apparent after running the post-fieldwork calibrations on the DPS sensors that the output had "drifted," shifting all values for sensor 1 approximately 2cm to the left and all values for sensor 2 approximately 1cm to the left (**Figures 3-23 and 3-24**). It is not known when the sensors drifted, because no other calibrations had been performed in the field. As a result of the lack of information on the drift (i.e. when or how it occurred), investigations were made into how to use the calibration error and minimize the error associated with the drift. In order to use the differential pressure data, a regression analysis was performed on the all calibration data from both before and after

the fieldwork. As part of the regression analysis, an RMS error is produced which describes how far away a given point falls from the regression line. The equations produced from the all calibration data are:

For Sensor 1: $\Delta h = (\Delta P - 1616.1) / 34.62$ where the rms error is $\Delta h \pm 1.05$cm

For Sensor 2: $\Delta h = (\Delta P - 1418.2) / 35.39$ where the rms error is $\Delta h \pm 0.68$cm

In these equations, ΔP is the sensor output (differential pressure) in mV and Δh is the differential head. At a 68% confidence interval, the RMS error is ± 1.05cm for sensor 1 and ± 0.68cm for sensor 2. At a 95% confidence interval, these errors become ± 2.1cm and ± 1.36cm, respectively. Because the errors involved have the same magnitude as most of the data, the DPS output cannot be trusted to resolve processes affecting the seabed. Despite this, the regression equations produced for each sensor were used to process the raw data from the differential piezometer system so that they could be plotted. **Figure 3-24** displays sensor data processed with both all calibration data (thin lines) and only post-field work calibration data (thicker lines).

The calibrations performed before and after the field study were conducted so that all procedures were the same, as much as possible. Yet the calibrations are obviously off by a considerable amount. Potential errors in the calibration tests could have been caused by multiple factors. The process used to de-air the water was changed after conducting pre-field calibrations. Initially, a vacuum of 85kPa was applied to a volume of water for 24 hours. For the preliminary field studies in Vancouver, the actual fieldwork in Florida and the post-calibrations, boiled water was used to de-air water for the sensors. Another potential source of error is the density of water used in DPS calibrations may have been different from the density of water used in DPS experiments in Florida. Vancouver tap

water (used for all calibration experiments, both pre and post fieldwork) has a lower TDS concentration than that of tap water at Florida State University Marine Lab. The density differential of the water used is likely to be extremely small and will not have much of an effect on the calibrations. A greater chance of error that may have caused the drift in the sensors is the severe temperature fluctuations experienced inside the plastic box where the sensors were housed during experimentation in Florida. The box underwent a maximum daily swing of 22°C during run 2 at site 1, with the temperature ranging from 25°C just prior to sunrise to 47°C in the late afternoon (See **Figure 3-26**). Pressure transducers can be sensitive to temperature fluctuations and may cause offset in the data. The temperature fluctuations inside the DPS box during the experiments are well within the operating temperature of the sensor, which is -18 to +80°C. There is a potential as well that the resistors used in the DPS box for transforming the electrical output from the sensors were not properly insulated against the high temperatures inside the box. As the resistors were not tested for temperature effects, it is unknown whether this affected the DPS output.

In light of these errors, it is still useful to examine the differential piezometer system output. As discussed previously, the differential pressure transducers used in the field are capable of resolving pressure differences of up to +/-0.34m of hydraulic head (+/-0.5 psid or +/- 3.45 Pa), which is within the range of head differences measured at the field area (Findlater 2001). Preliminary experiments conducted at a beach along the Spanish Banks of Vancouver prior to the Florida field work indicated that the port separation of 0.31m was sufficient to produce head differences on the order of 5 to 11cm for sensor 1 and 1 to 6cm for sensor 2. It is not clear why the sensors produced different

readings. It was not anticipated that the head differences measured at FSUML would require a larger port separation. Recharge was observed by both sensors (more common in sensor 2), a highly unlikely occurrence when constant discharge was recorded by the seepage meter 0.4m away. Differential head measurements were sampled at a rate of one measurement every 2 seconds initially so as to ensure that no signals affecting the DPS would be lost. It was determined, however, that one measurement every 6 seconds would be suitable and easier for data storage. Based on the calibration equations (discussed below), sensor 1 exhibited head differences for run 1 that ranged from -1.5cm to +4cm (average of 1cm) at site 1 (**Figure 3-27**) and a range of -2cm to +4.5cm (average of 1.5cm) at site 2 (**Figure 3-28**). Sensor 2 had output ranging from -1cm to +4cm (average 0.5cm) at site 1 (**Figure 3-29**) and from -3.5cm to +2cm (average 0cm) at site 2 (**Figure 3-30**). It should be noted that significant noise is present in the data, likely caused by wind and/or wave disturbances. Future experiments will require more vigilant efforts to reduce noise in the system.

The port separation was increased to 0.62m for run 2, producing better results but also introducing new concerns about the data. During run 2 at site 1, the head differences for both sensors were somewhat higher than those observed during run 1 and no negative readings were recorded (**Figure 3-31**). Notable, however, is that the sensor outputs are not just offset in magnitude as in the first run, they are also offset in direction. Whereas previously the sensors produced differential head measurements that oscillated in the same direction, S1R2 shows the sensors fluctuating in different directions. That the head difference recorded at each piezometer (measured at the same depths and separated by

only 1.4m, horizontally) would record opposite oscillations with tide is a surprising result and very difficult to interpret.

Included in **Figure 3-31** is the seepage discharge data. This data has been included because the original intent of the DPS experiment was to correlate all three data sets: tidal fluctuations, seepage rate and differential head in the seabed. As the DPS calibration errors did not allow the data to be resolved in a usable format, this goal could not be achieved. Despite this, S1R2 contains the highest quality DPS data collected at the field site.

Run 2 at site 2 recorded differential head for less than one tidal cycle and thus had similar issues as with the seepage data. Truncation of the experiment was mandatory due to the large spring tide occurring at that time, forcing the removal of the DPS datalogger and sensors. As will be described in the next section, no realistic analysis can be performed due to calibration issues.

In summary, the differential pressure experiment was not successful because (A) run 1 had to be discounted from analysis due to low head differences and observed recharge, (B) the RMS error from the regression of the calibration data is at the same magnitude as the data itself and (C) the calibration of the differential pressure sensors did not take into account environmental affects likely to be experienced in the offshore region of the FSUML. Future studies should include careful calibration of equipment under conditions likely to be experienced in the field.

Power Spectrum Density Analyses

Power Spectrum Density (PSD) transformations determine the dominant frequencies present in a given set of numbers. Assuming that tidal influences are present in both the seepage meter data and the onshore Levelogger data from wells P1 and N1, these data sets were examined. The numerical analysis tool, Matlab™, was used to process the data for these experiments. The window size for each analysis was defined as the number of samples in the data set, allowing for the highest resolution possible. As a result the figures provided tend to be noisy at higher frequencies.

PSD analyses were performed on the tidal data prior to the processing of other data sets. This would determine which frequencies should be returned by the analysis of the seepage and differential pressure system data. The tidal elevation was collected at two sampling frequencies; 10 minute intervals initially (1912 samples) and then reduced to 5 minute intervals (3195 samples). The dominant periods returned from these analyses are 24.5 hours (diurnal) and 12.3 hours (semi-diurnal) for the 10 minute data and 24.2 hours (diurnal) and 12.7 hours (semi-diurnal) for the 5 minute data. The periodograms for these estimates are shown in **Figures 3-32 and 3-33**, respectively. These periods are similar to those reported by Taniguchi (2002) who measured SGD and tidal fluctuations in Osaka Bay, Japan, over a period of 4.3 months. Taniguchi transformed 3 months of data, determining periods of 24.1 hours (diurnal) and 12.3 hours (semi-diurnal) for both the SGD and tidal measurements. Taniguchi also found a 341.4 hour signal, indicative of the 14 day lunar cycle (spring-neap tide). The tidal data collected at Turkey Point, which the most temporally extensive data set of all the experiments, did not extend beyond 24 days

and thus would not have captured more than one lunar cycle and would not have seen the lower frequency signal of the bi-monthly lunar tide.

PSD analyses were performed on three of the four seepage data sets; S1R1, S1R2 and S2R1. Seepage data collected during the second run at site 2 (S2R2) was below the detection limit of the meter and was not in place long enough to collect over a full, diurnal tidal cycle. For these reasons, S2R2 data was not analyzed. The S2R1 seepage data was investigated in two parts: first, as a partial data set with only the first 4 days of seepage data and then the entire data set. The reason for this is because data collected between August 28th and September 2nd does not contain a visually significant tidal influence. Data collected between August 24th and August 28th, however, exhibited strong tidal effects. The results for these analyses are summarized in **Table 3-4**. Periodograms are shown in **Figures 3-34, 3-35 and 3-36**.

Table 3-4. Seepage Data PSD results

Site and Run	Number of Samples	1st Dominant Period (hours)	2nd Dominant Period (hours)	3rd Dominant Period (hours)
S1R1	1669	46.5	23.2	11.6
S2R1	992 (partial)	27.6	11.8	8.3
S2R1	2555	42.6	12.5	NA

The power spectrum density results show that some of the seepage data sets exhibit diurnal and semi-diurnal tidal frequencies while others have not captured easily identifiable frequencies. Periodograms for S1R1 and S2R1 (**Figures 3-34, 3-35 and 3-36**) exhibit frequencies that are nearly diurnal and/or nearly semi-diurnal. The 42.6 and 46.5 hour signals observed in S1R1 and S2R1 sequences are a two-day tidal cycle that is not visually observed in the non-transformed data (**Figures 3-13 and 3-14**).

S1R2 PSD results (actual data plotted in **Figure 3-15)** do not have a visually obvious tidal frequency because of anomalously low discharge rates for over half of the run time. Also, later in the run, discharge rates increase sharply but do not appear to be driven by tidal signals. This data did not produce tidal periods and is not presented.

Finally, the onshore well data was investigated. Although not visible in the plotted water table elevations at wells P1 and N1, the analysis of these wells showed that they captured semi-diurnal as well as diurnal tide signals very well. Both wells, sampled every 10 minutes, had nearly continuous data over the entire experiment period (August 14th to September 6th). Tidal signals analyzed at well P1, with 2891 samples, had a dominant period of 24.09 hours and a secondary period of 12.04 hours (**Figure 3-37**). Well N1, with 3178 samples, experienced tidal influences with a dominant period of 24.08 hours and a secondary period of 12.04 hours (**Figure 3-38**). While lacking sharp peaks indicating strong signals, the tidal influences expected within the coastal aquifer, captured by the onshore wells, are present.

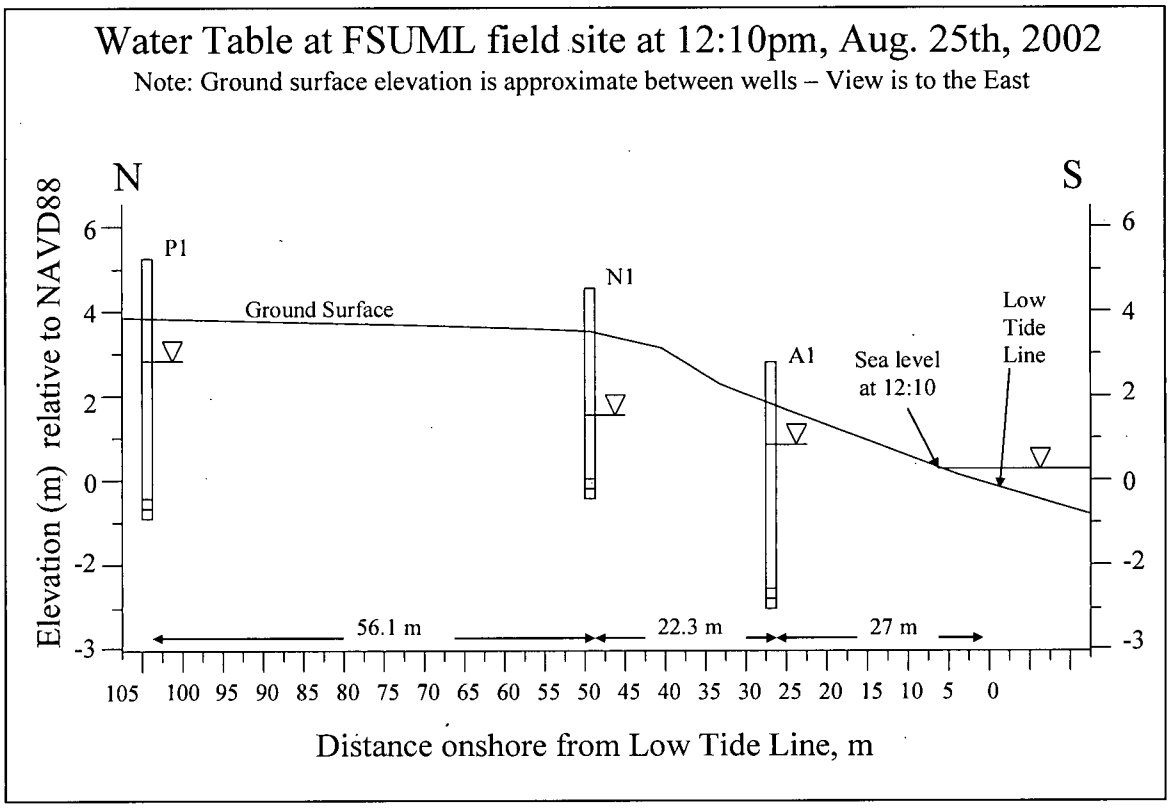

Figure 3-1. Onshore Cross-section showing location of P, N and A nests (and the water table position at 12:10pm on August 25th, 2002)

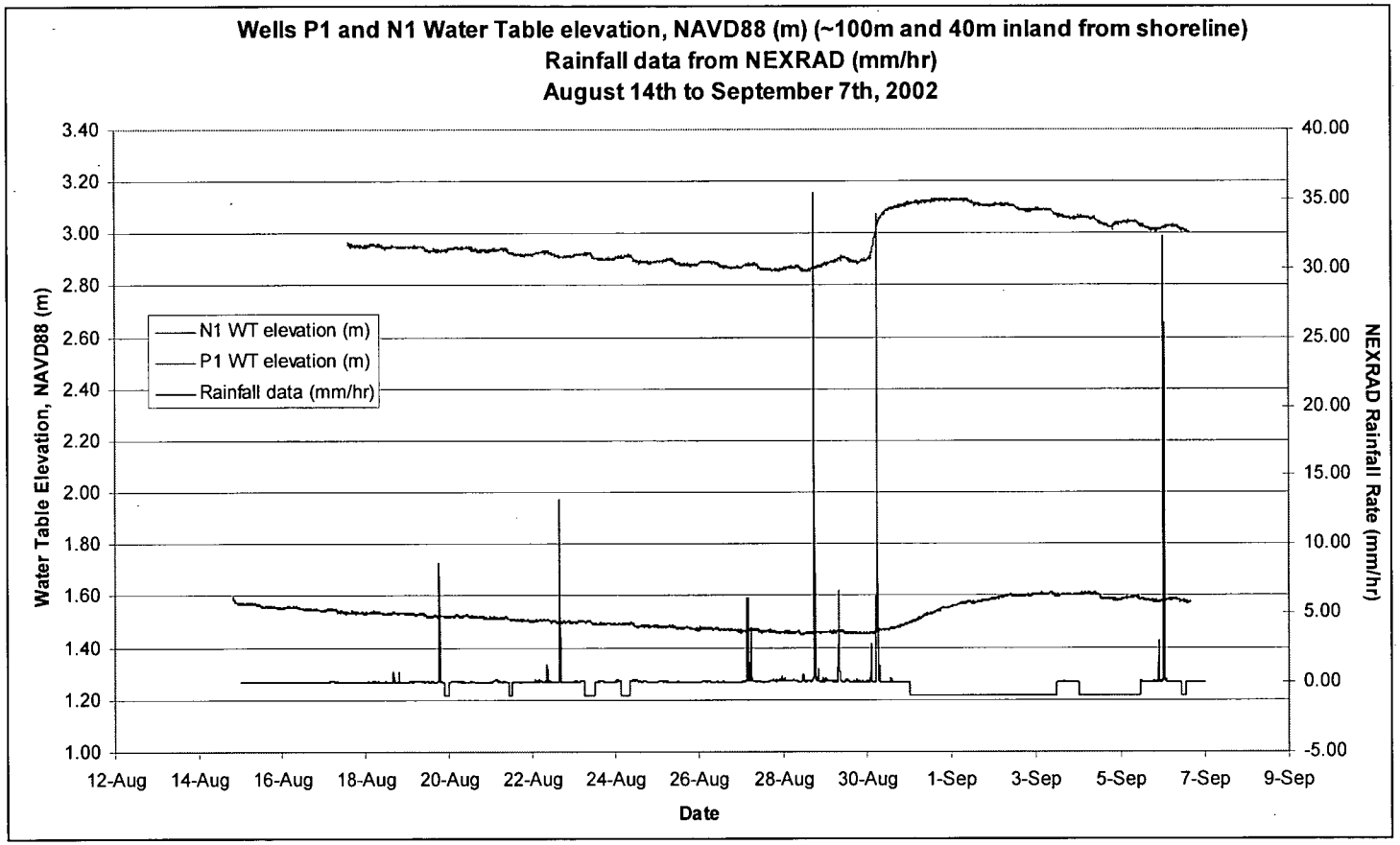

Figure 3-2. Water Table Elevation (NAVD88) and Rainfall Data

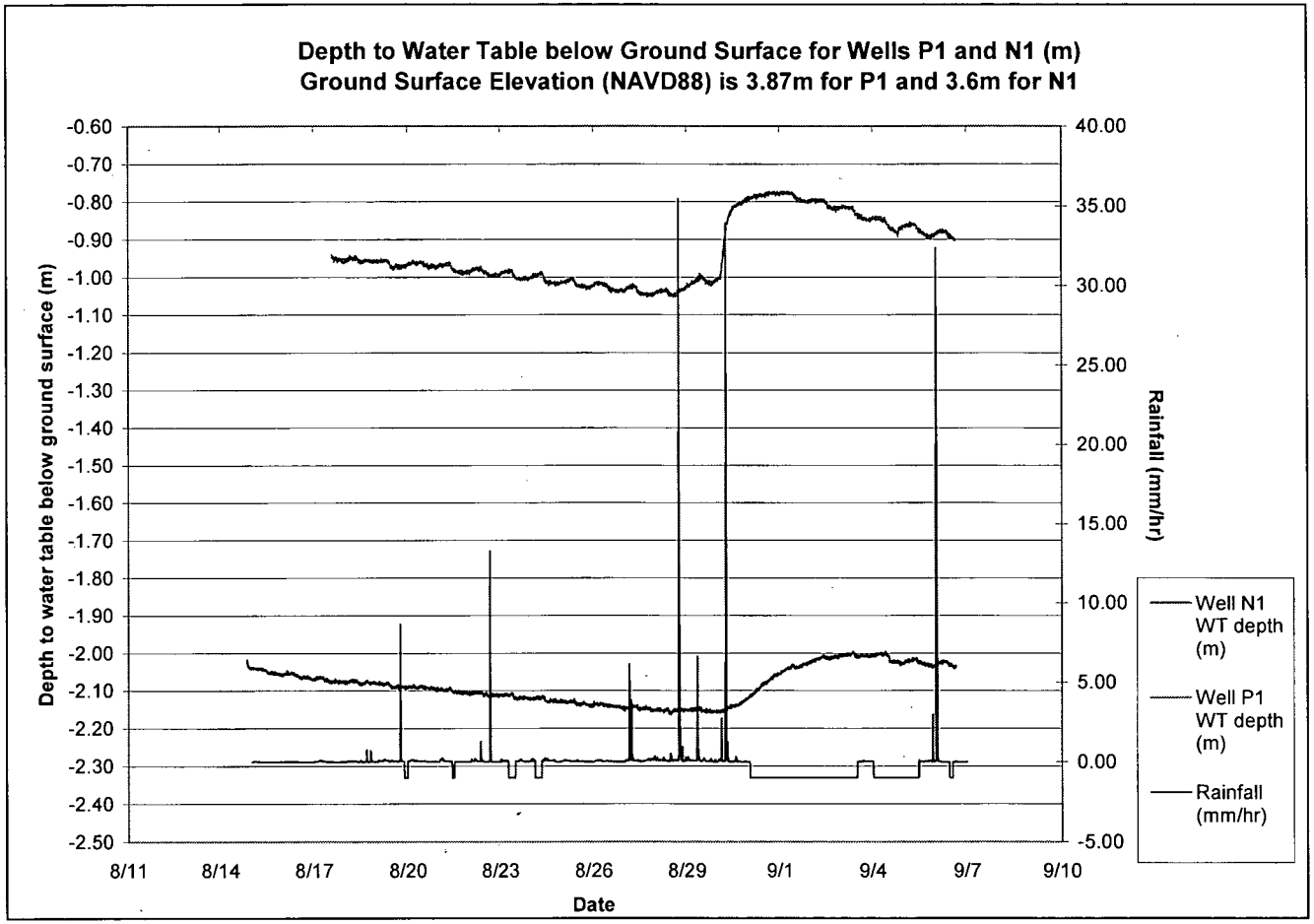

Figure 3-3. Depth to Water Table and Rainfall Data

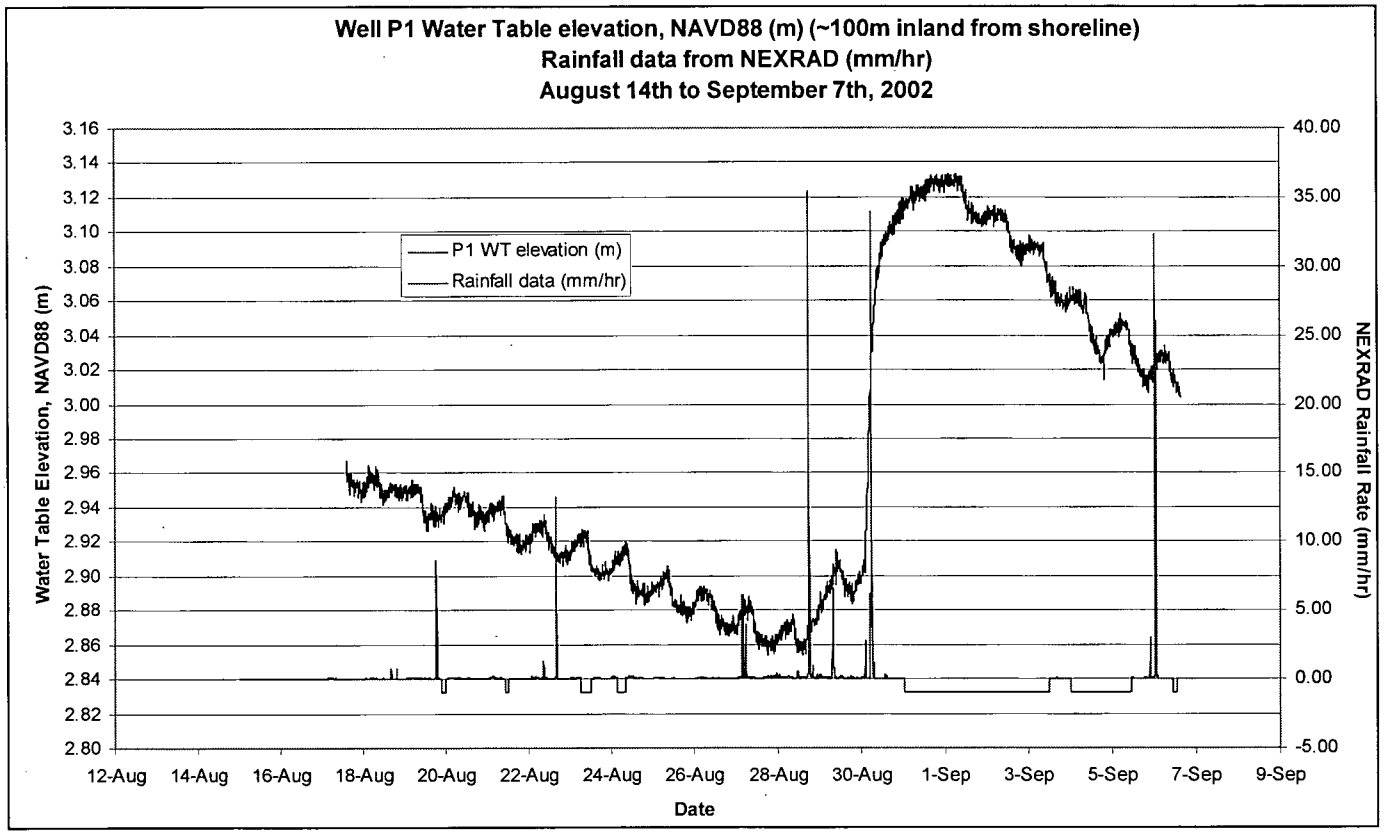

Figure 3-4. Well P1 Water Table Elevation and Rainfall Data

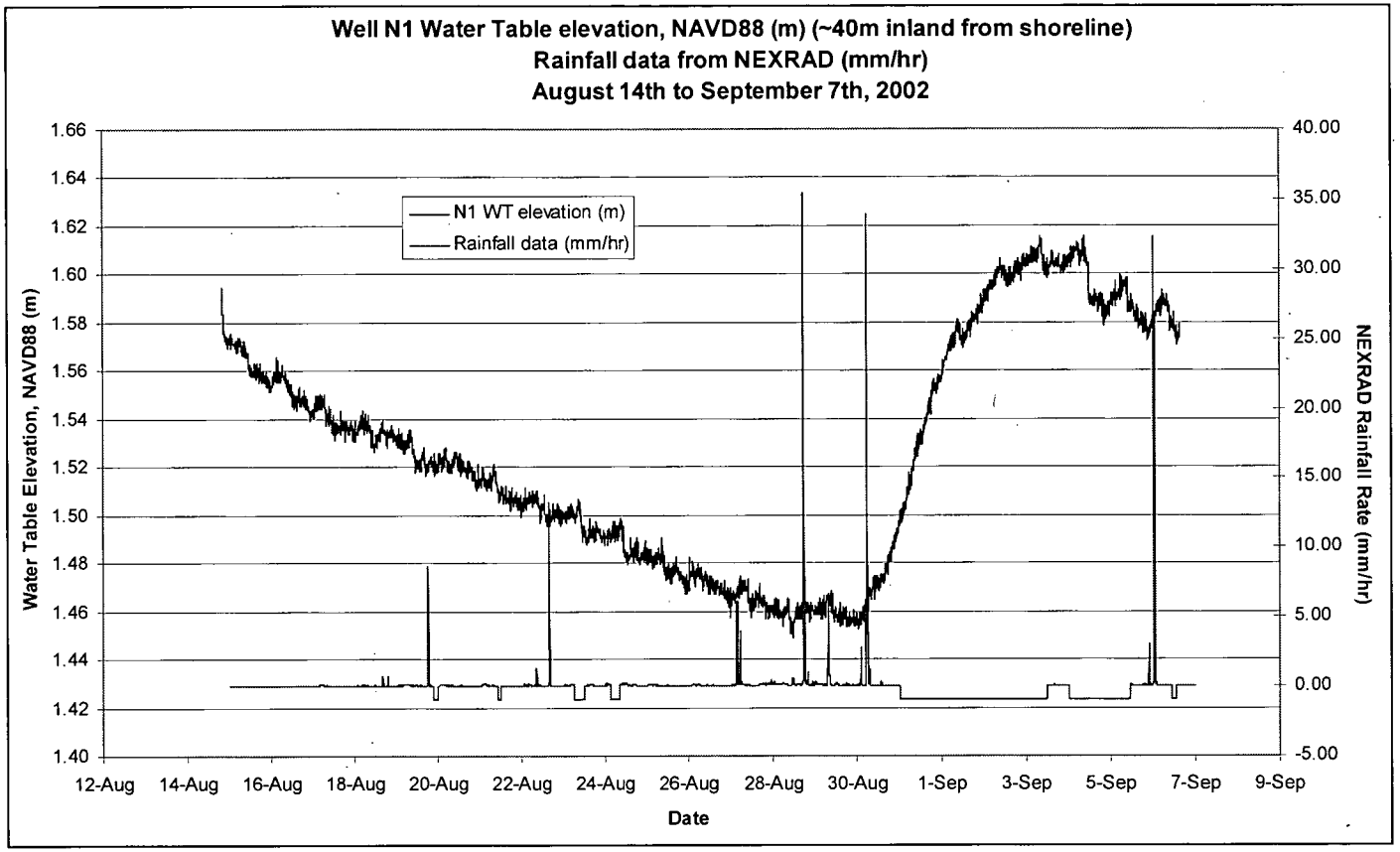

Figure 3-5. Well N1 Water Table Elevation and Rainfall Data

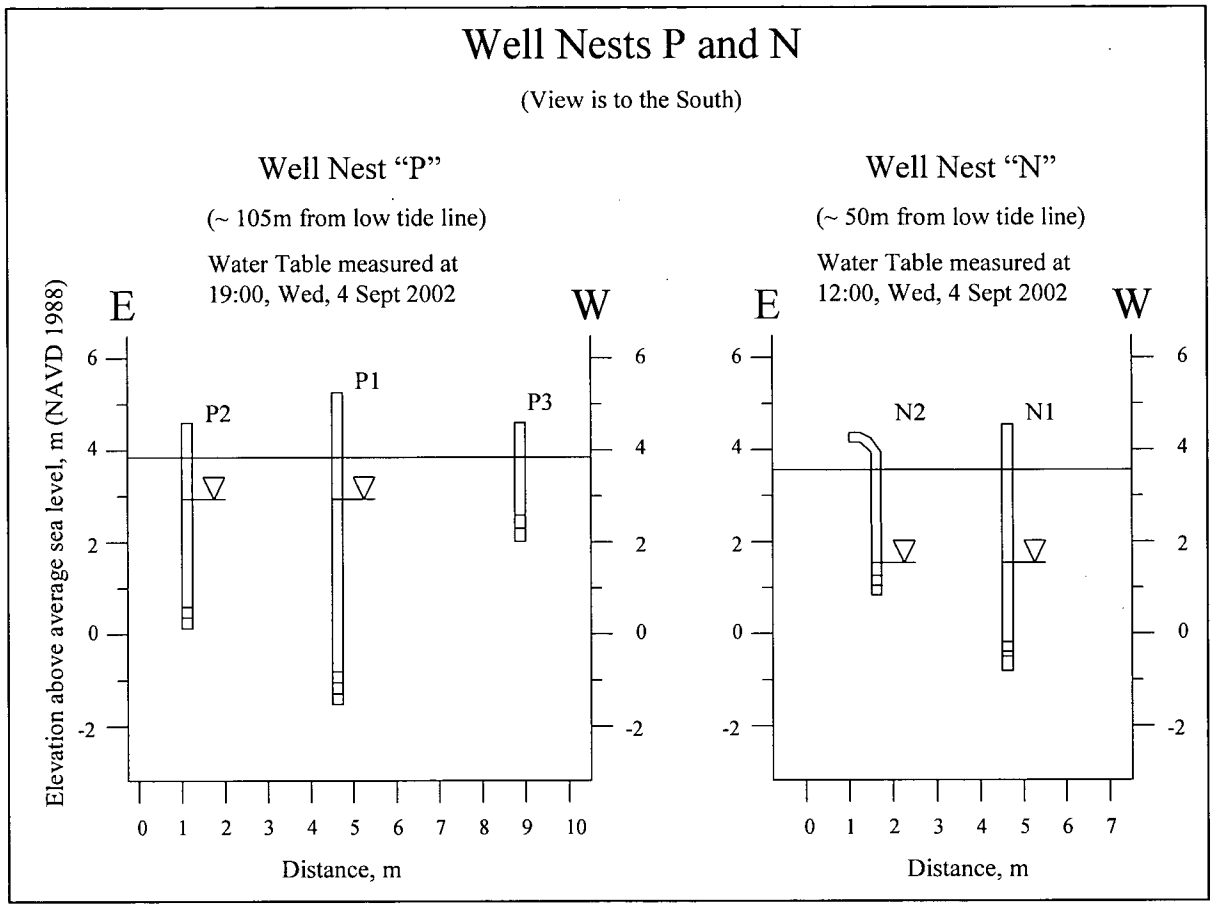

Figure 3-6. Wells Nest P and N with water table "snapshots"

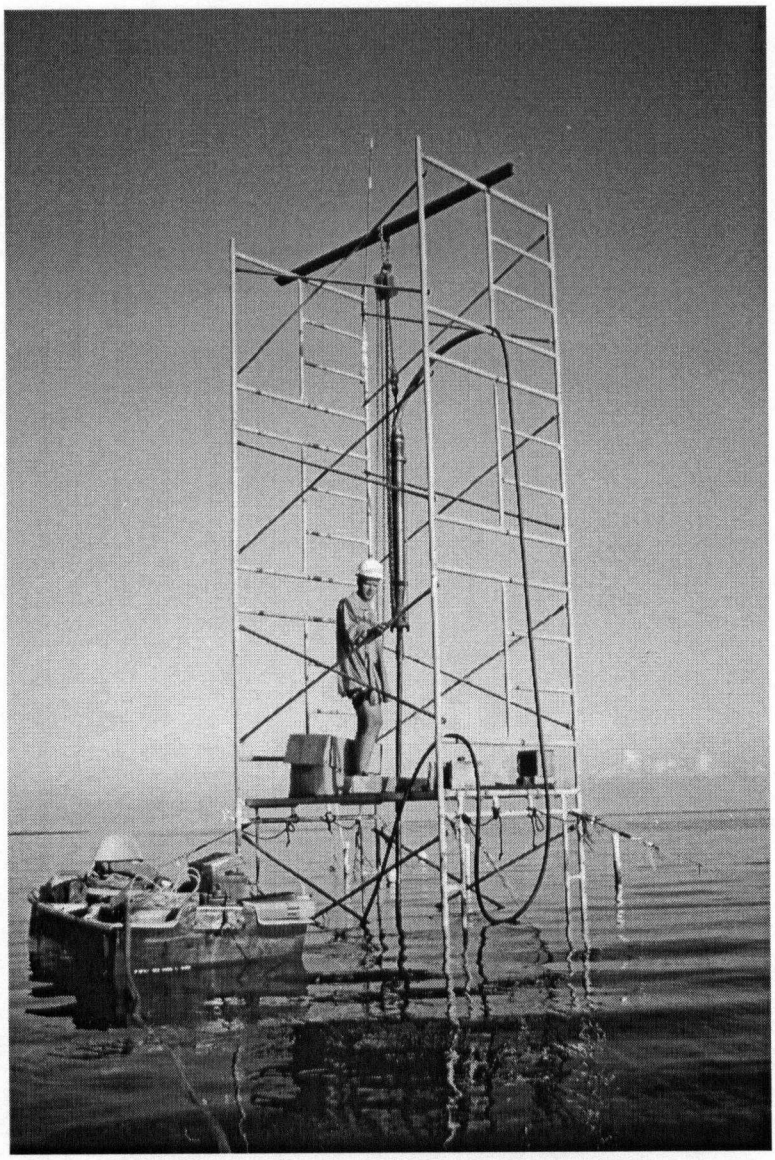

Figure 3-7. Waterloo Profiler sampling at offshore site (site 1). Note: Wells behind the scaffolding are those of BC-nest

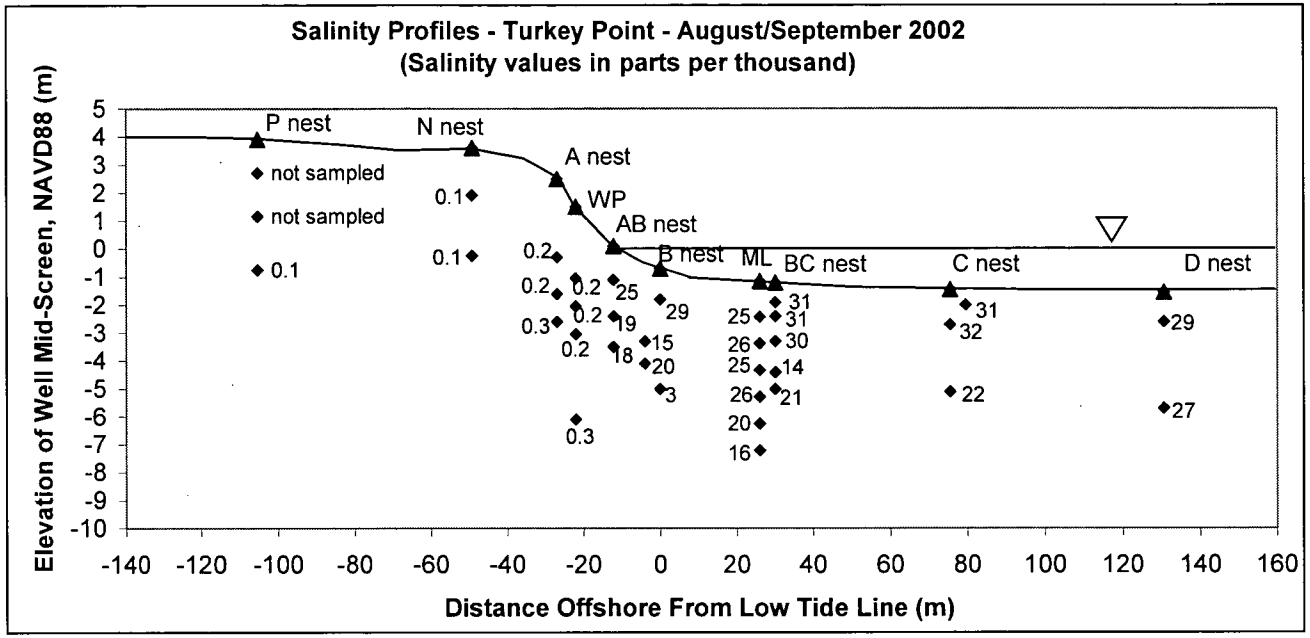

Figure 3-8. Salinity Profile with Depth – August/September 2002

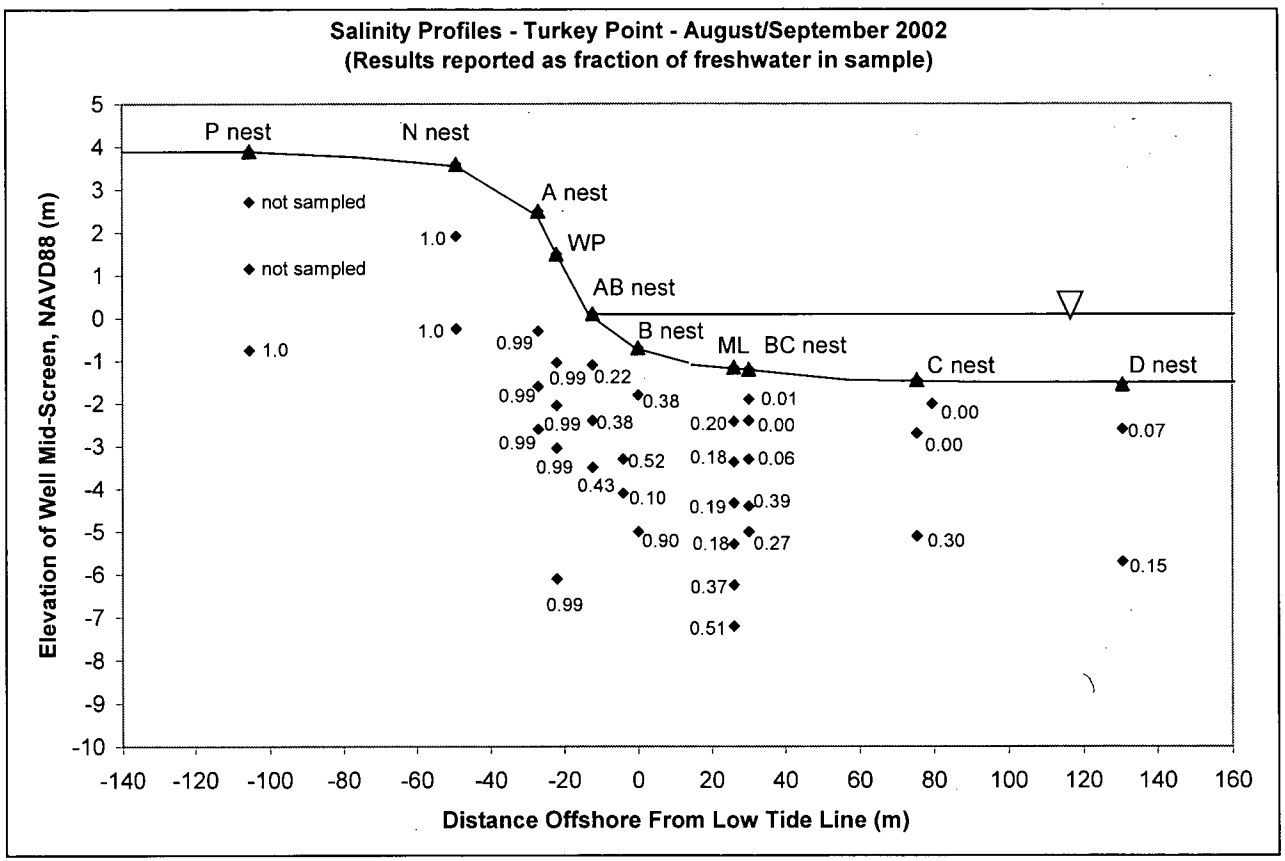

Figure 3-9. Salinity Profile as Percent Freshwater – August/September 2002

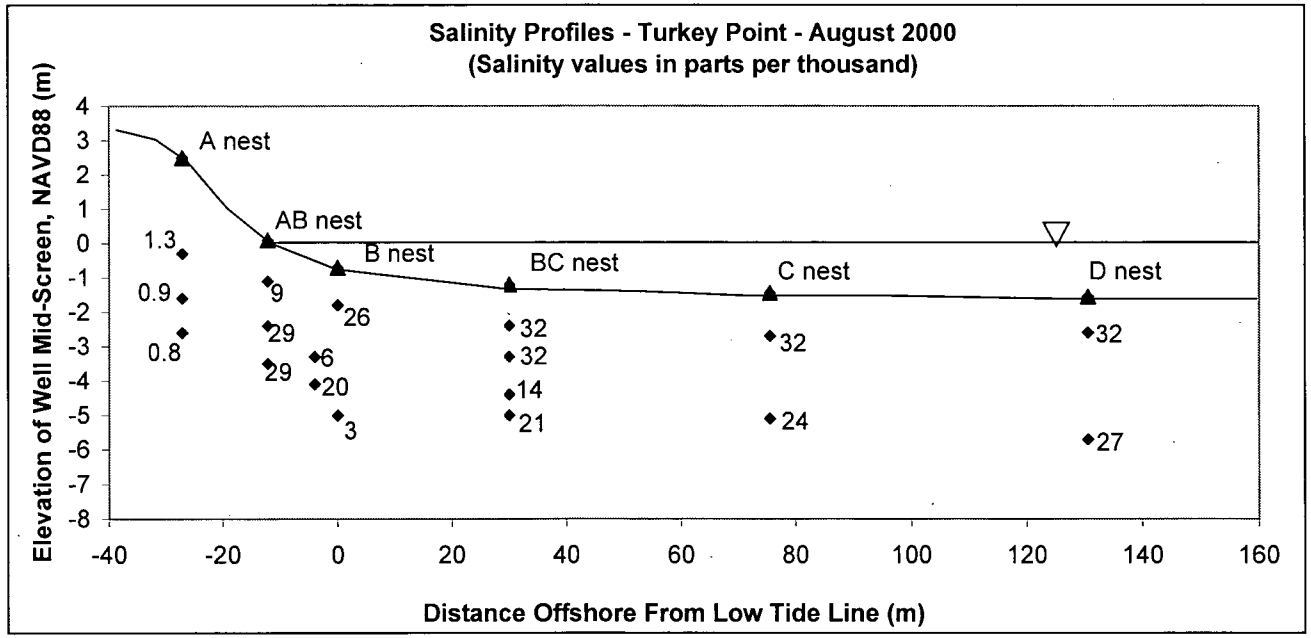

Figure 3-10. Salinity Profile with Depth – August/September 2000

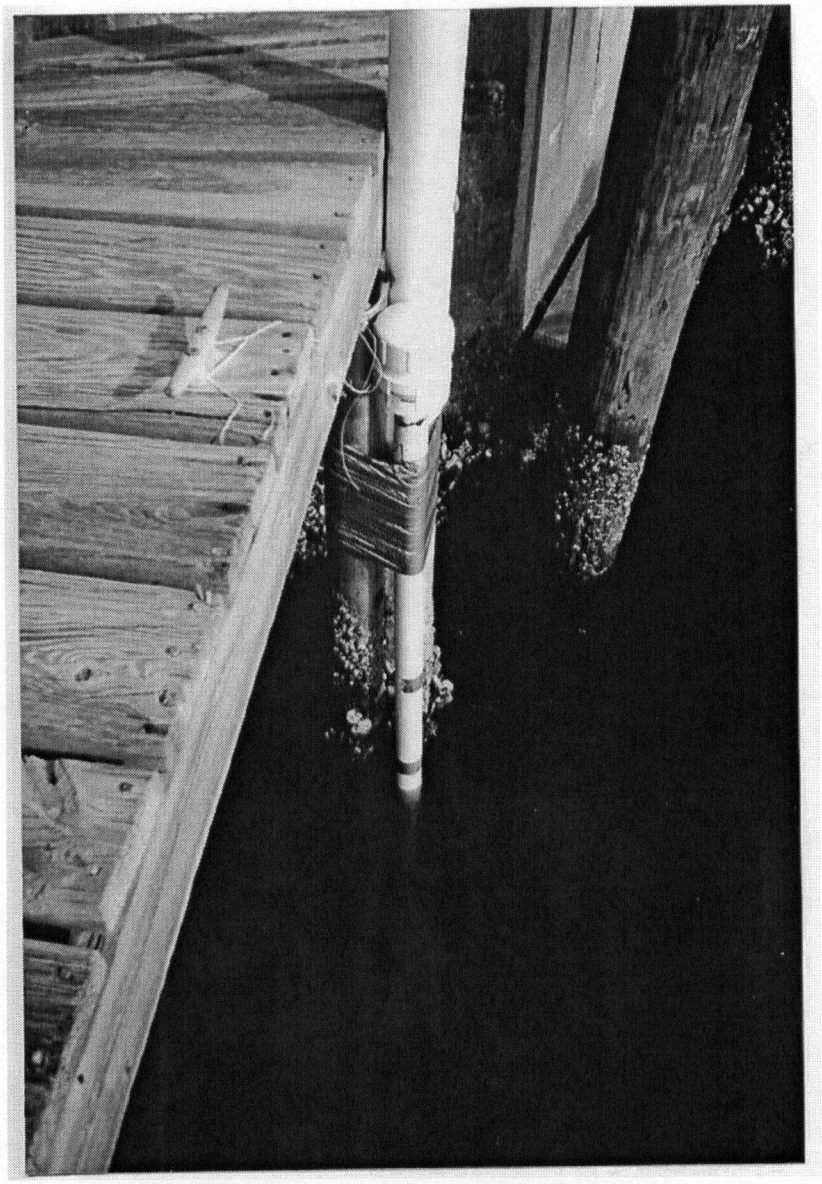

Figure 3-11. Tide Meter

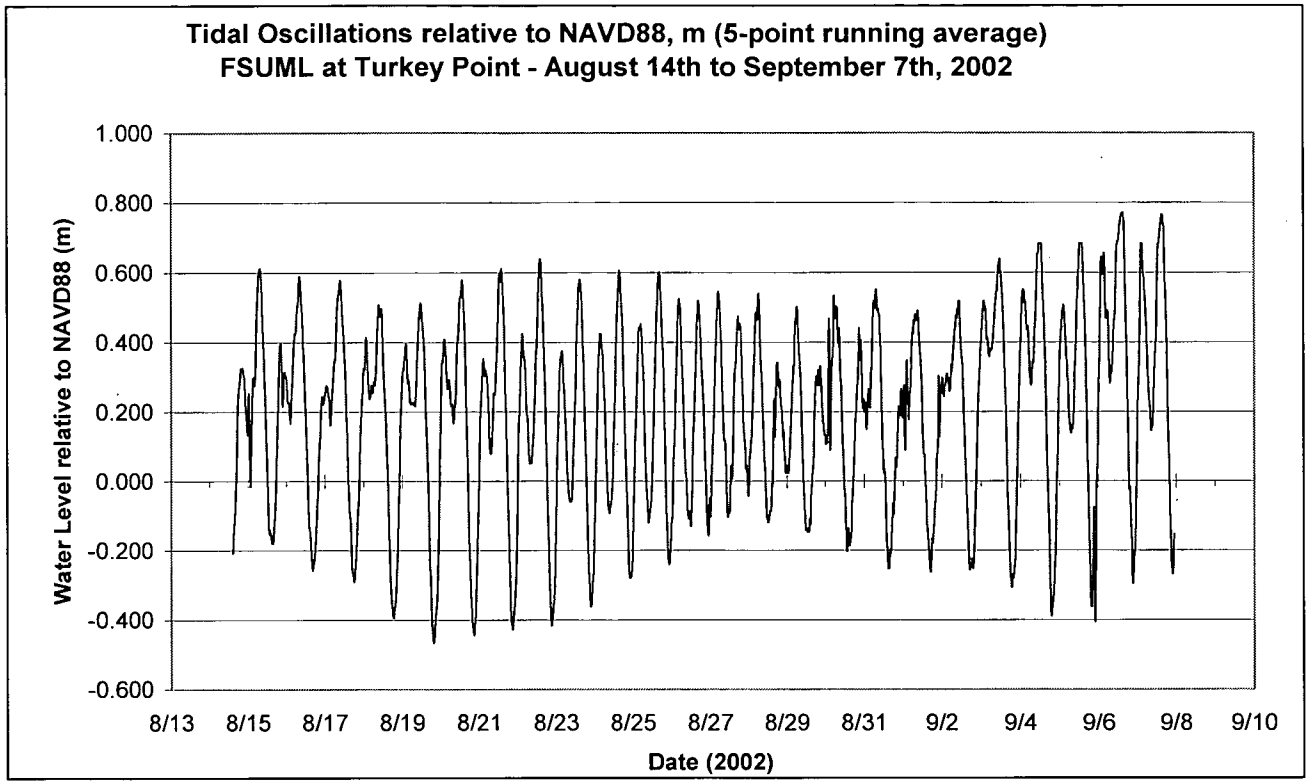

Figure 3-12. Tidal Oscillations at FSUML

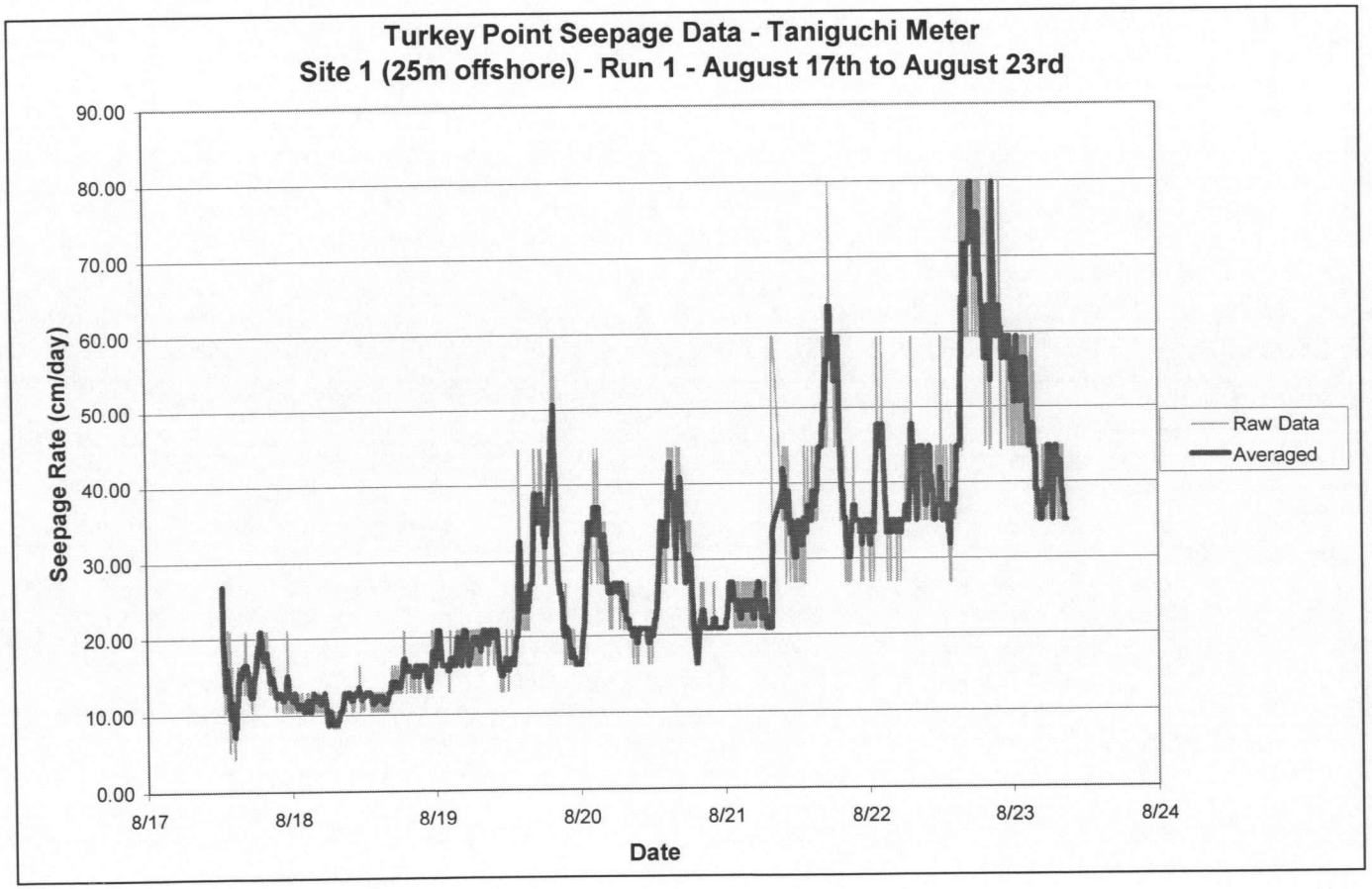

Figure 3-13. Seepage Rate for Run 1 at Site 1

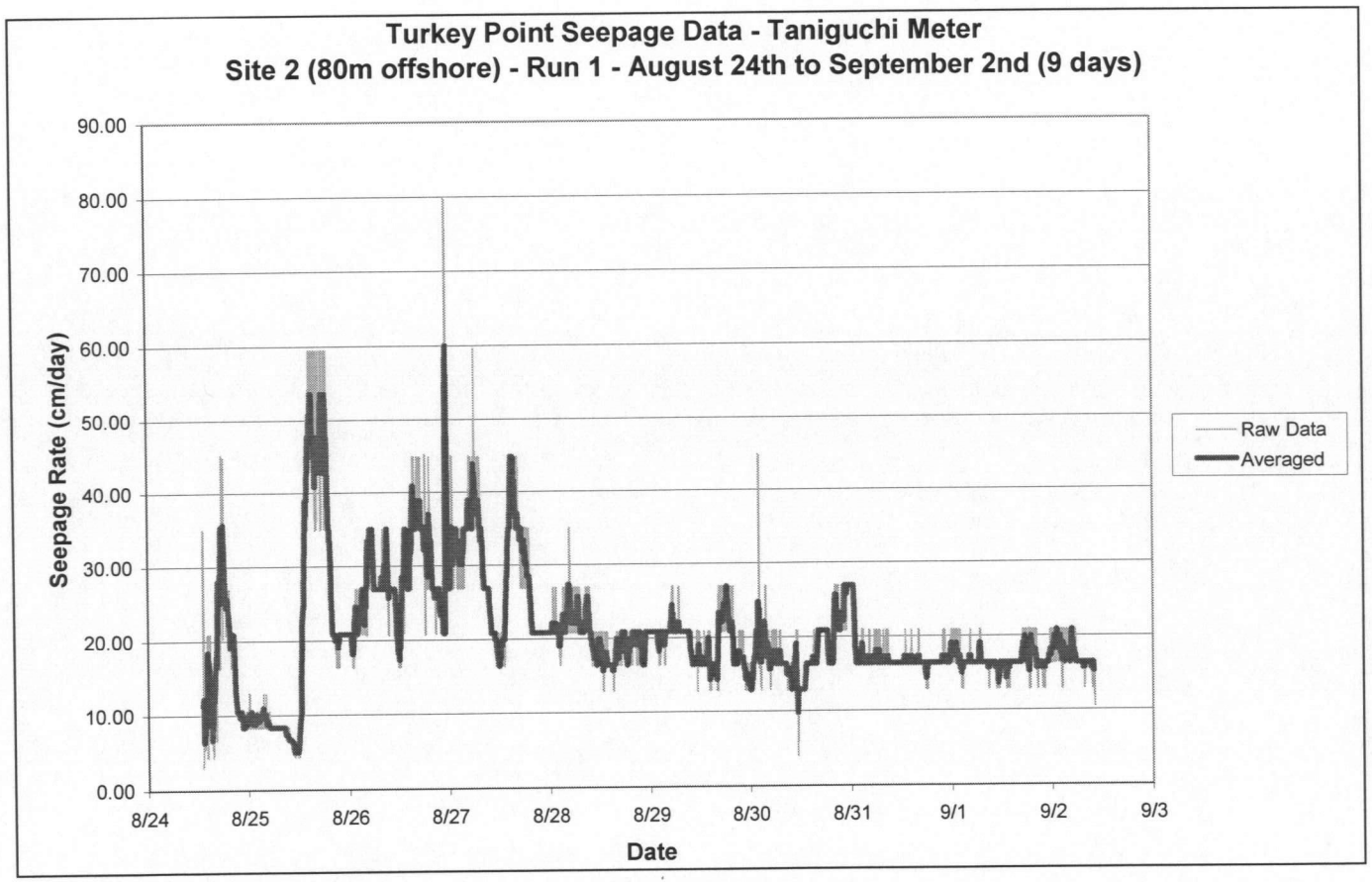

Figure 3-14. Seepage Rate (cm/day) for Run 1 at Site 2

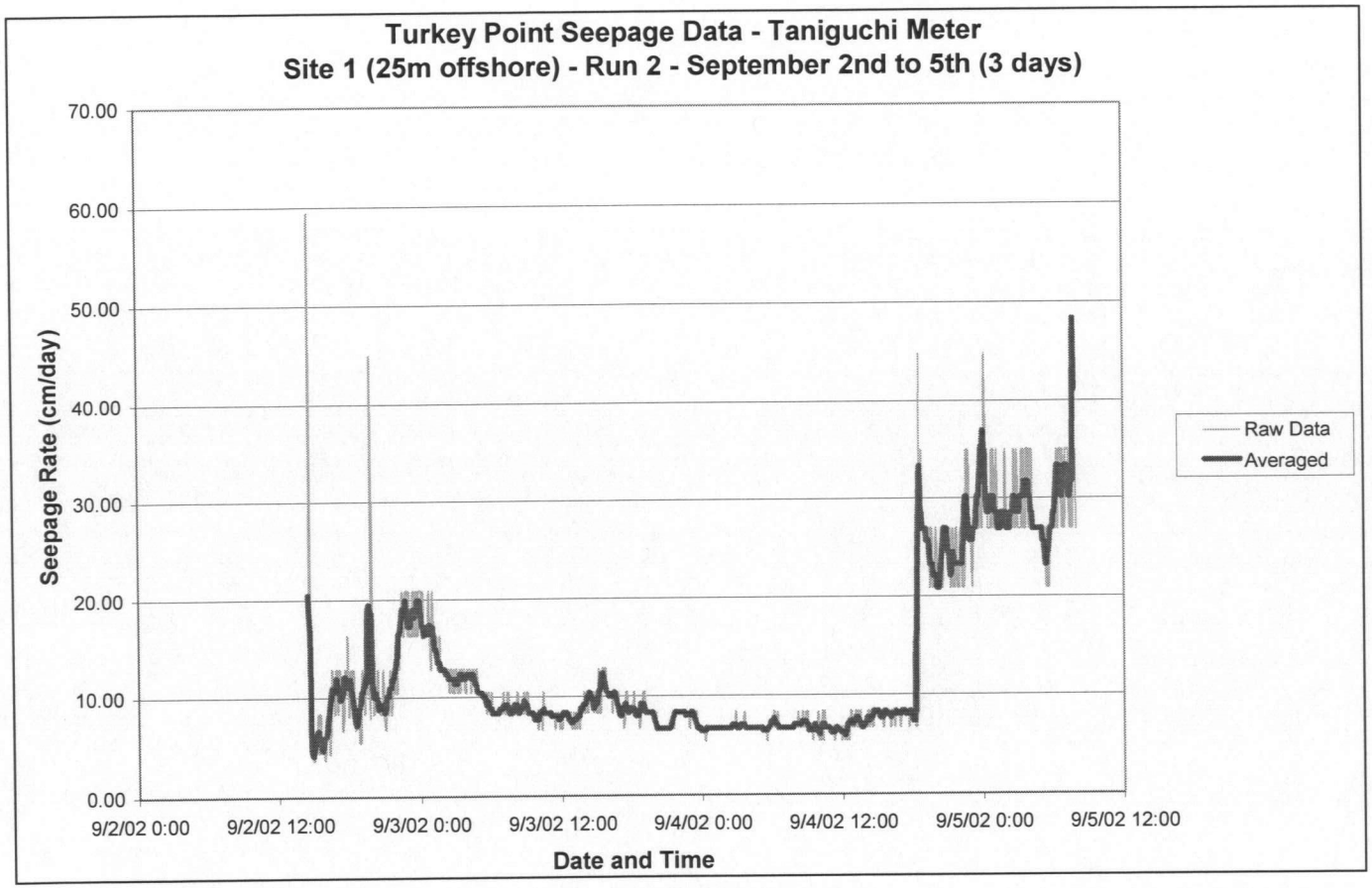

Figure 3-15. Seepage Rate (cm/day) for Run 2 at Site 1

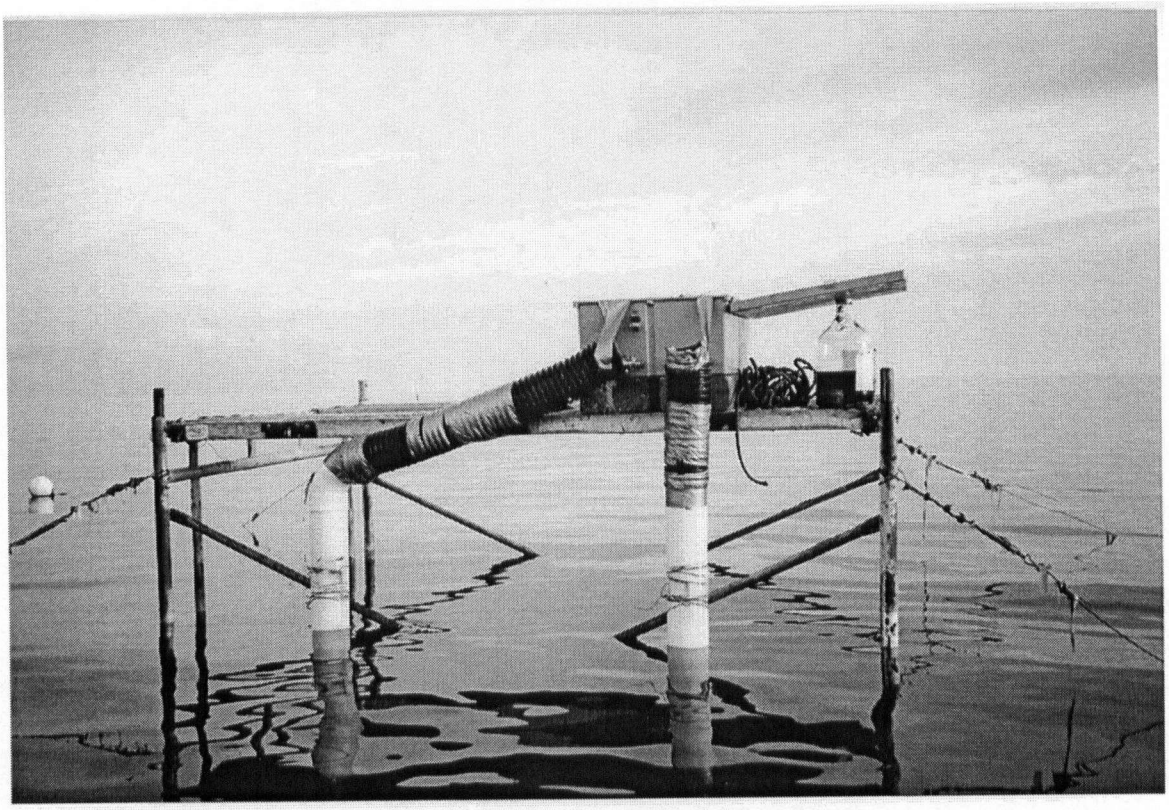

Figure 3-16. Photograph of DPS at Site 2

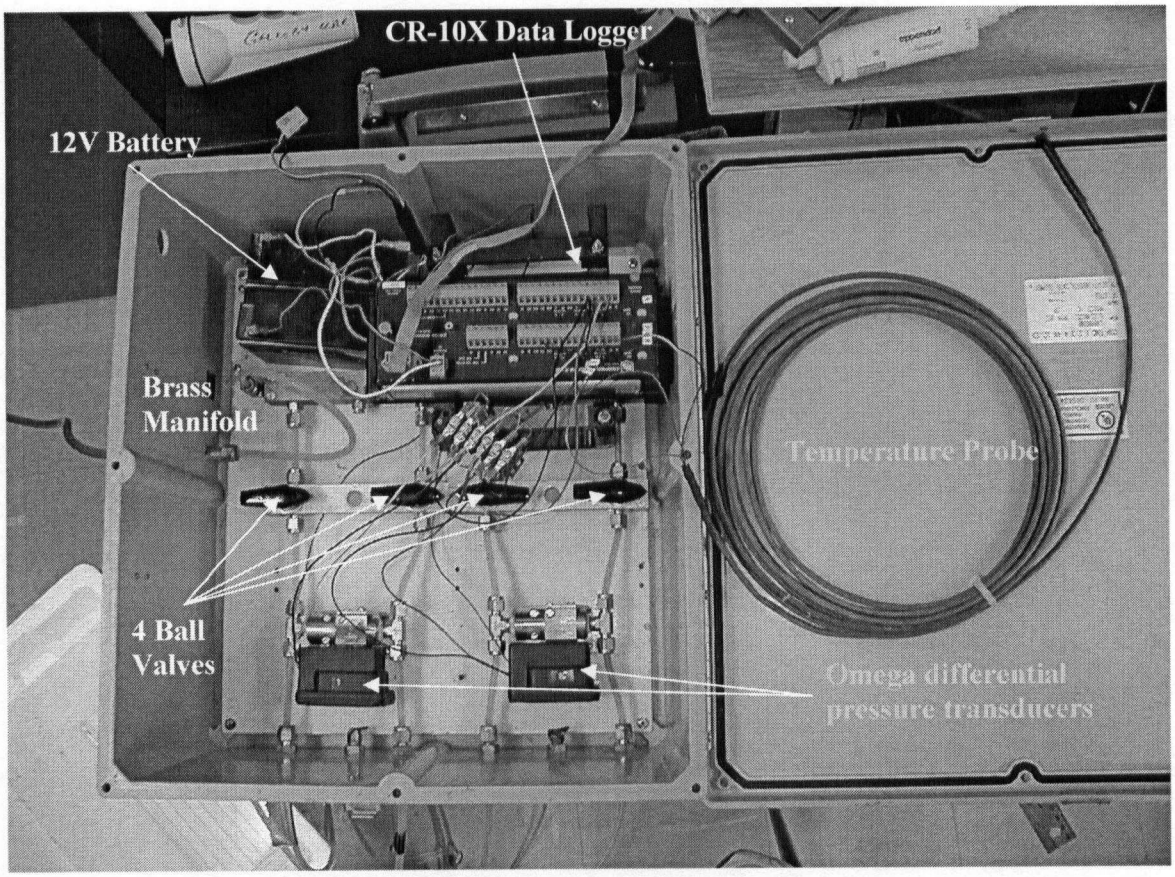

Figure 3-17. Inside the DPS Box

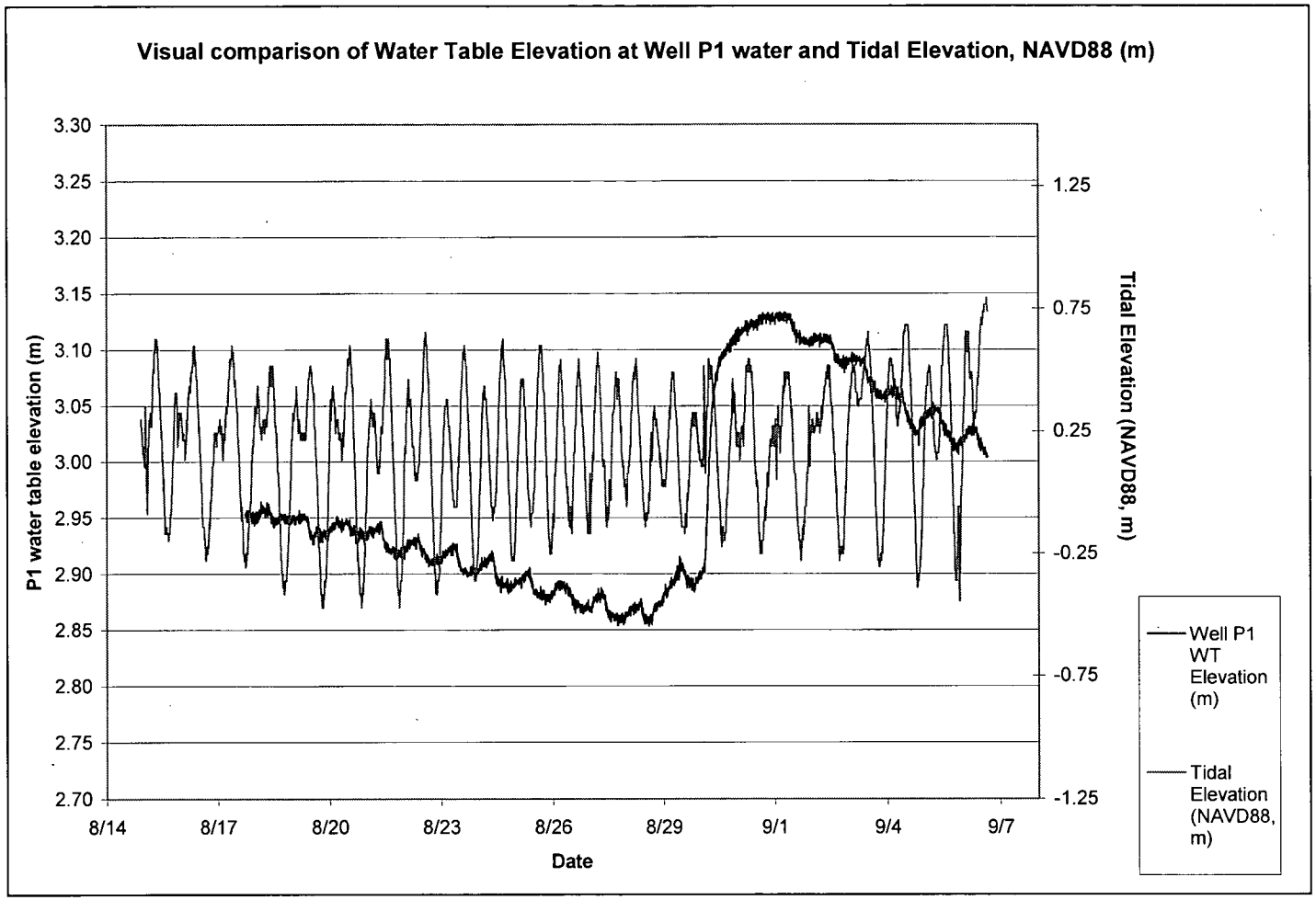

Figure 3-18. Tidal Fluctuations at Well P1

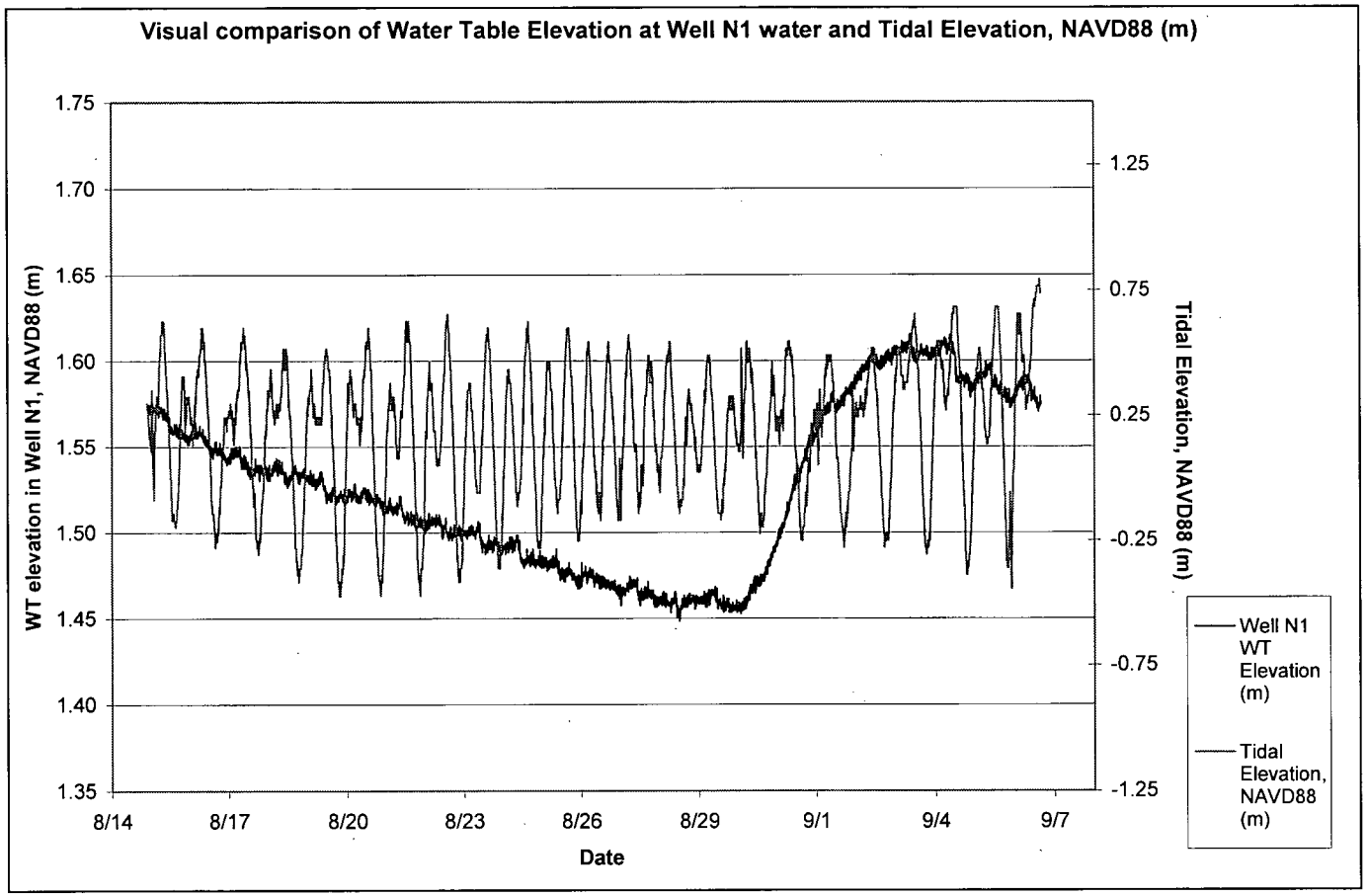

Figure 3-19. Tidal Fluctuations at Well N1

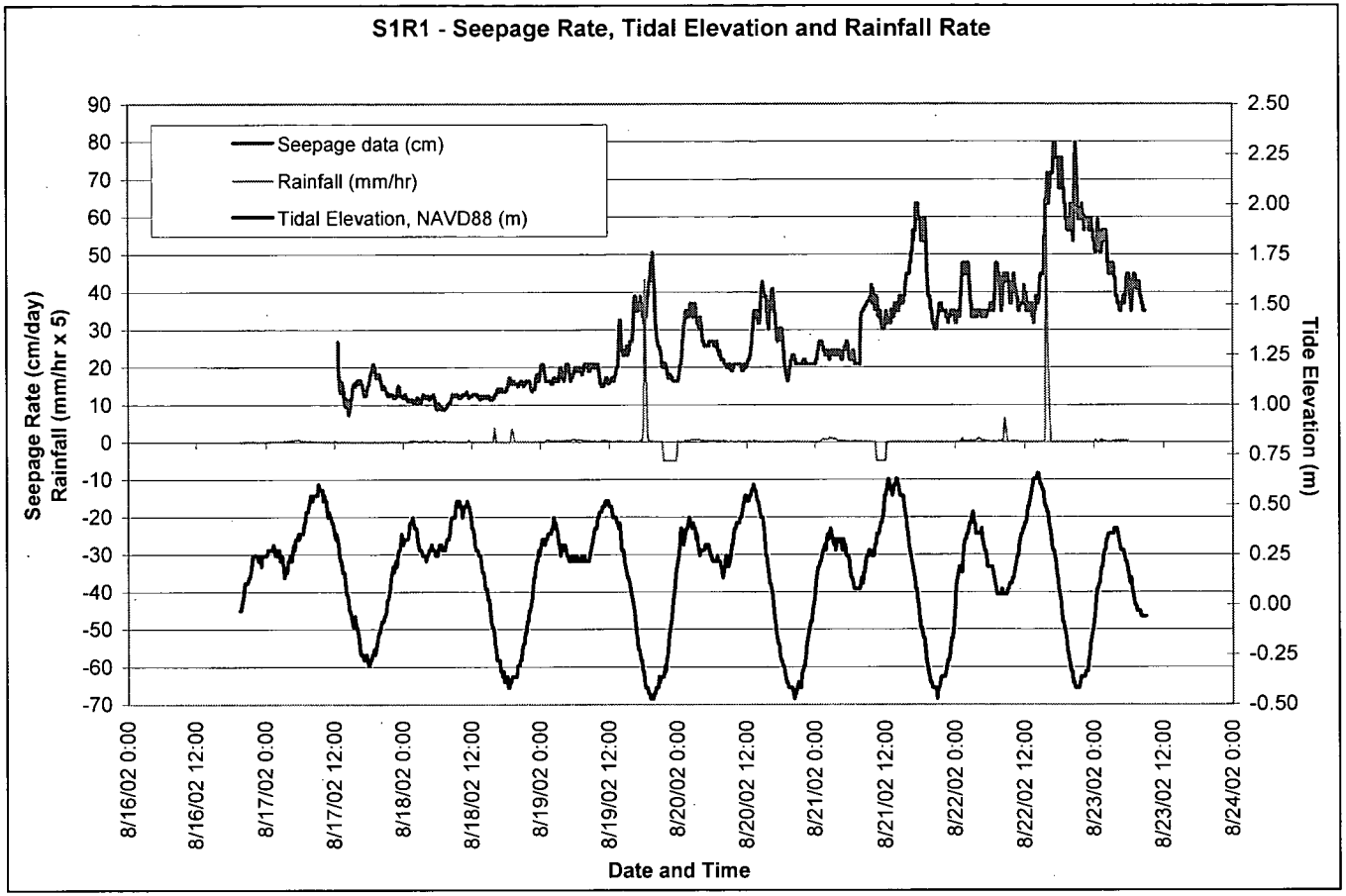

Figure 3-20. Seepage Rate, Tidal Elevation and Rainfall Rate during S1R1

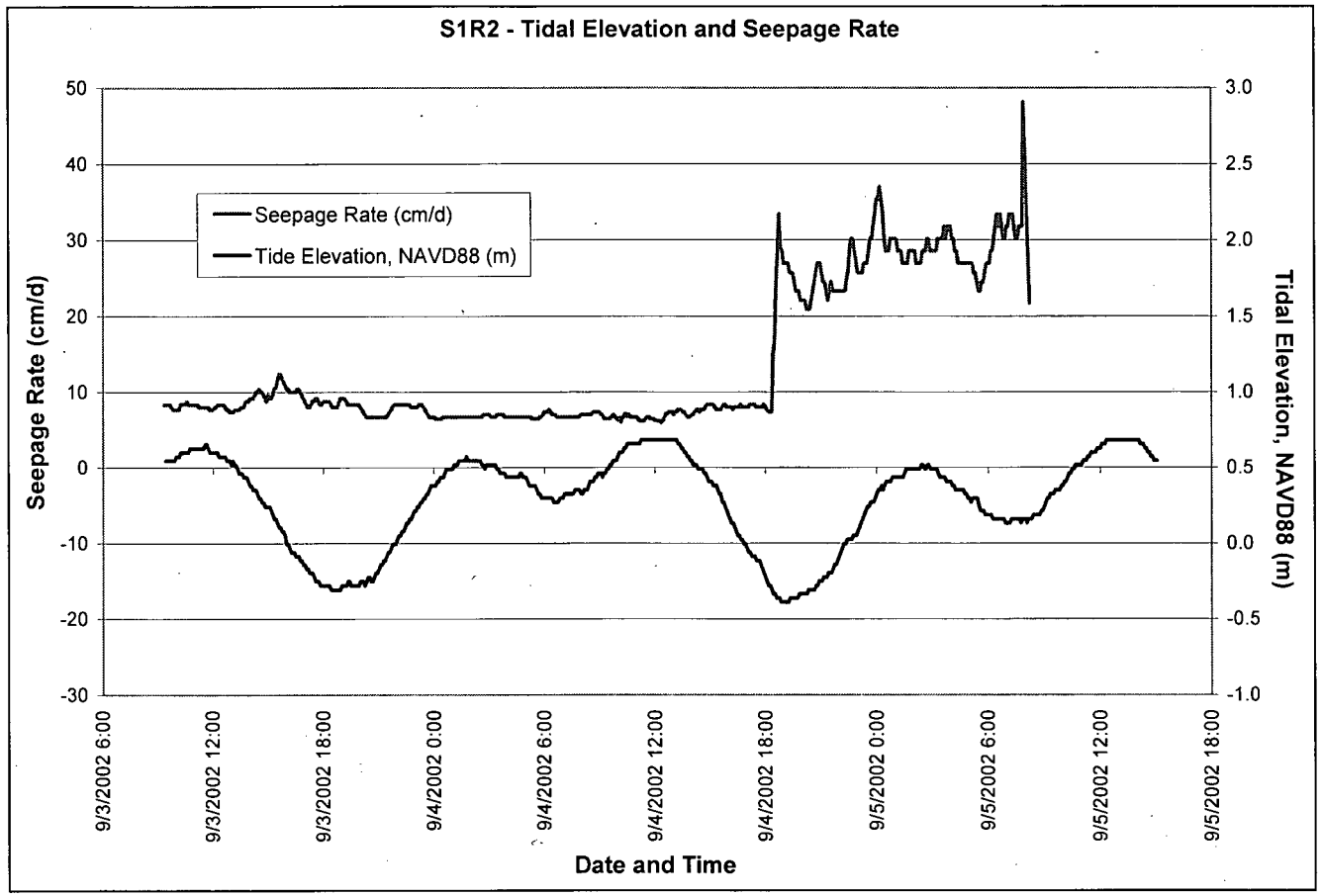

Figure 3-21. Tidal Elevation and Seepage Rate for S1R2. No significant rainfall was recorded.

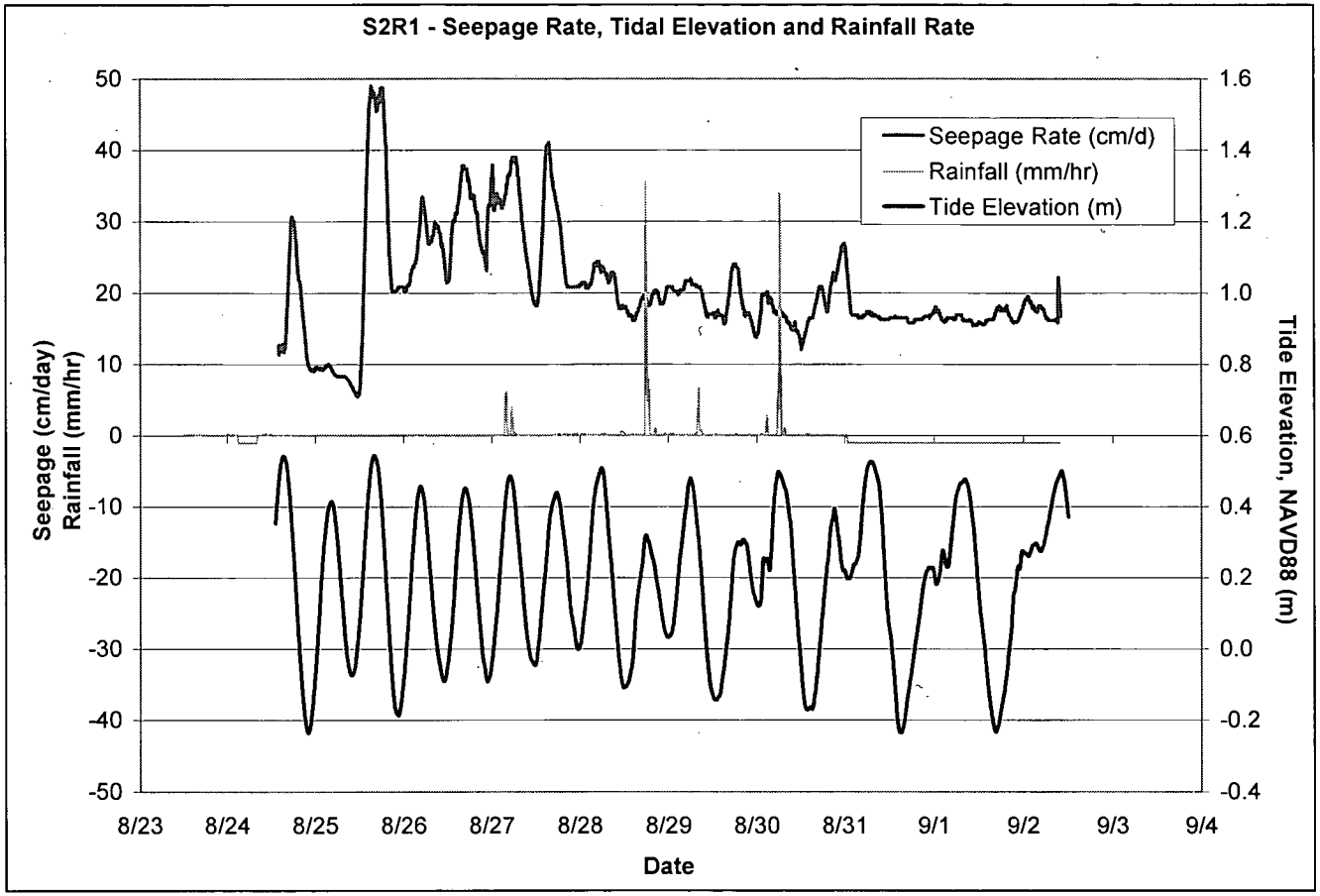

Figure 3-22. Seepage Rate, Tidal Elevation and Rainfall Rate during S2R1

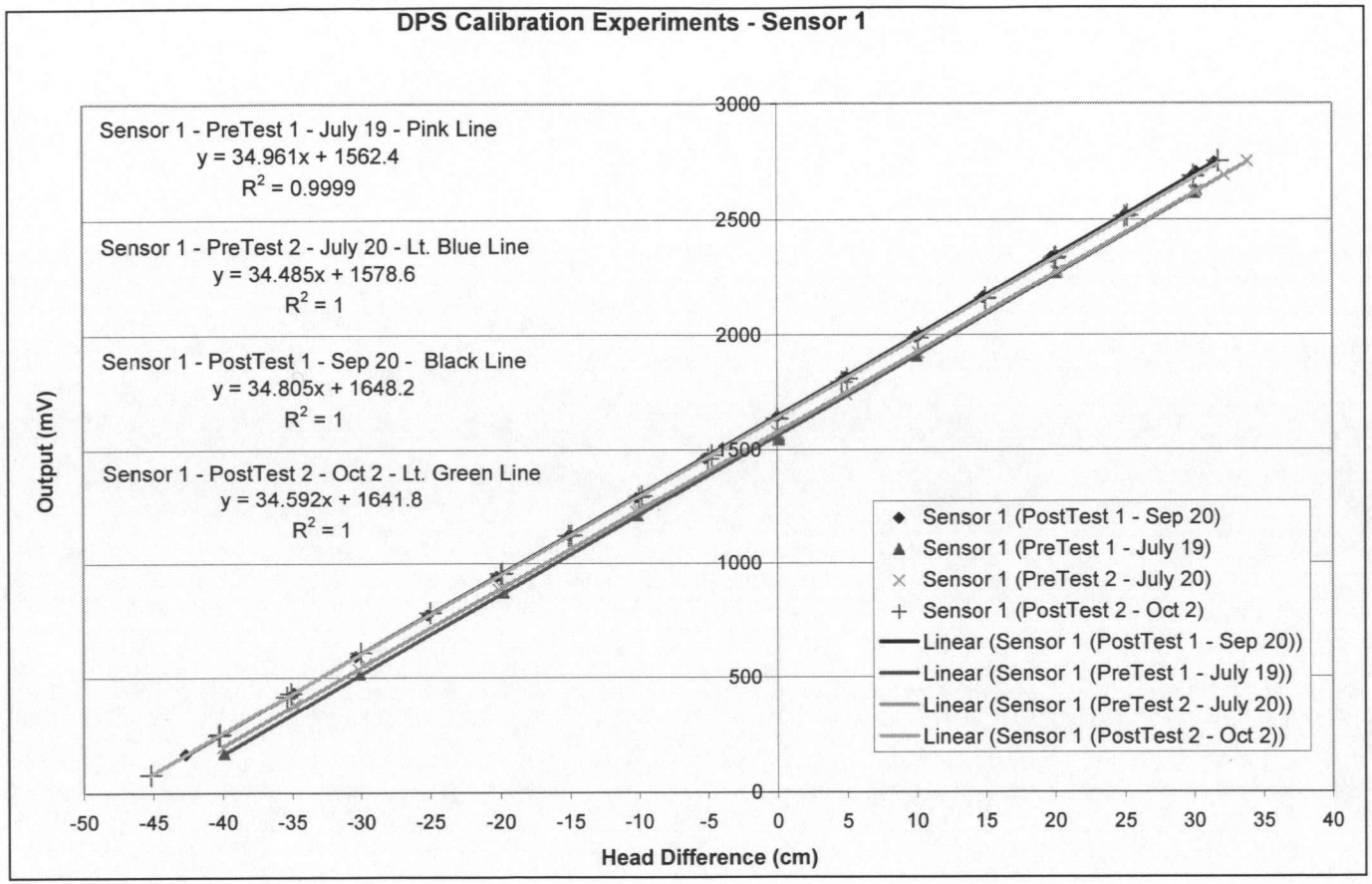

Figure 3-23. DPS Calibration Experiments for Sensor 1

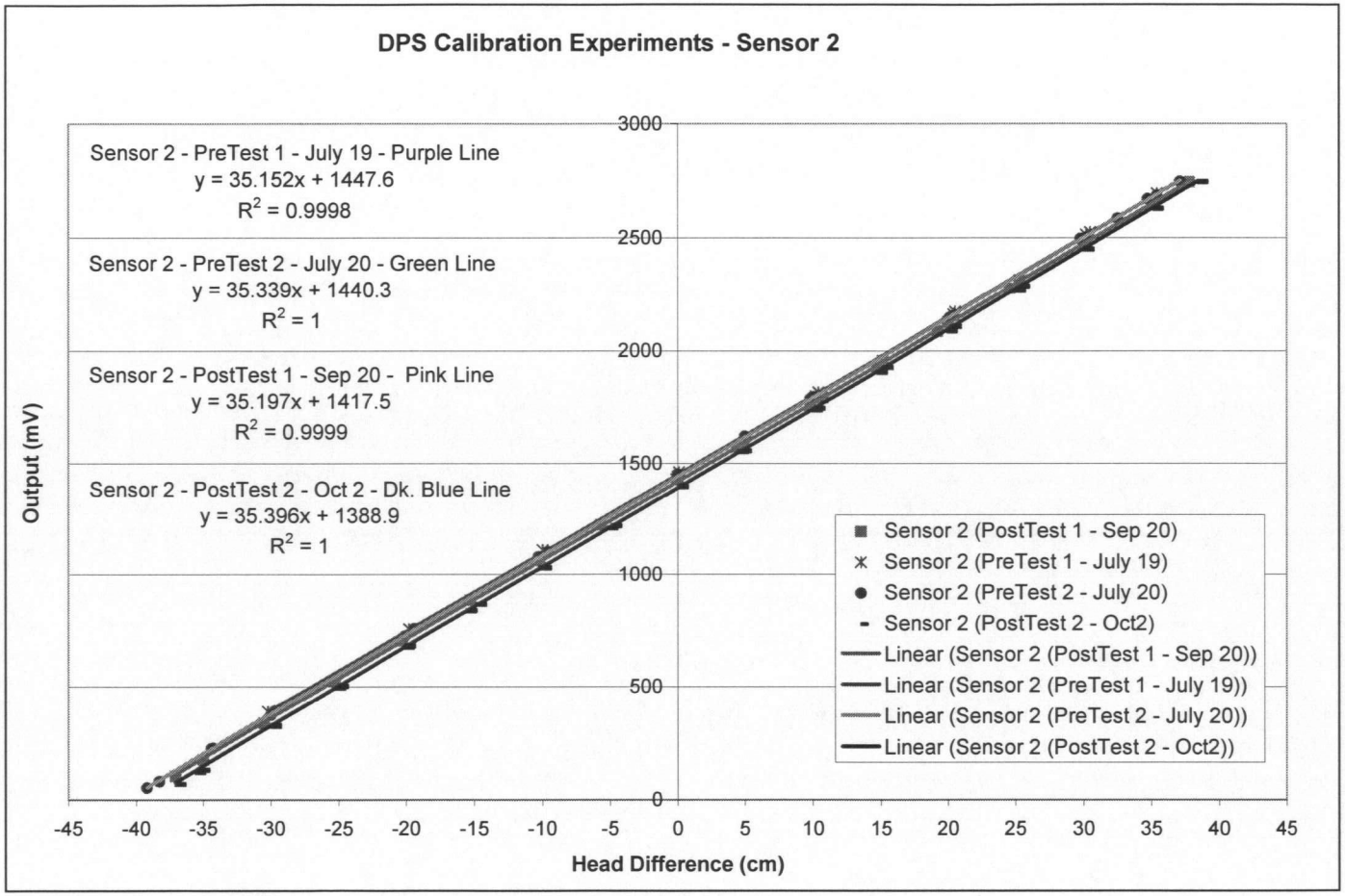

Figure 3-24. DPS Calibration Experiments for Sensor 2

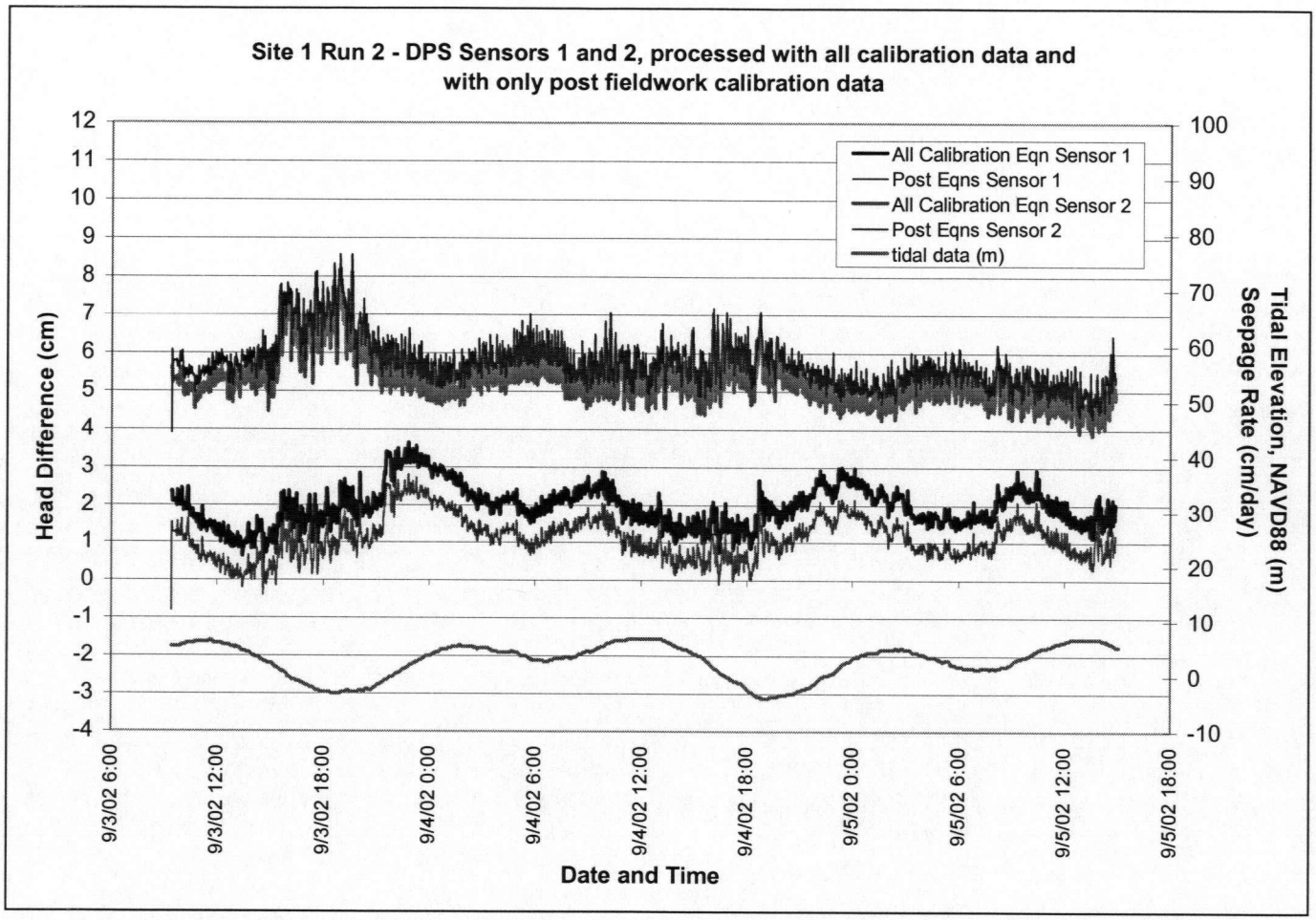

Figure 3-25. S1R2 – DPS Sensors 1 and 2 – Processed with all calibration data and Post field work calibration data. Data processed with post field work calibration is plotted with thicker lines.

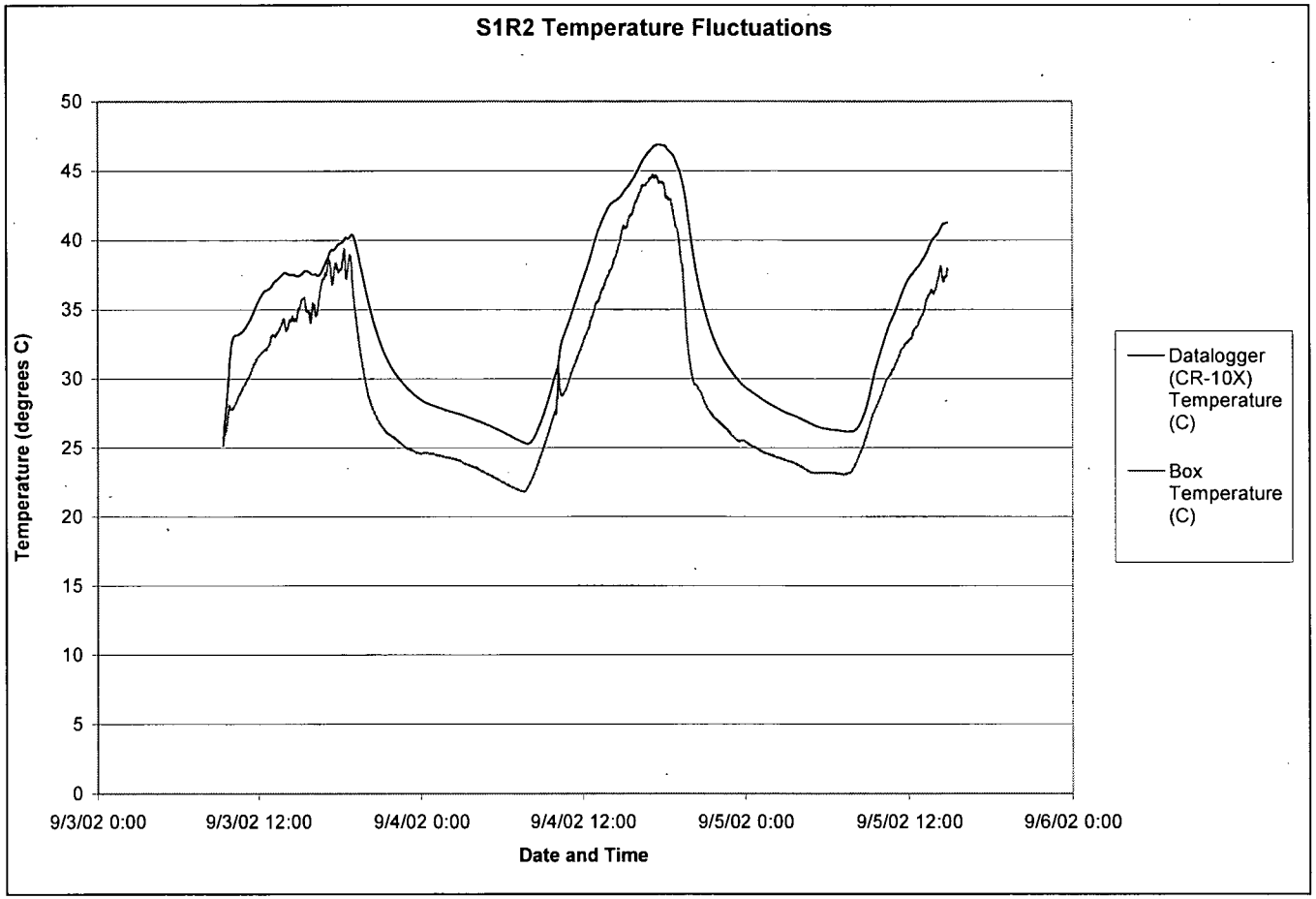

Figure 3-26. Temperature Range in DPS Box for S1R2

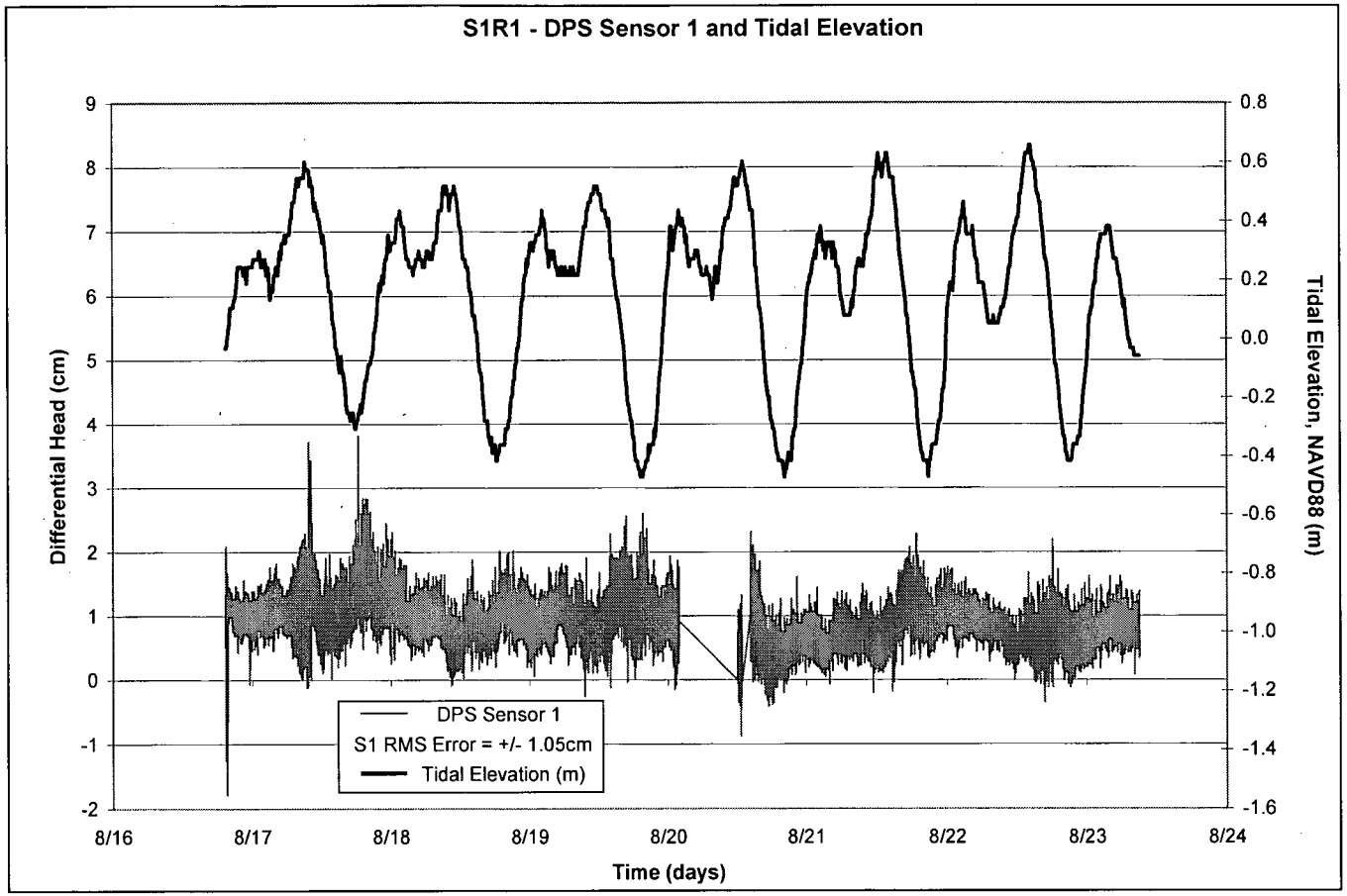

Figure 3-27. S1R1 – DPS Sensor 1 and Tidal Elevation

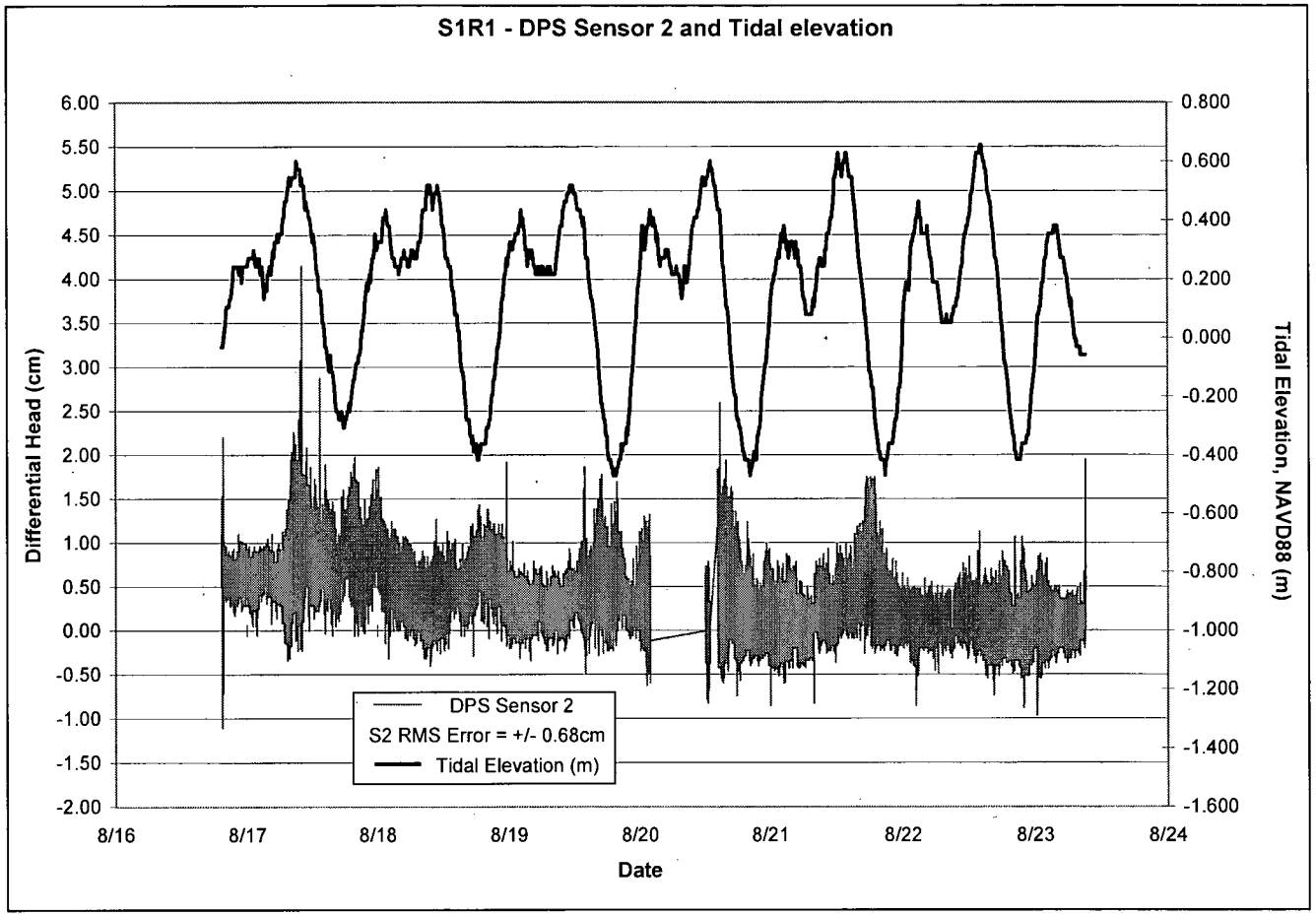

Figure 3-28. S1R1 – DPS Sensor 2 and Tidal Elevation

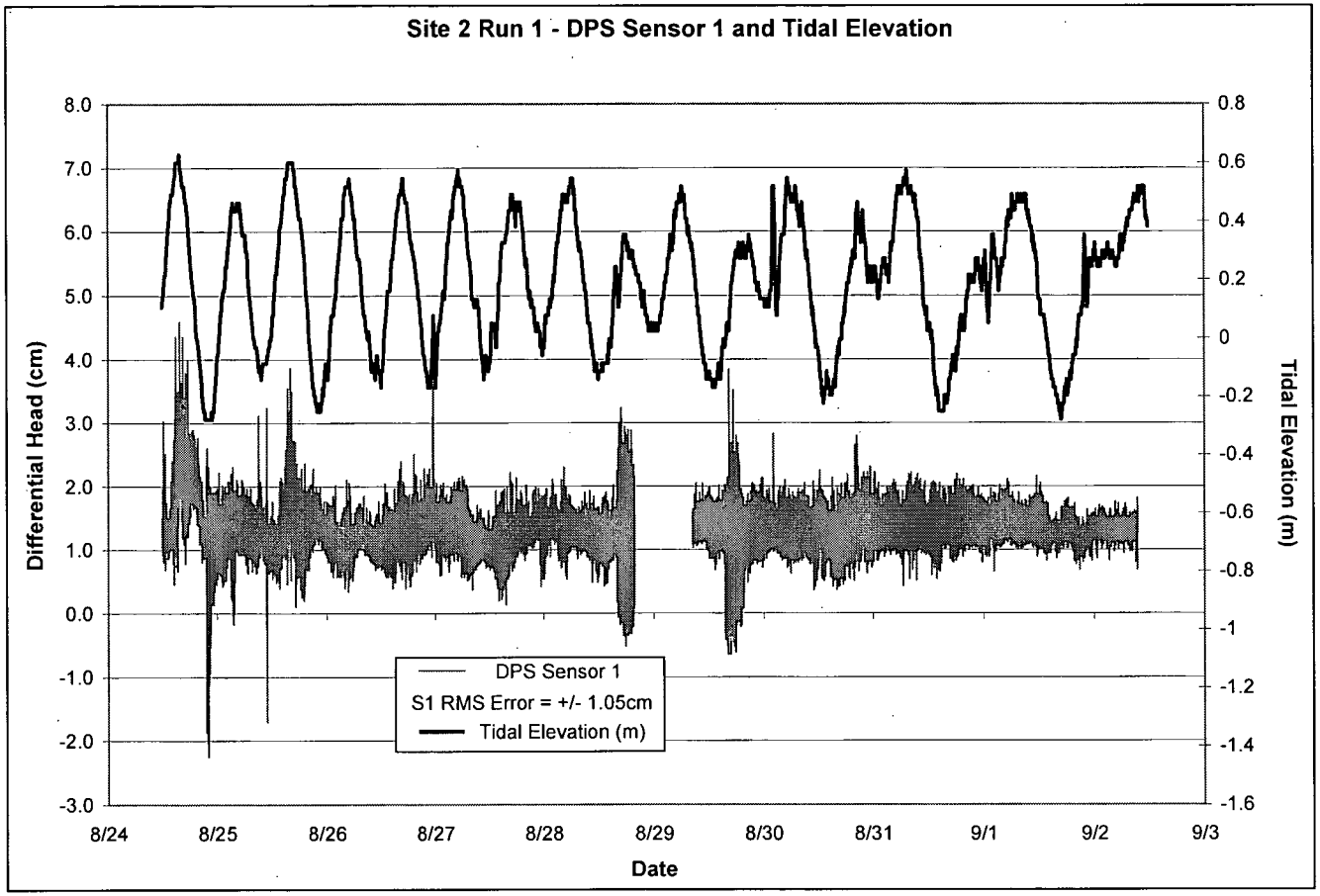

Figure 3-29. S2R1 – DPS Sensor 1 and Tidal Elevation

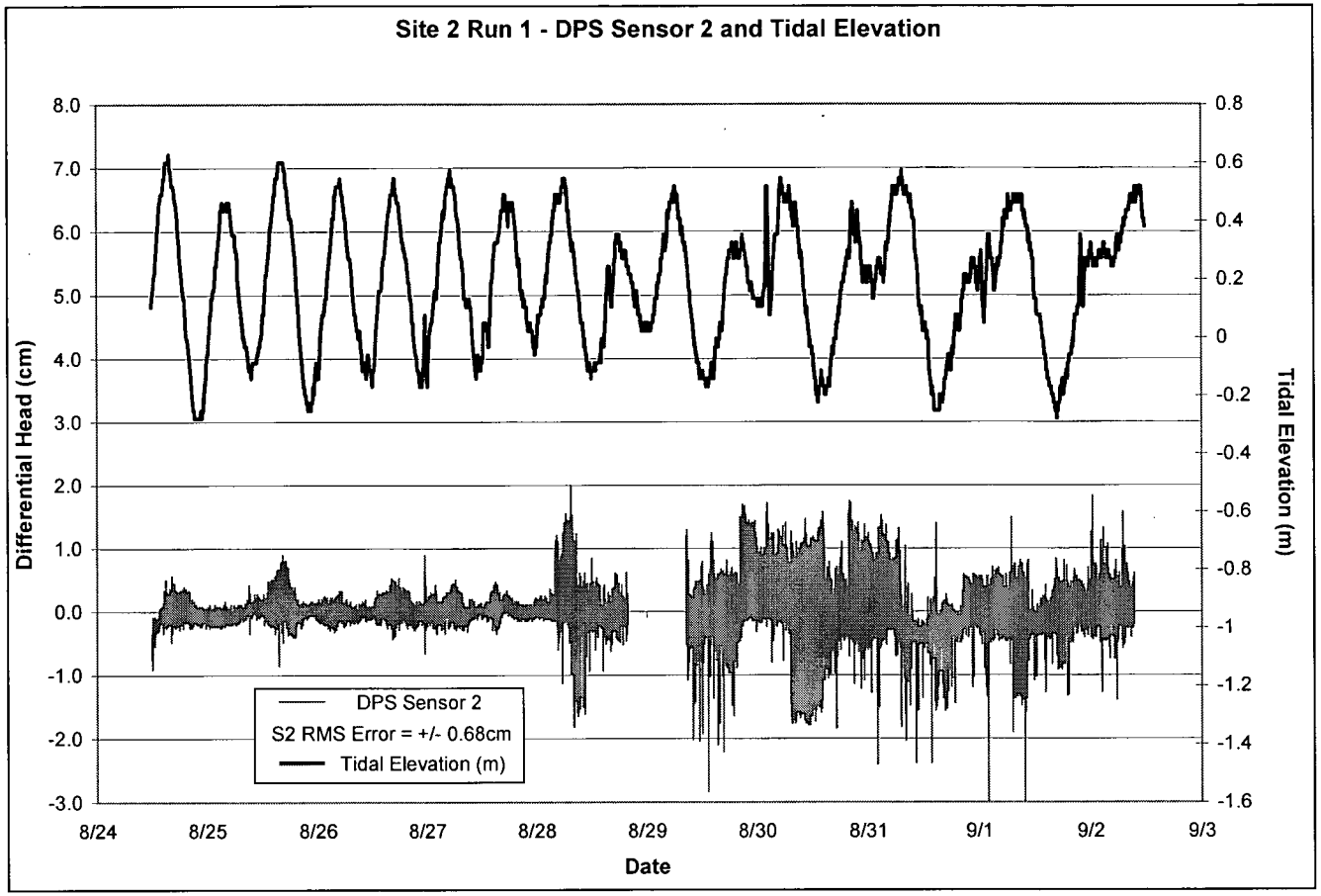

Figure 3-30. S2R1 – DPS Sensor 2 and Tidal Elevation

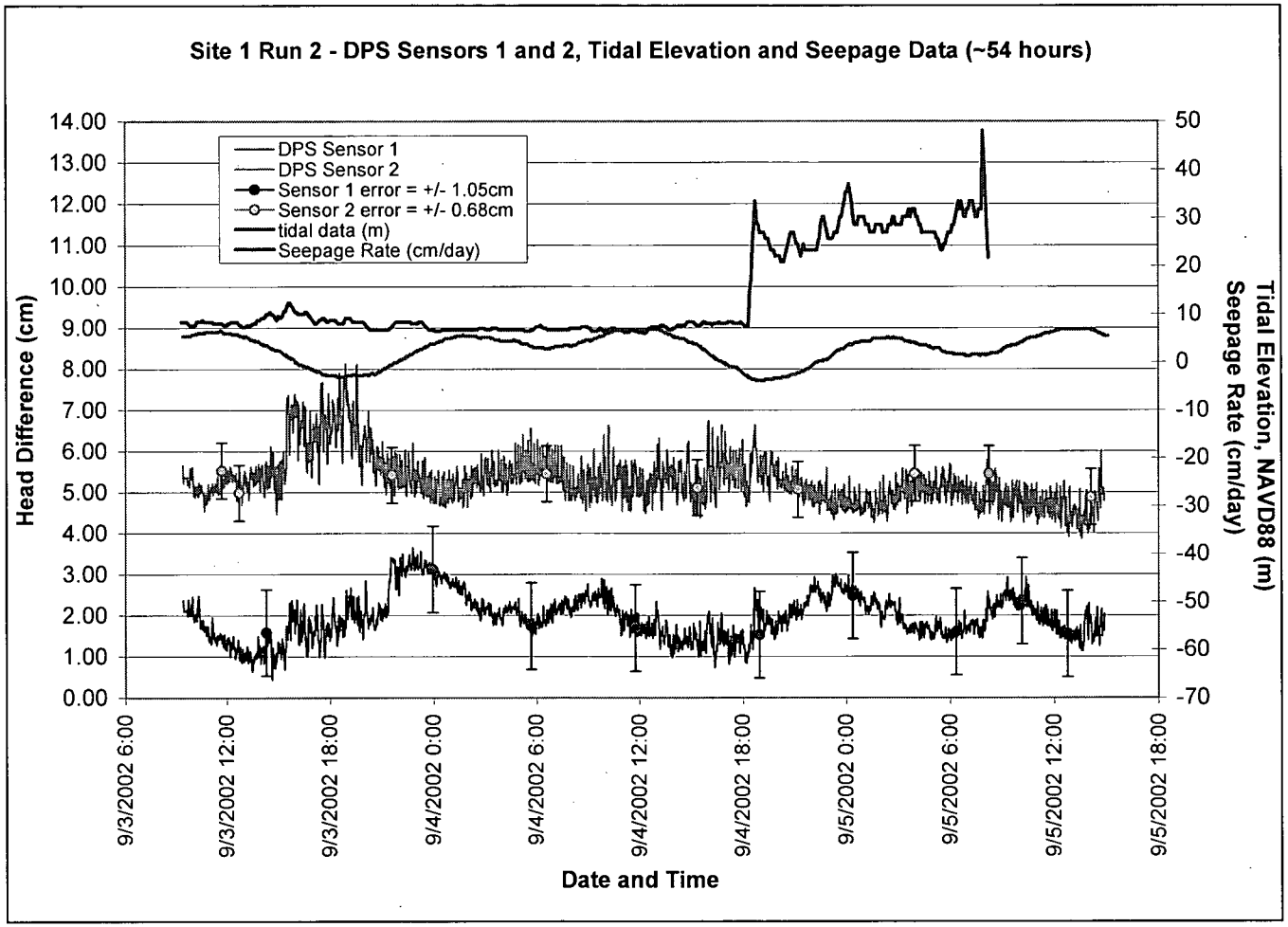

Figure 3-31. S1R2 – DPS Sensors 1 and 2 and Tidal Elevation

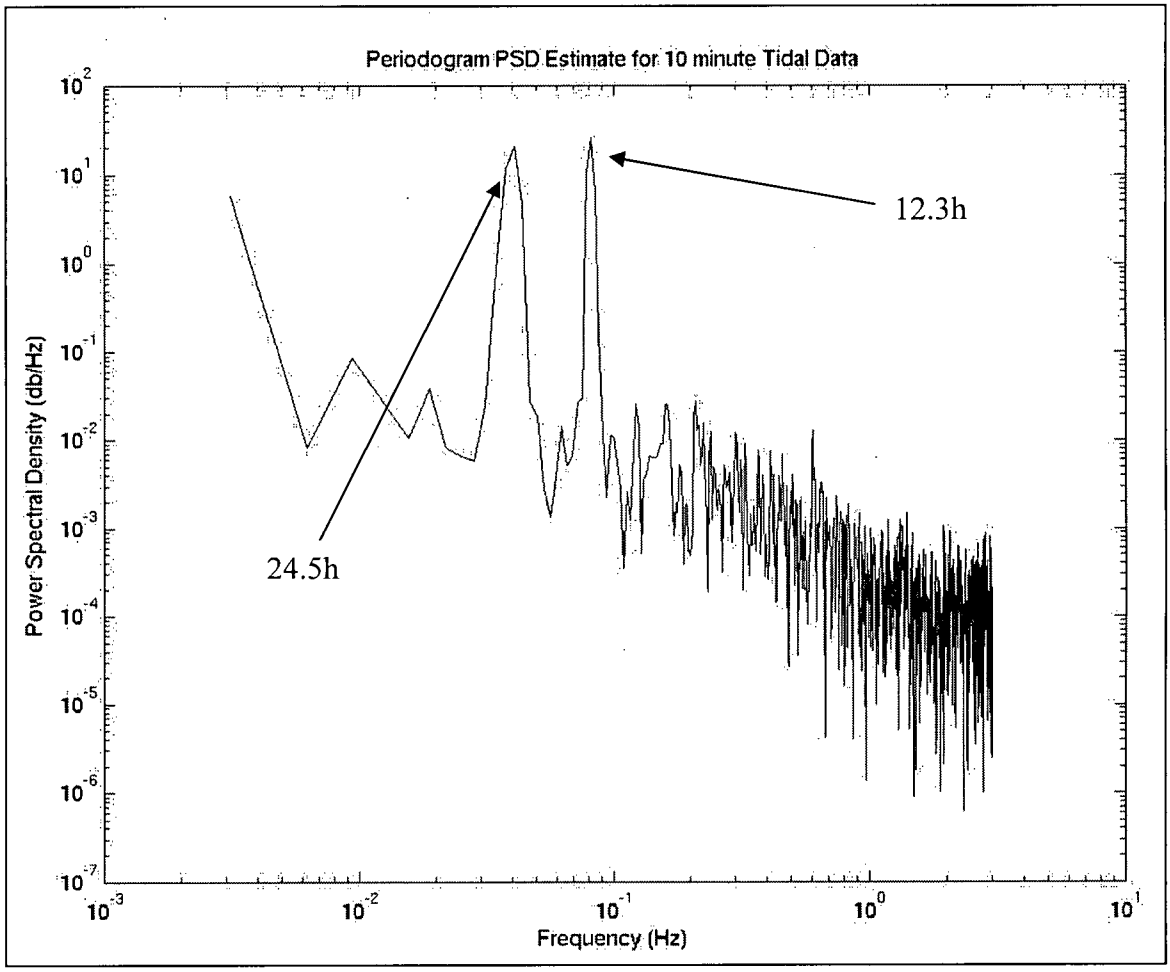

Figure 3-32. Periodogram for Tidal Data with 10 minute sampling frequency

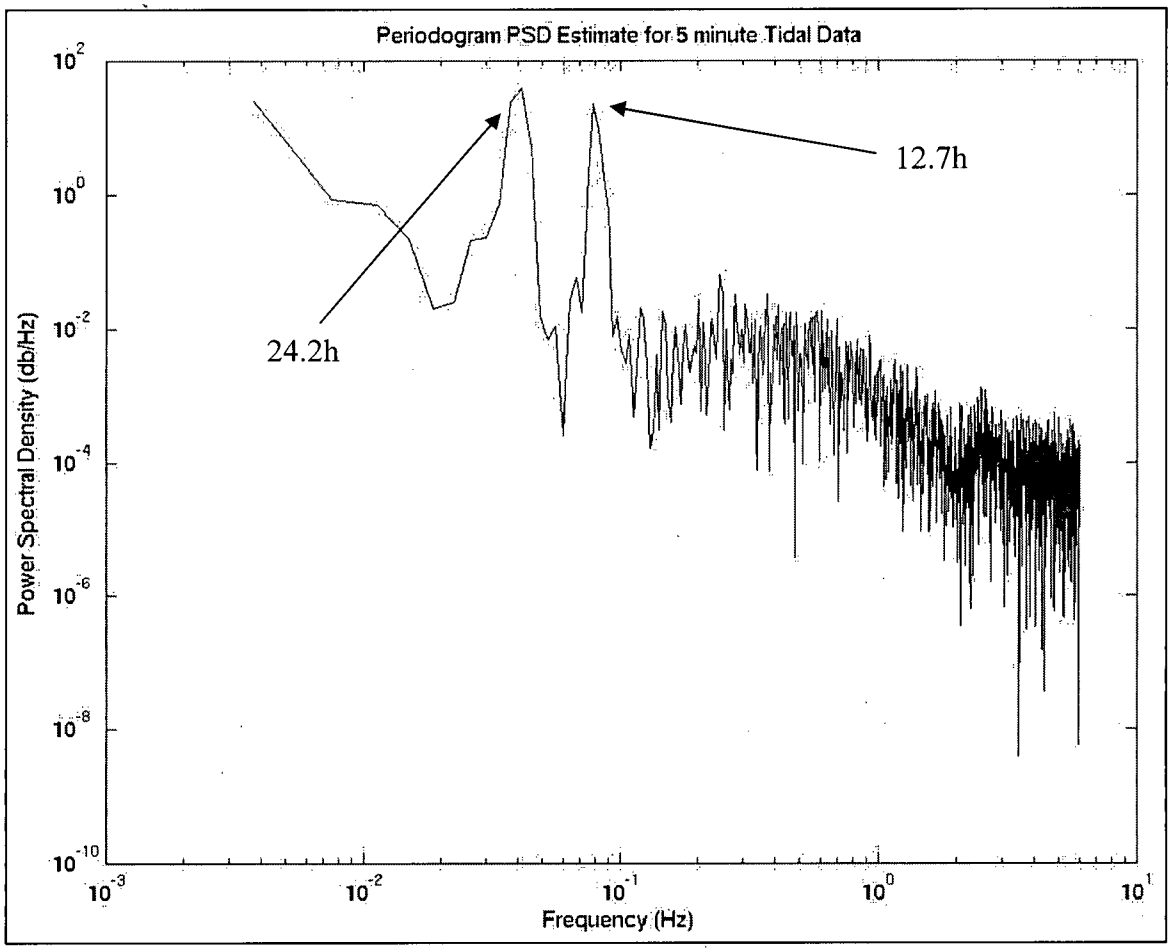

Figure 3-33. Periodogram for Tidal Data with 5 minute sampling frequency

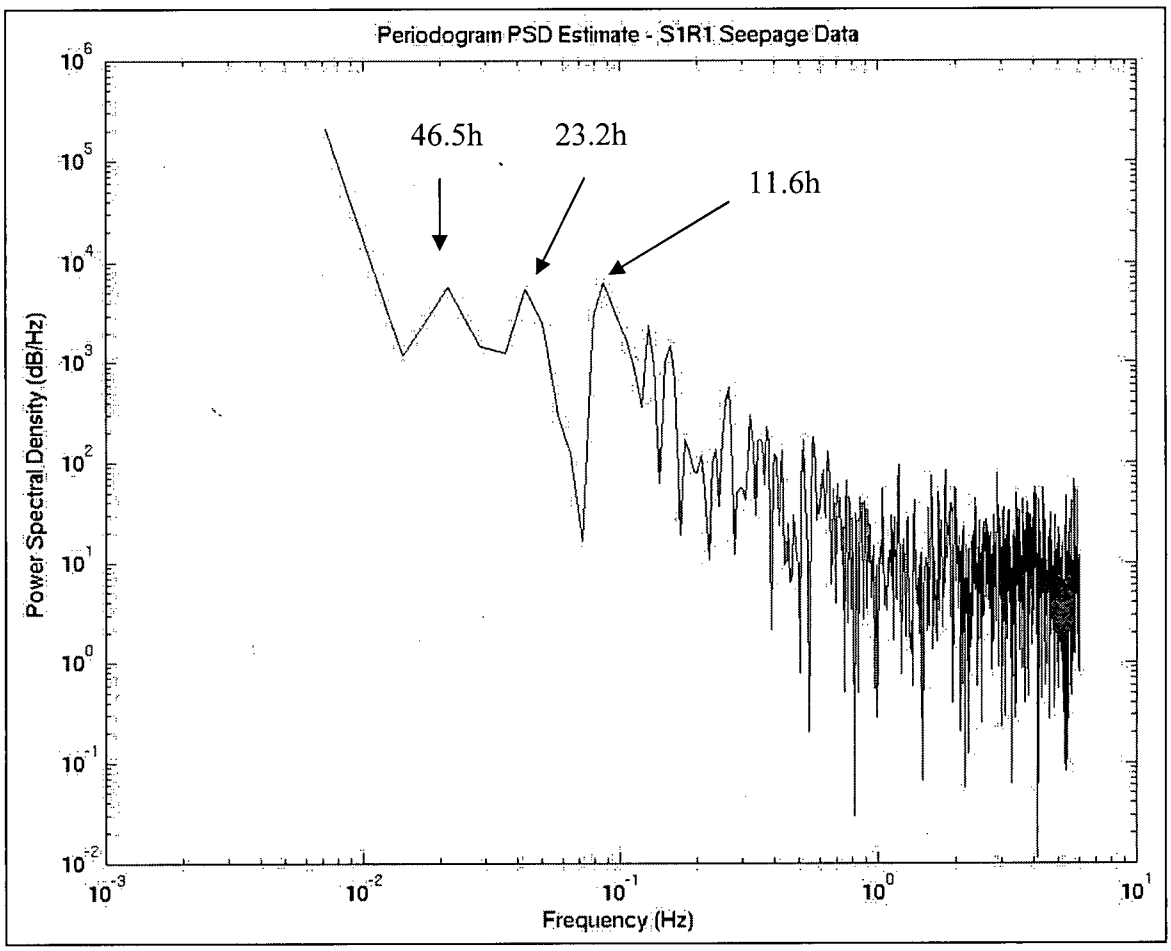

Figure 3-34. Periodogram for Seepage Data of S1R1

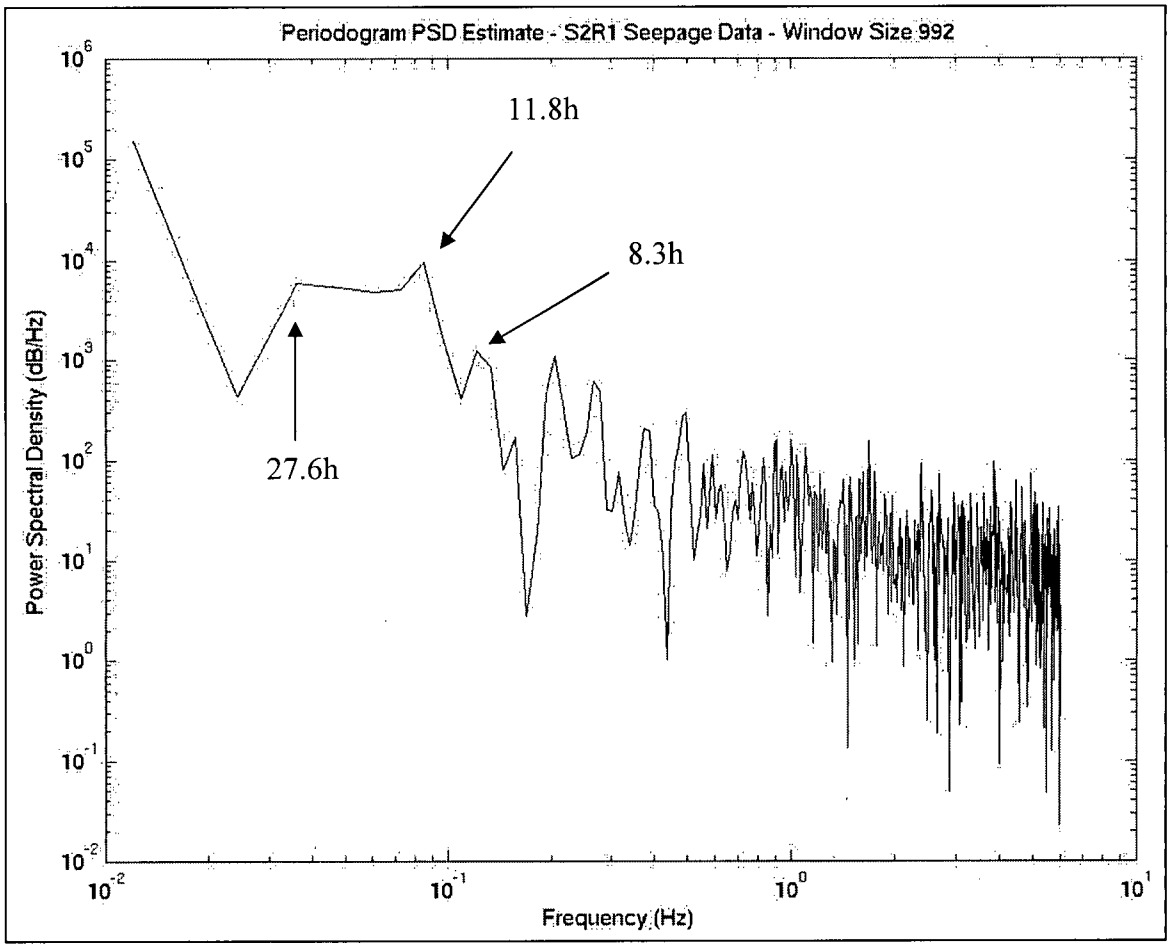

Figure 3-35. Periodogram for Seepage Data of S2R1

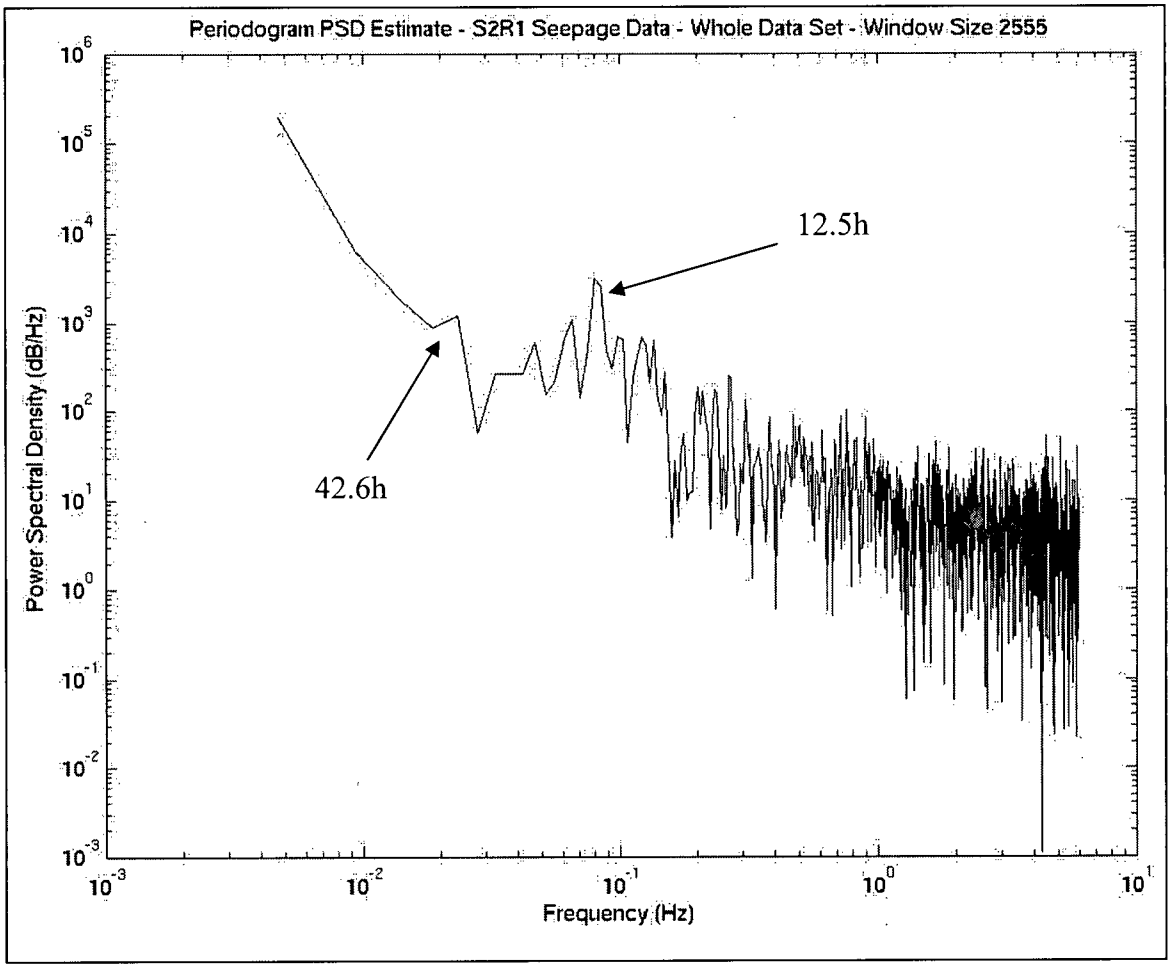

Figure 3-36. Periodogram for Seepage Data of Run 2 at Site 1

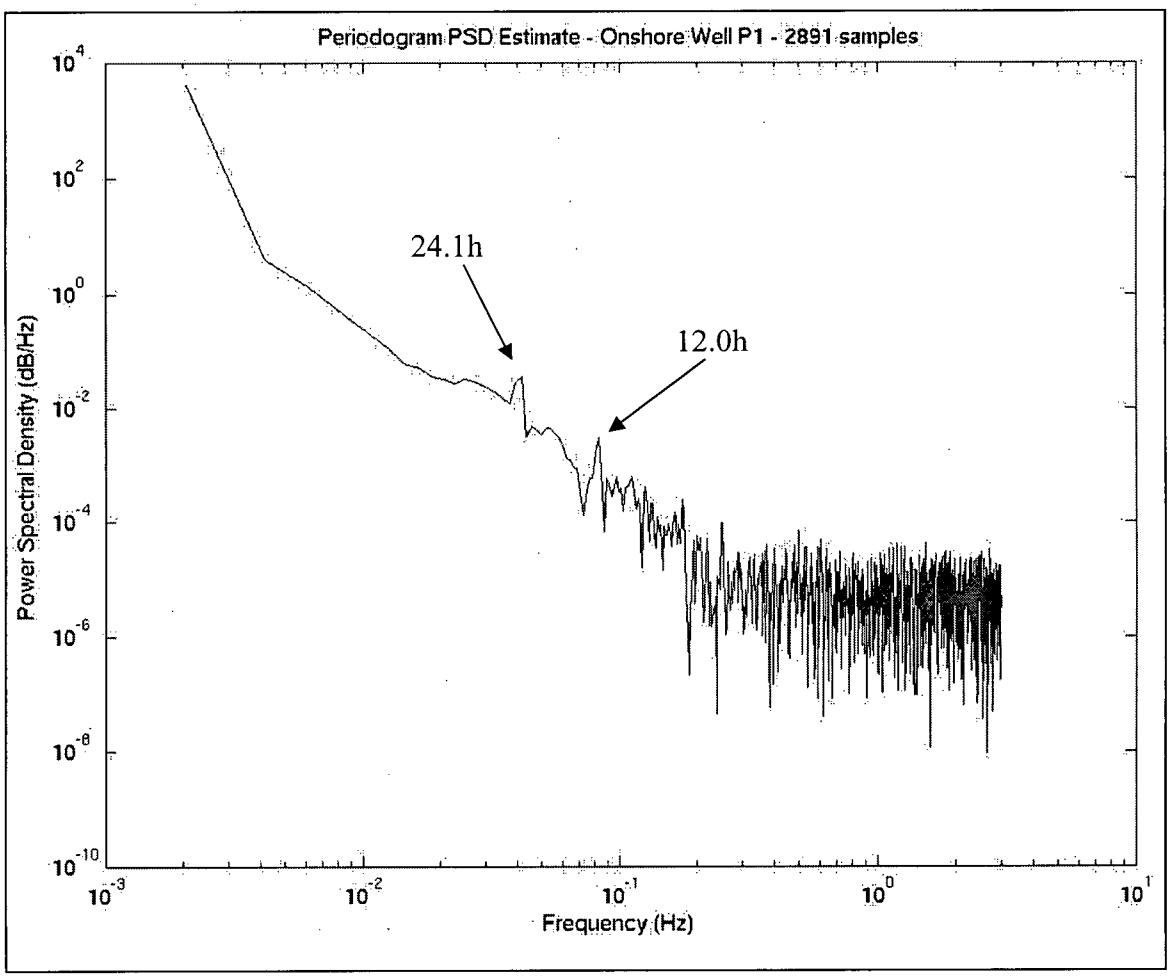

Figure 3-37. Periodogram for Well P1 Water Table Elevation Data

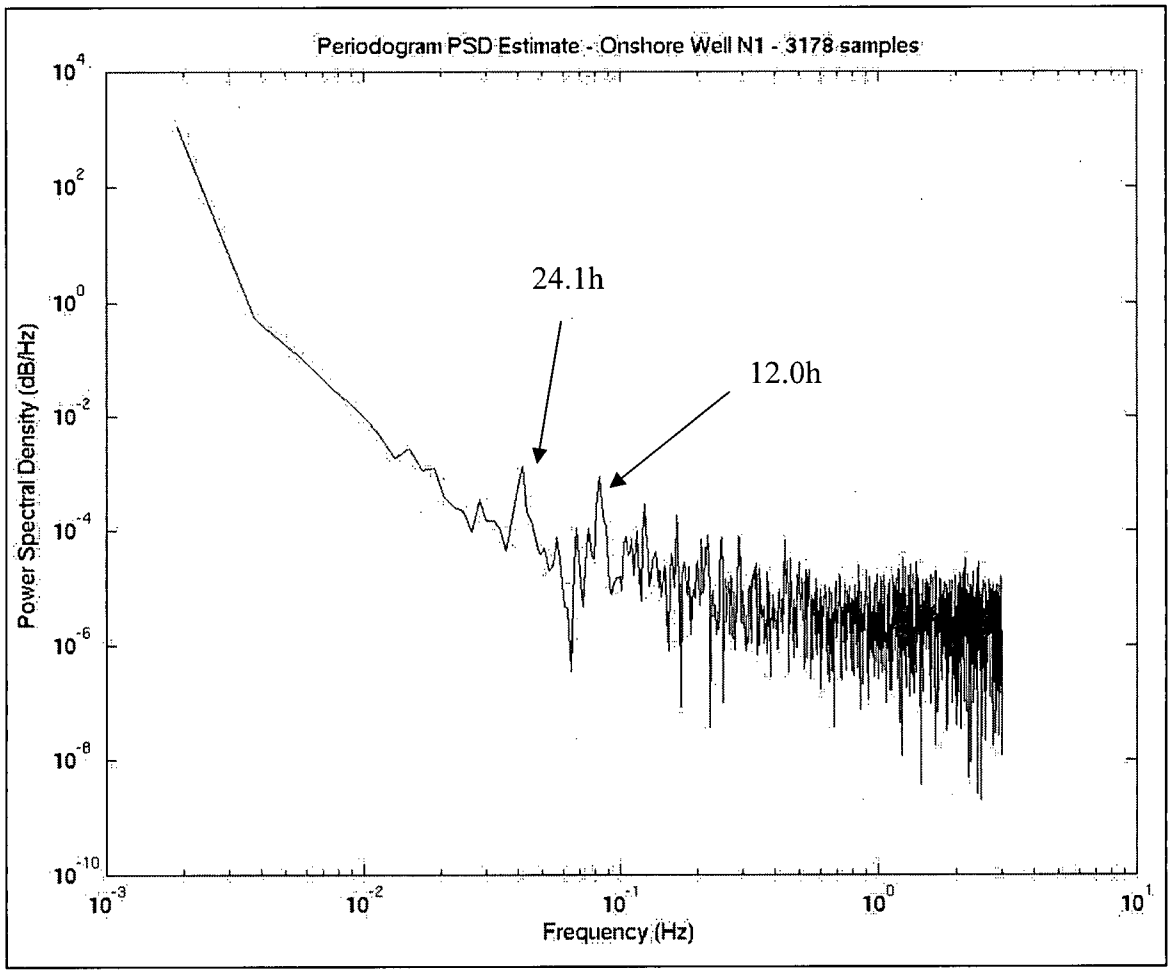

Figure 3-38. Periodogram for Well N1 Water Table Elevation Data

4. Numerical Model of the FSUML Site

4.1 One-Dimensional Computer Simulation

4.1.1 Rationale and FRAC3DVS Description

Researchers examining wave, tide and groundwater interactions in coastal aquifers and nearshore environments have used numerical models to shed light on the phenomena of submarine groundwater discharge, saltwater intrusion and freshwater/seawater mixing (Ataie-Ashtiani et al. 1999; Uchiyama et al. 2000; Langevin 2003; Smith and Zawadzki 2003). The results of a few of these investigations are worth describing here. Ataie-Ashtiani et al. (1999) modeled the effects of tidal fluctuations on saltwater intrusion in unconfined aquifers, where one finding was that small discharge velocity vectors are produced during a rising tide and that large discharge velocity vectors are produced during a falling tide. In addition, Ataie-Ashtiani et al. (1999) discovered that the seaward freshwater flux in the aquifer has considerable influence on both the shape and location of the seawater/freshwater contact. Finally, the authors found that by neglecting tidal fluctuation effects resulted in an inaccurate evaluation of the water table elevation in the onshore region of the aquifer. Uchiyama et al. (2000) used a numerical model to simulate nutrient discharge from groundwater discharge into the Kashima Sea off the east coast of Japan based on field measurements and compared with nutrient concentrations measured in the Tone River. They discovered that while nutrient fluxes from SGD were minor compared to those from the Tone River, it is recognized that SGD may have been underestimated because macropore and wave-setup effects were not included in their model. Langevin (2003) used a density-dependent, three-dimensional flow model, SEAWAT, to predict SGD into Biscayne Bay, Florida. The

author determined that for 6 of the 9 years modeled, the SGD magnitude was approximately 10% of the surface water discharge to Biscayne Bay while the 3 driest years produced SGD exceeding surface water discharge. Langevin (2003) notes, however, that results contain a high level of uncertainty as the field measurements of SGD proved problematic and were not used to validate the model.

Numerical modeling in this context is useful to test assumptions made about coastal aquifers and the processes driving SGD.

4.1.2 Construction Details

A 1-dimensional column model was developed to simulate seepage and differential pressures in the seabed, given tidal conditions at the site. The column model dimensions are 1m by 1m by 10m (XYZ) with the column subdivided at the centimeter scale (0.01m vertical spatial resolution). The vertical subdivisions enable the calculation of small-scale changes in hydraulic head. Only non-density-dependent flow was used in the simulation. This is because unrealistic head distributions were produced using density-dependency as a result of irresolvable errors.

The domain for the model includes the Surficial Aquifer (SA) and the Intracoastal Formation (IF), both of which are assumed to be homogenous. The upper 6m of the column are designated as SA, this depth is based on the refusal depth of the Waterloo Profiler at site 1. The bottom four meters of the column are designated as IF. The hydraulic conductivity of the SA was chosen to be 1×10^{-5} m/s, which is the geometric mean of wells BC1 and BC4, the wells closest to site 1 where K values had been determined. The hydraulic conductivity of the IF was chosen to be 1×10^{-9} m/s, estimated

from descriptions of the IF by Schmidt (1984). Other material properties included in the model are listed in **Table 4-1**. A conceptual diagram of the 1-dimensional model is presented in **Figure 4-1**.

Table 4-1. Material properties of Surficial Aquifer and Intracoastal Formation

Parameter	Surficial Aquifer	Intracoastal Formation
Hydraulic Conductivity (m/s)	1×10^{-5}	1×10^{-9}
Storage Coefficient	0.001	0.0001
Porosity	0.3	0.05

A constant head of 1.5m was applied at the top of the Upper Floridan Aquifer, which is the base of the model at the IF/Floridan Aquifer contact. The model was run to steady-state with constant heads at both the top and the bottom of the model. Once steady-state was reached, heads ranging from 0.331 to 1.403m were applied at the top of the SA, simulating tidal fluctuations. The fluctuations are based on real tidal elevation data collected at the site during each period of time under examination. The time periods examined were between 2 and 4 days, enough time to allow for at least two tidal cycles to be analyzed. The tidal elevations, referenced to NAVD88, were corrected to be representative of the height of the water column above the seabed at site 1. The head fluctuations in the model are programmed to occur at either 5 or 10 minute intervals over the course of the run, depending on the collection rate of tide data. The model is simulating a zone 20-40m beyond the low tide line where no input from the surficial aquifer is considered.

Observation points are included in the model at intervals of 0.2m (vertical depth) to observe the hydraulic head fluctuations with depth. Differences between observed

hydraulic head at depth simulate the differential piezometer system output. The depths used from the simulation are 0.4m and 1m below the seabed, providing a Δz of 0.6m. Despite the errors associated with the calibrations of the DPS, it is useful to examine how hydraulic heads are fluctuating in the seabed. Seepage rates (described as flux rates in FRAC3DVS) across the seabed are also predicted using the 1D model. A flux output node was specified at the top of the column (at the seabed), which should approximate the observed submarine groundwater discharge rate measured with the automated seepage meter. The model was calibrated by varying the hydraulic conductivity of the SA and the IF to see how these changes would affect the SGD and DPS results.

4.2 Results and Discussion

The model results indicate that given the tidal data recorded in the field and with the estimated aquifer properties indicated above, discharge and recharge should be observed at the field site (**Figures 4-2**). In this figure, a tidal sequence of approximately four semi-diurnal cycles is superimposed with the simulated discharge rate and the simulated differential head. The simulated processes of discharge and differential head are driven in the same direction by the fluctuating tide. Assuming the automated seepage meter was performing accurately, no recharge was recorded in the experiments during August and September 2002. While the seepage meter cannot measure recharge, a reading of zero or the minimum reading is expected if recharge is occurring. It is possible, although unlikely, that the uncalibrated seepage meter was producing discharge readings when in reality recharge was occurring, yet there is no way to verify if this was the case. Recharge may explain the periods of absent tidal signals in the seepage data but

again, verification of this hypothesis is not an option. The discrepancy between the model and the field results is not currently understood. No recharge at the FSUML site was reported by Taniguchi et al. (2003) for the intercomparison study nor has previous work at the marine lab discussed observations of recharge. Yet recharge can occur at high tides as documented by Paulsen et al. (2003), where two ultrasonic automated seepage meters spaced 2 meters apart in West Neck Bay, New York, recorded discharge in one meter and recharge at the other. The authors concluded that spatial heterogeneities may exist at the meter scale and this may account for the field seepage measurements.

In regards to the timing of the flux rates, it is observed from the model that the highest discharge rates occur during the transition from highest to lowest tide (**Figure 4-2**). Burnett et al. (2002) also note that the highest flux rates observed at FSUML in August 2000 occurred during the transition from highest to lowest tide (**Figure 2-3**), an observation identical to what was found during the current research (**Figures 3-17, 3-19, 3-21**). Conversely, recharge is at a maximum in the model results during the transition from low to high tide. This corresponds to discharge being at a minimum at the field site both in 2000 and 2002. The fact that the simulation is able to predict the occurrence of seepage oscillations with tide as seen in the field implies that the conditions applied within the model are accurate to some degree. It is interesting to note, however, that the field results from Paulsen et al. (2003) do not match those found by this study or Burnett et al. (2002). Paulsen et al. (2003) record that seepage rates are at a maximum immediately after the low tide in all data displayed yet they do not speculate on this. The discrepancy may be caused by the fact that the aquifer at West Neck Bay is composed of glacio-fluvial medium to coarse-grained sand, which is highly conductivity material

while the Surficial Aquifer at FSUML is composed of silty sand (geometric mean hydraulic conductivity of SA is 8×10^{-6} m/s). No hydraulic conductivity data is provided by Paulsen et al. (2003).

Head vs. depth profiles created from the 1D model are presented in **Figure 4-3**. This figure demonstrates head fluctuations with depth over a period of 17 hours. Notice that there is continuous discharge from the Intracoastal Formation, albeit widely varying with the tides, caused by the applied boundary condition at the base of the model. The sequence of discharge and recharge across the seabed is also controlled by the tidal influences applied to the seabed surface at the top of the Surficial Aquifer. Comparing **Figures 4-2 and 4-3**, the simulated discharge can be explained by closely examining how the tidal oscillations affect the sediments at depth.

At high tide, hydraulic head in the seabed is static and discharge is at zero but begins to climb immediately after high tide is passed, indicating that pressure is decreasing and allowing brackish water to discharge. As the tide drops, the rate of discharge increases with the decreasing pressure. At just after midway between high and low tide, when the slope of the falling tide is at its maximum (highest rate of pressure change or highest differential head), the seepage rate reaches its maximum, which implies that the rate of pressure change at the seabed controls the rate of change in the discharge. As the rate of tidal elevation decline begins to slow (decreasing slope of the tide), the discharge rate begins to drop as well. When the tide reaches its minimum, the seepage rate is again at zero because the head has equalized across the SA. With increasing pressure at the seabed from the increasing tide, recharge rates increase, reaching a maximum at the point of maximum tidal increase (maximum slope). Finally, as the tidal

elevation flattens again towards high tide, the recharge rate declines, reaching zero at high tide.

Thus, the model indicates that the rate of discharge from (or recharge into) the Surficial Aquifer is really caused by the rate of change in pressure caused by the fluctuating tides and the hydraulic head assigned at the top of the Upper Floridan Aquifer.

One-dimensional simulations were run from tidal data collected during run 1 at both sites (S1R1 and S2R1) and run 2 at site 1 (S1R2). The hydraulic conductivity at site two, 3.59×10^{-6} m/s, based on the geometric mean of the hydraulic conductivities of wells C1 and C3, the wells closed to site 2. All other variables were kept the same for this simulation. Seepage data was plotted with model results along with the tidal fluctuations inputted to the model because it would be useful to see how the field results compare to the simulation. The S1R2, S1R1 and S2R1 plots are presented in **Figures 4-4, 4-5 and 4-6**, respectively. Notable in **Figure 4-5** is the observation that the model clearly predicts temporal variations in discharge rates measured in the field. Discharges peak at about 1cm and with hydraulic conductivities of 1×10^{-4} m/s for the SA and 1×10^{-5} m/s for the IF, discharges peaked at about 2cm. The model calibrations, however, as described above were unable to predict accurate discharge magnitudes, the simulated discharge rates always falling much lower than the field rates even at extreme parameter values.

The relationship between tidal height above the seabed and seepage rate is presented in **Figures 4-7, 4-8 and 4-9**. As discussed previously, a non-linear relationship appears to exist between the seepage rate and the tidal fluctuations. As can be seen clearly in these figures, a distinct circular cycle is noted, following the tidal cycle. When

the tide is at an extreme, high or low, discharge is at or near zero. When tides are at mid-levels, discharge is at a maximum or minimum, depending on the direction of the tide.

As expected, simulated differential heads behave in a way very similar to that of simulated discharge as described above. The greatest differential heads are produced when the highest rate of pressure change is achieved, which is at the point of greatest slope of the falling or rising tides. These two processes act in tandem and quality field data should allow for prediction of the magnitude and direction of one process from the other. While the current research did not produce data where prediction of this nature could be achieved, future work should aim to minimize chances of calibration and instrument error in order to collect high quality differential head data.

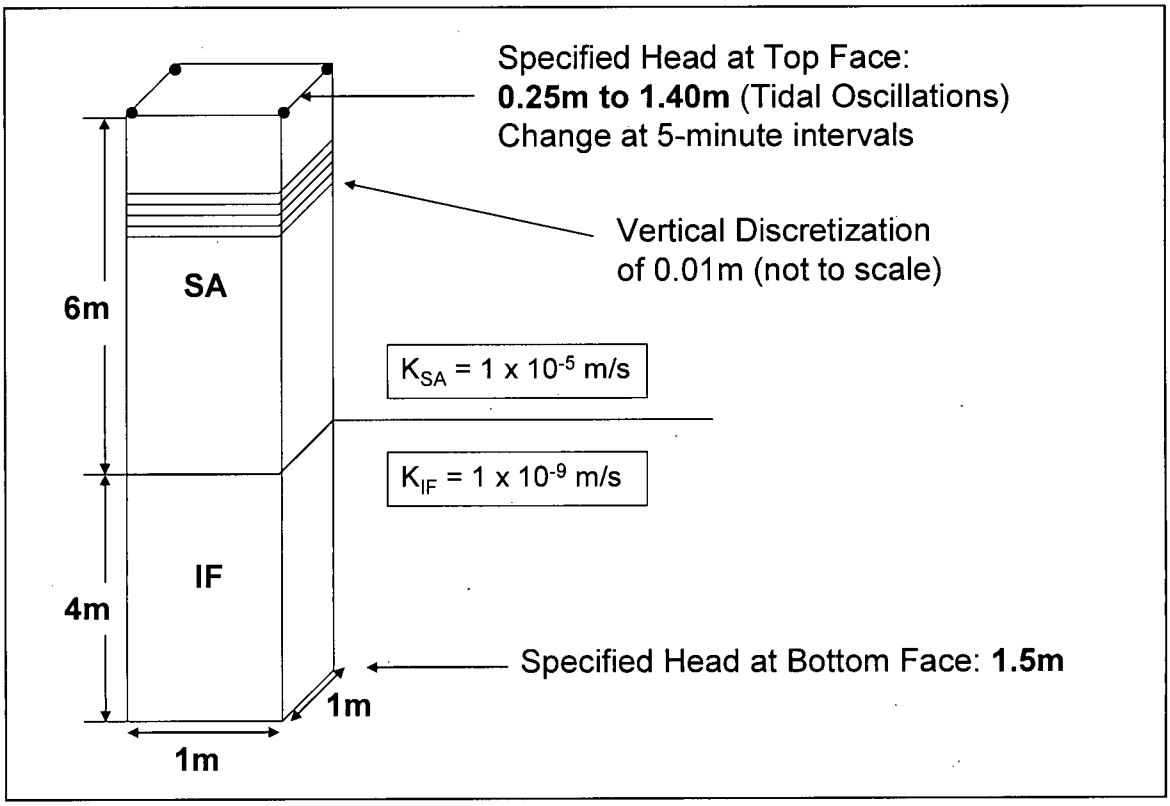

Figure 4-1. Conceptual Model for 1-Dimensional Simulation

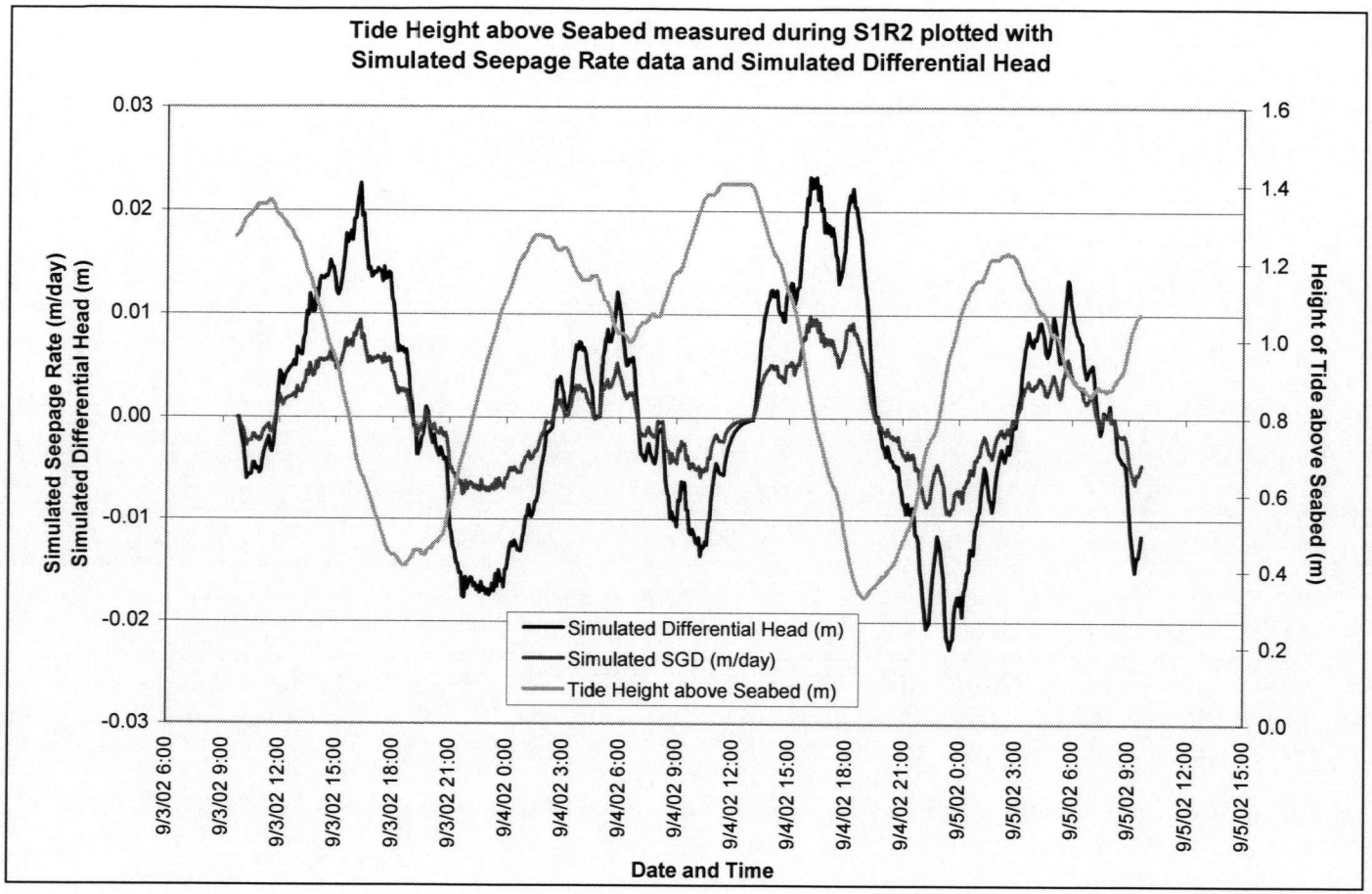

Figure 4-2. Simulated Differential Head and Seepage Rate from 1D Column Model using Tidal Data collected during S1R2

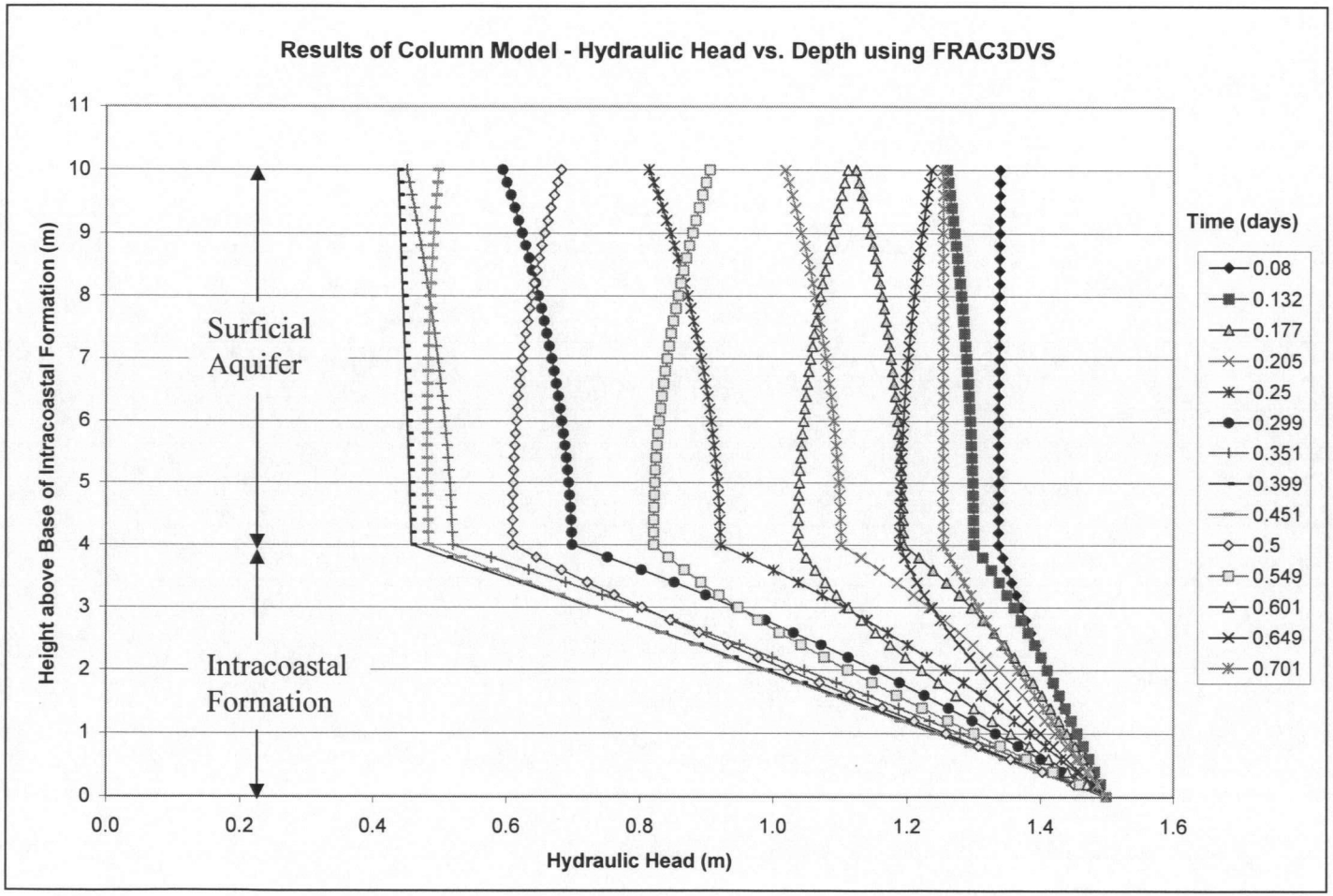

Figure 4-3. Model results from 1-dimensional model using tidal data collected during S1R2

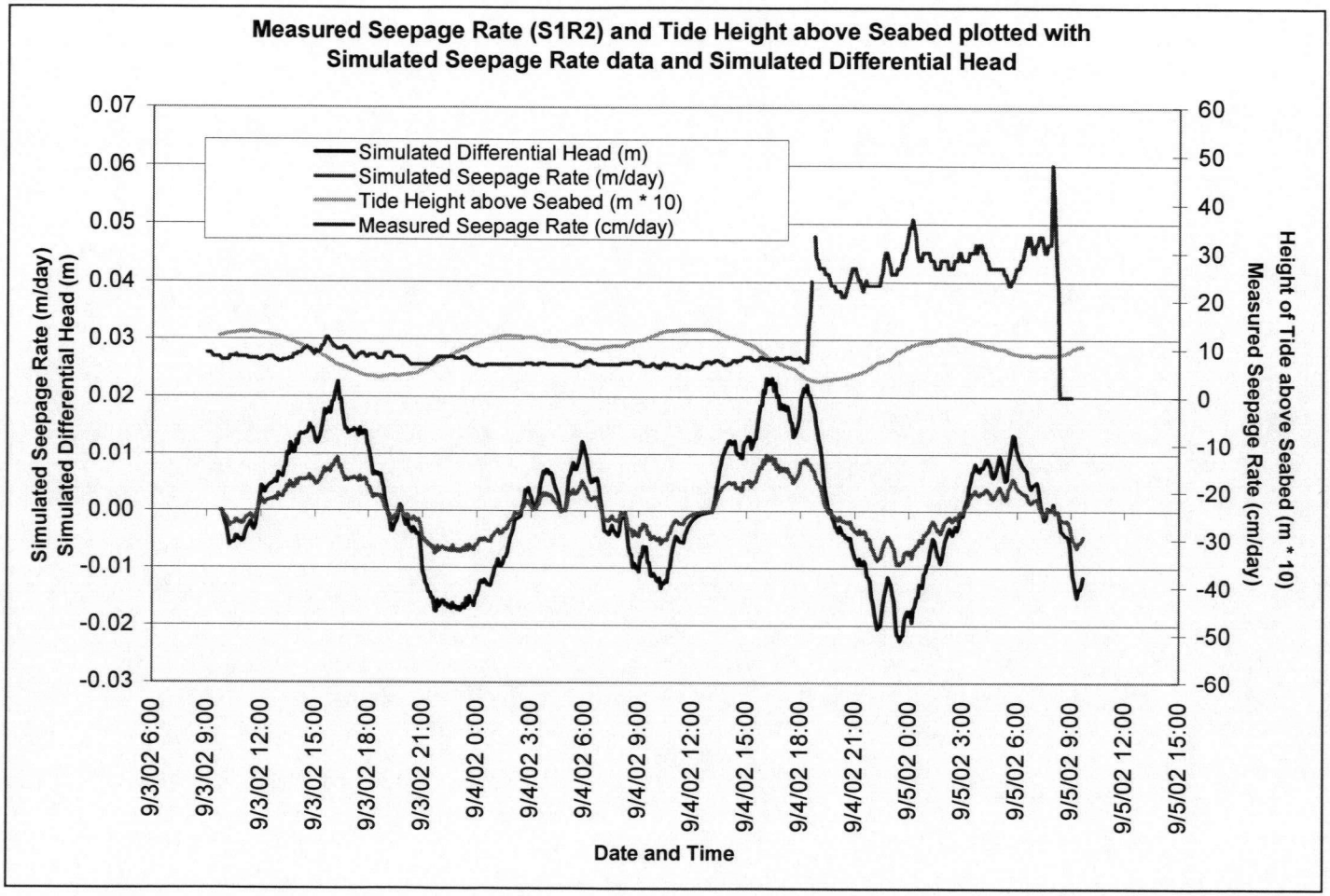

Figure 4-4. Measured Seepage Rate from S1R2 plotted with Simulated Seepage Rate and Differential Head from 1D Column Model. Note that the simulated seepage rate is in units of m/day, while the measured rate is in cm/day.

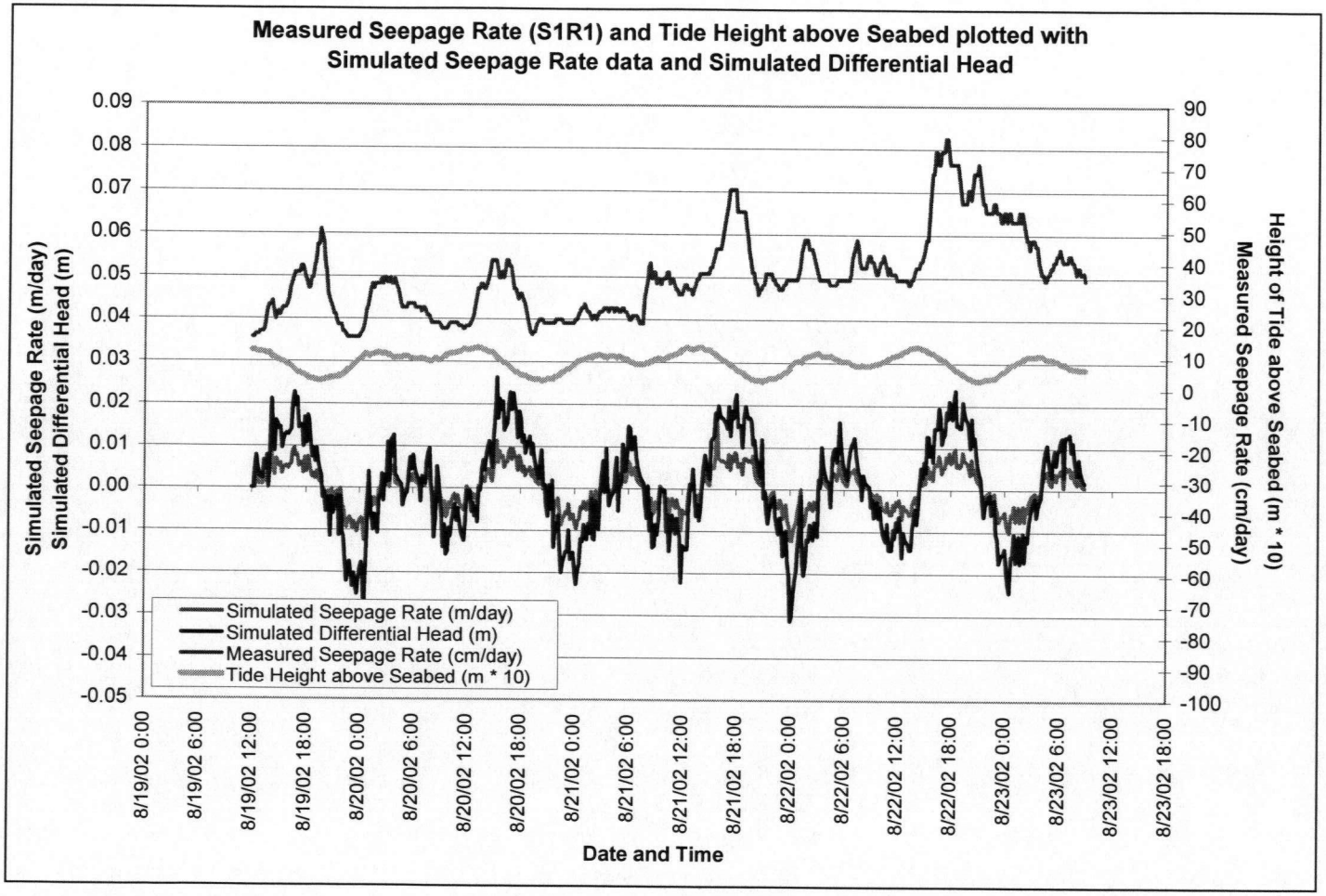

Figure 4-5. Measured Seepage Rate from S1R1 plotted with Simulated Seepage Rate and Differential Head from 1D Column Model. Note that the simulated seepage rate is in units of m/day, while the measured rate is in cm/day.

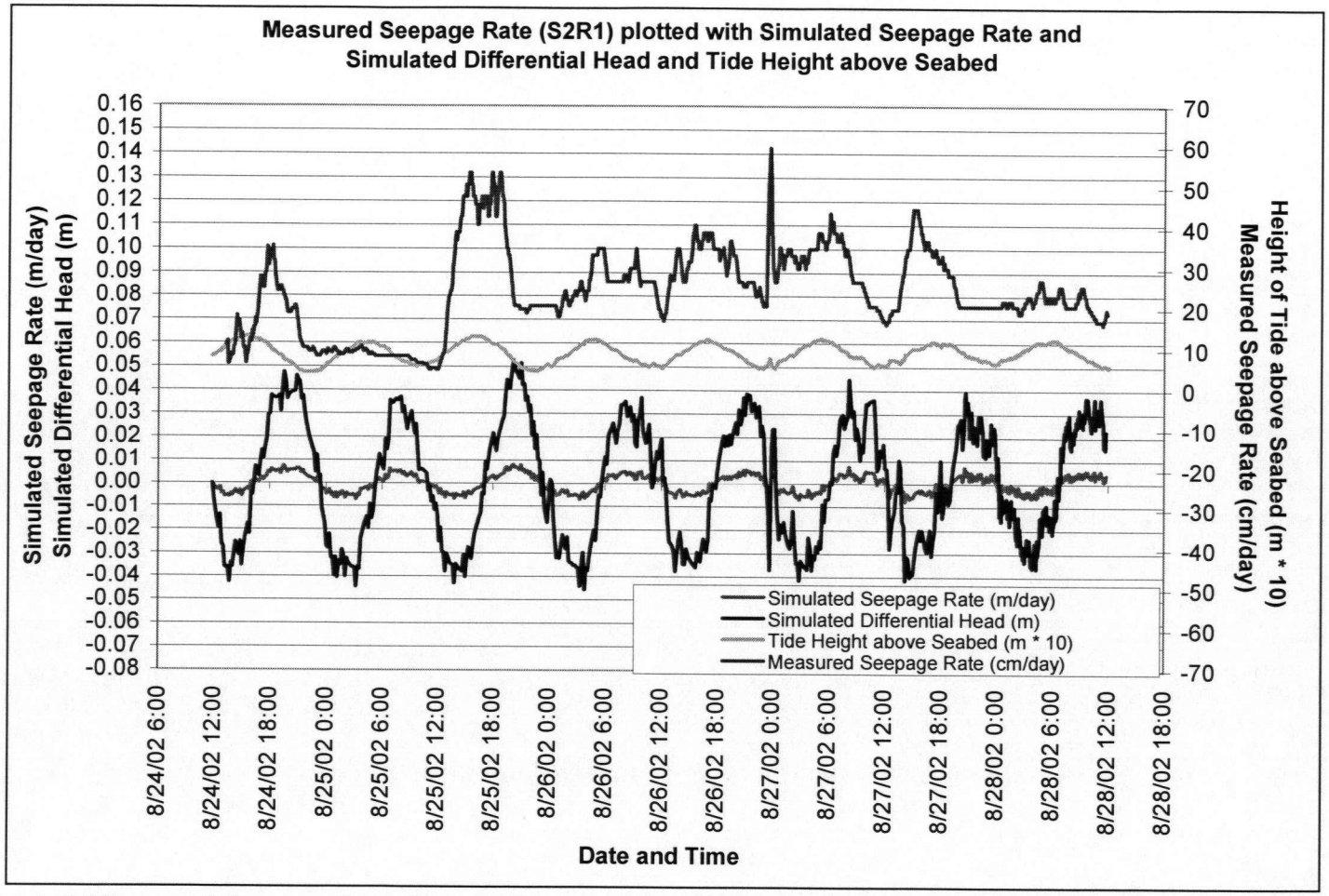

Figure 4-6. Measured Seepage Rate from S2R1 plotted with Simulated Seepage Rate and Differential Head from 1D Column Model. Note that the simulated seepage rate is in units of m/day, while the measured rate is in cm/day.

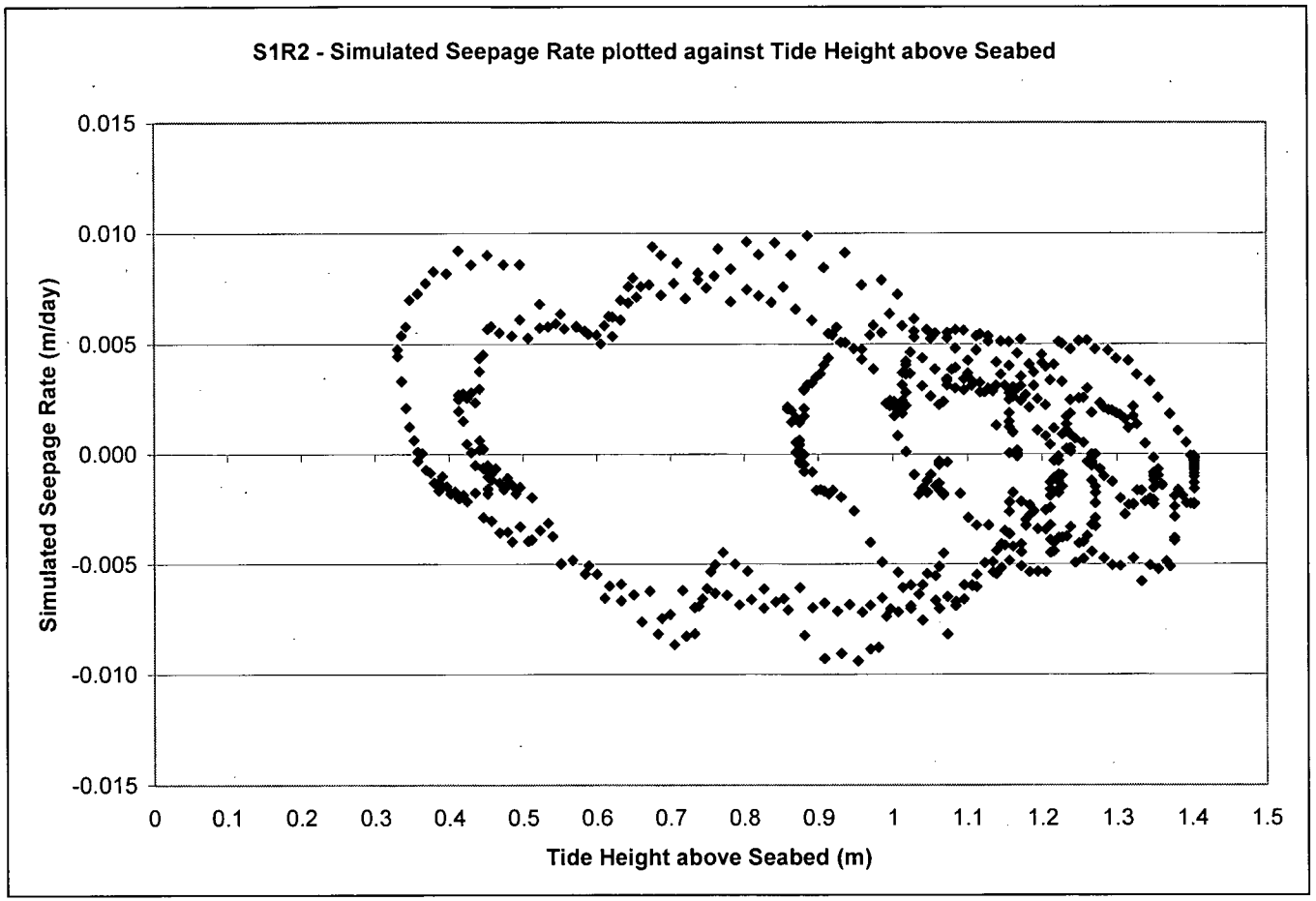

Figure 4-7. Simulated Seepage Rate based on tidal data from S1R2 period plotted against Tide Height above Seabed. Note the circular nature of the plot.

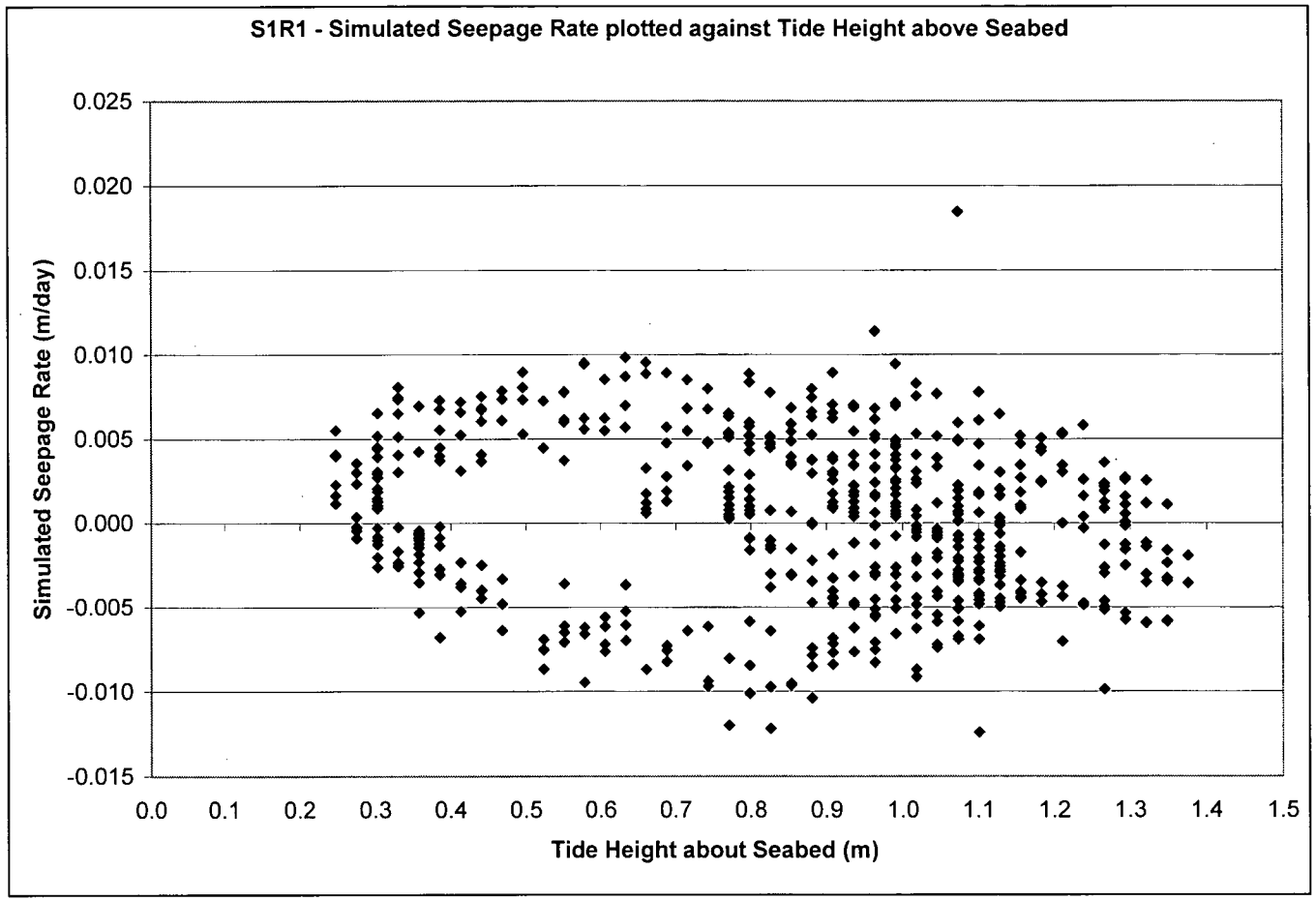

Figure 4-8. Simulated Seepage Rate based on tidal data from S1R1 period plotted against Tide Height above Seabed.

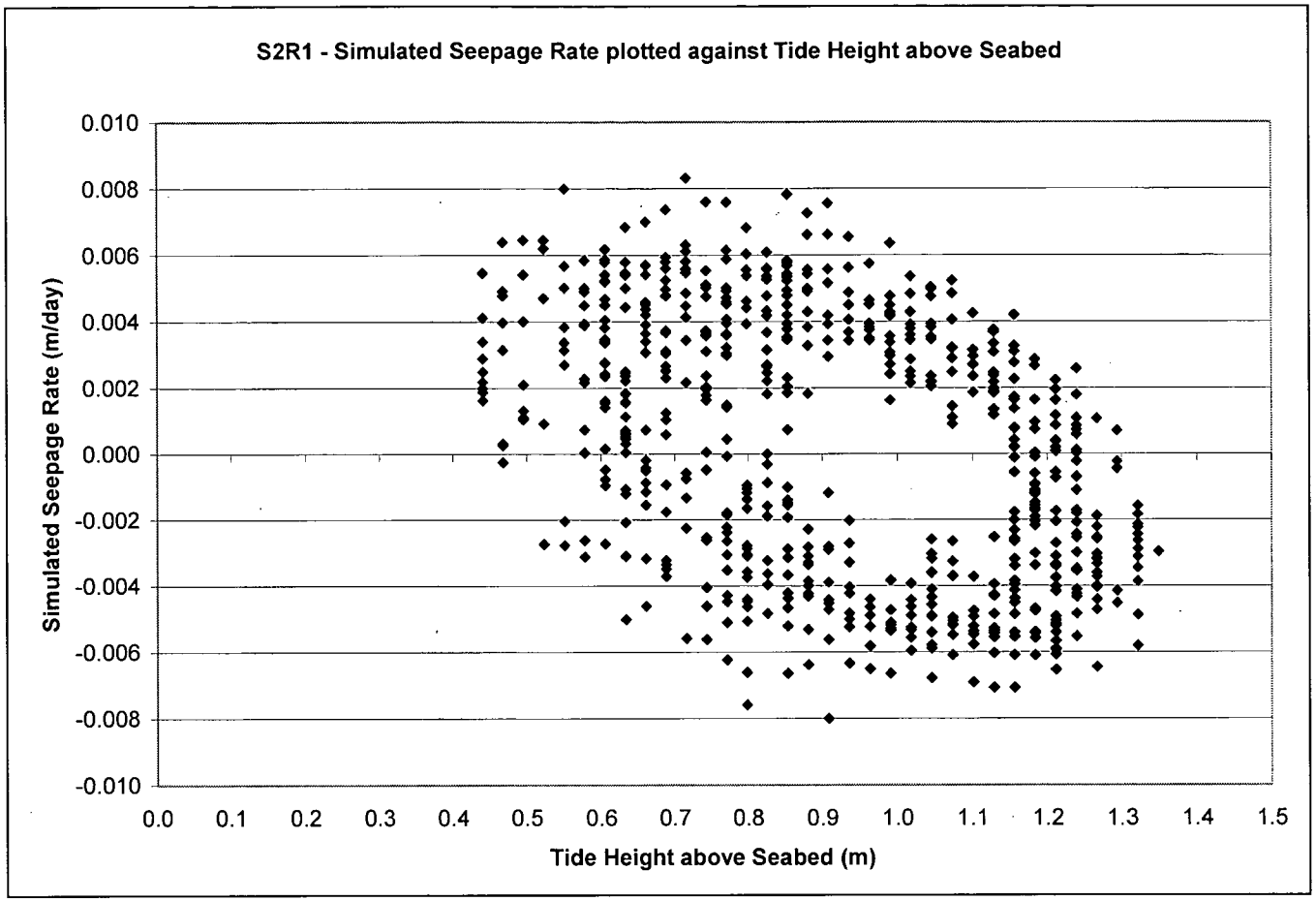

Figure 4-9. Simulated Seepage Rate based on tidal data from S2R1 period plotted against Tide Height above Seabed.

5. Conclusion

This research attempted to investigate the processes driving submarine groundwater discharge from three basic perspectives: characterization of the coastal aquifer, offshore analysis of SGD and a numerical modeling approach.

Characterization of the coastal aquifer involved the analysis of onshore water table levels in order to calculate an appropriate horizontal hydraulic gradient, found to be 0.025, based on the average drop in hydraulic head between wells P1 and N1. Slug testing of these wells and well P2 using the Hvorslev method produced hydraulic conductivity values that may point to a vertical structure of decreasing hydraulic conductivity with depth within the Surficial Aquifer as postulated by Smith and Zawadzki (2003). The geometric mean and arithmetic mean of these three wells is 6.4 x 10^{-5} m/s and 1.3 x 10^{-4} m/s, respectively, which is within the range of other wells at the site. Two major storm events provided insight into the nature of flow in the onshore region, indicating that well P1 responded more quickly to infiltration than well N1 despite being in sediment 31 times less conductive. From observations of tidal oscillations present in these wells it is likely that a low conductivity unit exists just shoreward of well N1, damping the effects of tidal influences. A discharge rate over an offshore area comparable to the 2000 intercomparison study, based on the onshore well hydraulic conductivity values and horizontal hydraulic gradient, was calculated to be lower than that measured by the intercomparison researchers by 1-2 orders of magnitude. This result is consistent with a model by Smith and Zawadzki (2003) whose vertically layered Surficial Aquifer model obtained a value of 0.15m^3/min while the Darcy's law calculation from this study obtained values of 0.14 m^3/min and 0.07 m^3/min for the

onshore well K value arithmetic and geometric means, respectively. One possible explanation for this is leakage across the Intracoastal Formation into the Surficial Aquifer.

Submarine groundwater discharge experiments were focused on two offshore sites where an automated seepage meter was coupled with a new apparatus, a differential piezometer system, which was designed to measure differential head fluctuations in the seabed. Seepage rates across the seabed had measured rates varying between 20-40 cm/day on average although peaks of up to 80cm/day were observed. While recharge cannot be recorded with the seepage meter, continuous discharge as observed is equivalent to no observed recharge. Occasional periods of "low" discharge rates (10-20 cm/day) with minimal tidal influence were observed over the course of several tidal cycles. Large calibration errors associated with the DPS differential pressure transducers, which are of the same magnitude as the measured data, prevent the use of the DPS data in an analysis. Despite this, a preliminary assessment of the data is completed. Difficulties with the differential piezometer system can be avoided in the future by careful lab calibrations of any system planned for use in the field and running calibrations while in the field. Acquiring a commercially available 2-port, differential pressure probe should be considered for future experiments.

A 1-dimensional numerical simulation was used to examine how simulated seepage rates compare with observed rates. The model results support the field evidence in regards to temporal periodicity of seepage with tidal fluctuations. It is observed that the relationship between the seepage rate and the tidal stage appears to be a non-linear one with maximum discharge or recharge occurring at times of maximum slope of tidal

oscillations. It is determined that the rate of pressure change at the surface and the hydraulic head assigned at the top of the Upper Floridan Aquifer drive the changes in discharge rate.

Appendix A – Slug Test Recovery Data

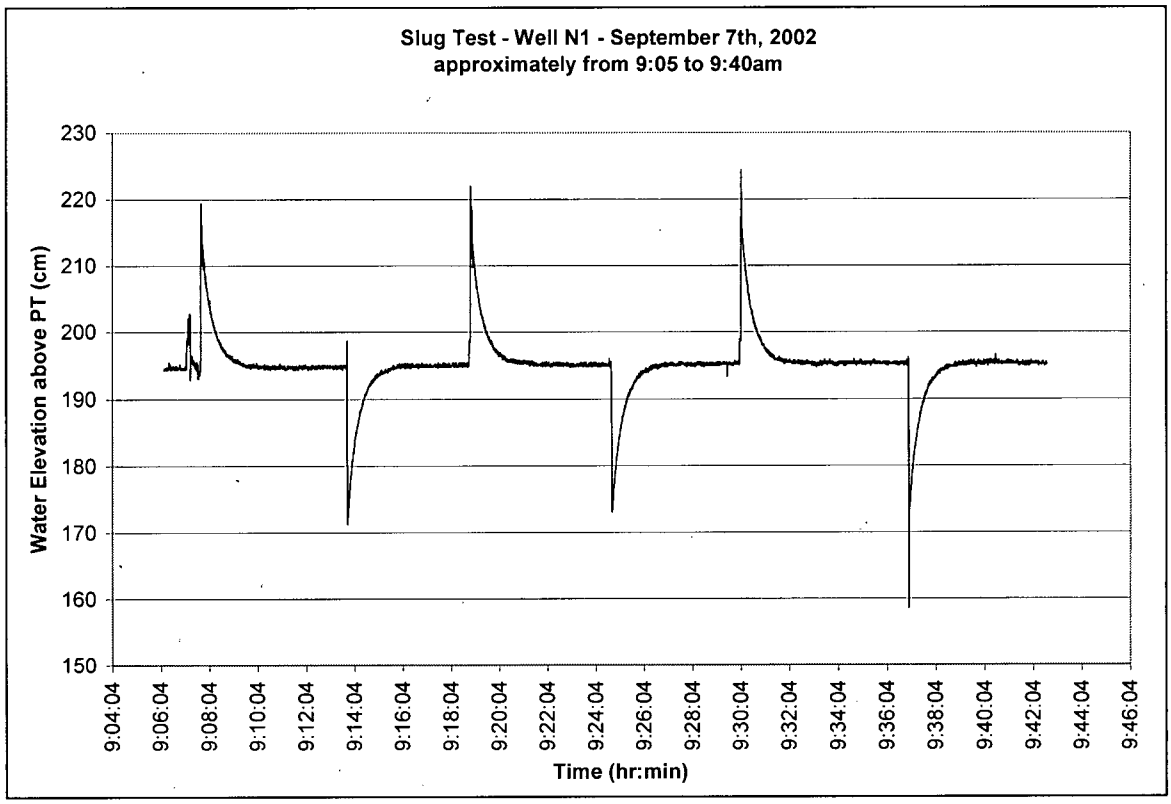

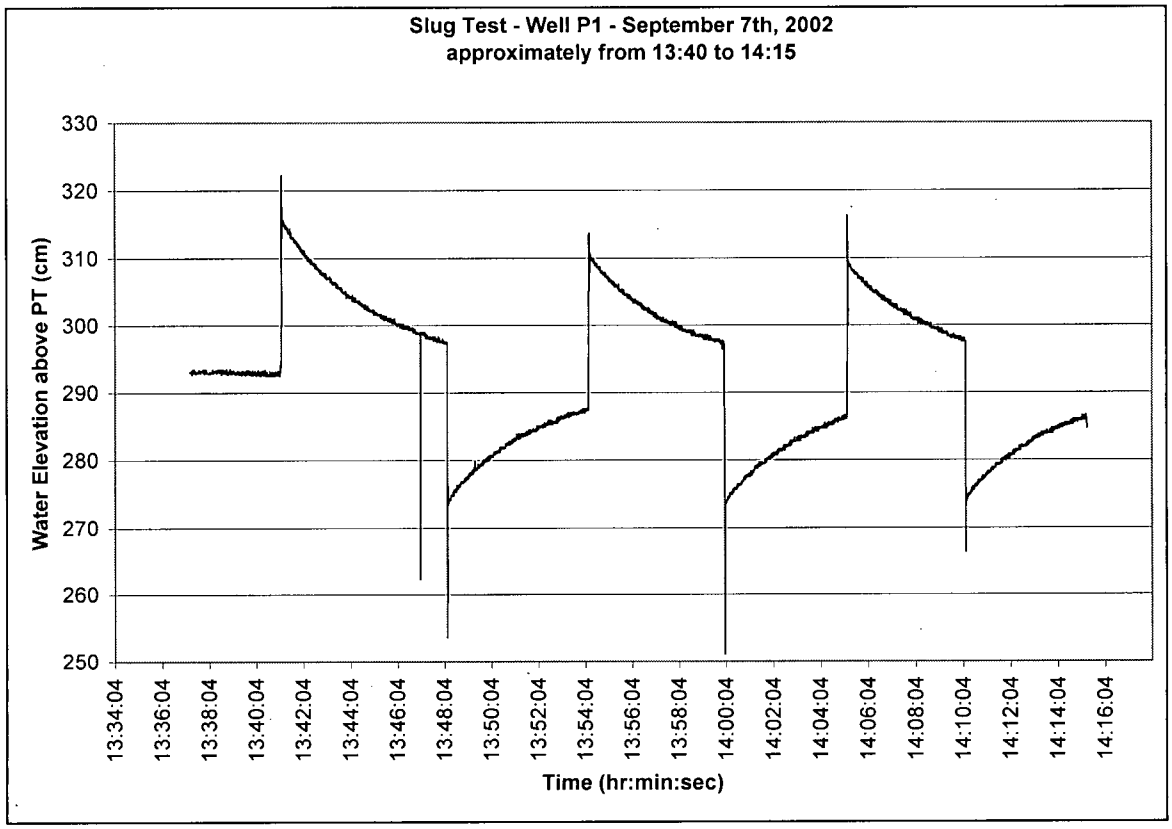
Slug Test - Well P1 - September 7th, 2002
approximately from 13:40 to 14:15
Water Elevation above PT (cm)
330
320
310
300
290
280
270
260
250
13:34:04
13:36:04
13:38:04
13:40:04
13:42:04
13:44:04
13:46:04
13:48:04
13:50:04
13:52:04
13:54:04
13:56:04
13:58:04
14:00:04
14:02:04
14:04:04
14:06:04
14:08:04
14:10:04
14:12:04
14:14:04
14:16:04
Time (hr:min:sec)

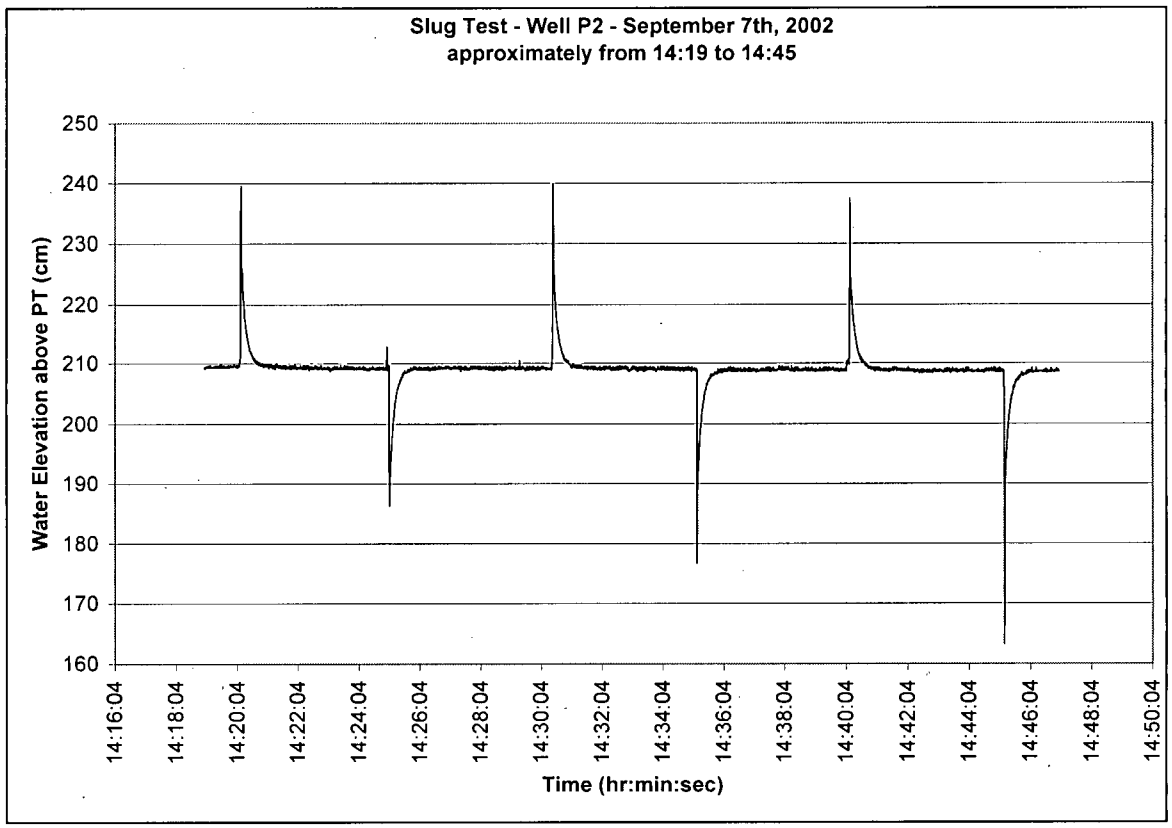
Slug Test - Well P2 - September 7th, 2002
approximately from 14:19 to 14:45
Water Elevation above PT (cm)
250
240
230
220
210
200
190
180
170
160
14:16:04
14:18:04
14:20:04
14:22:04
14:24:04
14:26:04
14:28:04
14:30:04
14:32:04
14:34:04
14:36:04
14:38:04
14:40:04
14:42:04
14:44:04
14:46:04
14:48:04
14:50:04
Time (hr:min:sec)

Appendix B – Slug Test Recovery Data

Slug Test Results for new onshore wells at FSUML

well	N1						
r	0.0254	m	well screen radius				
Le	0.4064	m	screen length				
R	0.0254	m	borehole radius				
			t37 min	K [m/min]	K[m/d]	K[m/s]	Method
N1	i1	in	0.367	0.0059966	8.64	0.00010	Hvorslev
N1	o1	out	0.45	0.0048905	7.04	0.00008	Hvorslev
N1	i2	in	0.41	0.0053677	7.73	0.00009	Hvorslev
N1	o2	out	0.46	0.0047842	6.89	0.00008	Hvorslev
N1	i3	in	0.379	0.0058067	8.36	0.00010	Hvorslev
N1	o3	out	0.225	0.0097811	14.08	0.00016	Hvorslev
N1 Average K [m/s] =			**1.02E-04**	**(med. to coarse sand)**			

well	P1						
r	0.0254	m	well screen radius				
Le	0.4445	m	screen length				
R	0.0254	m	borehole radius				
			t37 min	K [m/min]	K[m/d]	K[m/s]	Method
P1	i1	in	3.83	0.0005423	0.78	0.0000090	Hvorslev
P1 Average K [m/s] =			**9.04E-06**	**(med. to coarse sand)**			

Note: P1 - Only the first slug test (i1) was used
Well P1 had not fully recovered when the slug was removed from the borehole

well	P2						
r	0.0254	m	well screen radius				
Le	0.9144	m	screen length				
R	0.0254	m	borehole radius				
			t37 min	K [m/min]	K[m/d]	K[m/s]	Method
P2	i1	in	0.092	0.0137412	19.79	0.0002290	Hvorslev
P2	o1	out	0.15	0.0084279	12.14	0.0001405	Hvorslev
P2	i2	in	0.077	0.016418	23.64	0.0002736	Hvorslev
P2	o2	out	0.0875	0.0144478	20.80	0.0002408	Hvorslev
P2	i3	in	0.093	0.0135934	19.57	0.0002266	Hvorslev
P2	o3	out	0.0375	0.0337116	48.54	0.0005619	Hvorslev
P2 Average K [m/s] =			**2.79E-04**	**(med. to coarse sand)**			

Appendix C – Slug Tests – Normalized drawdown versus time

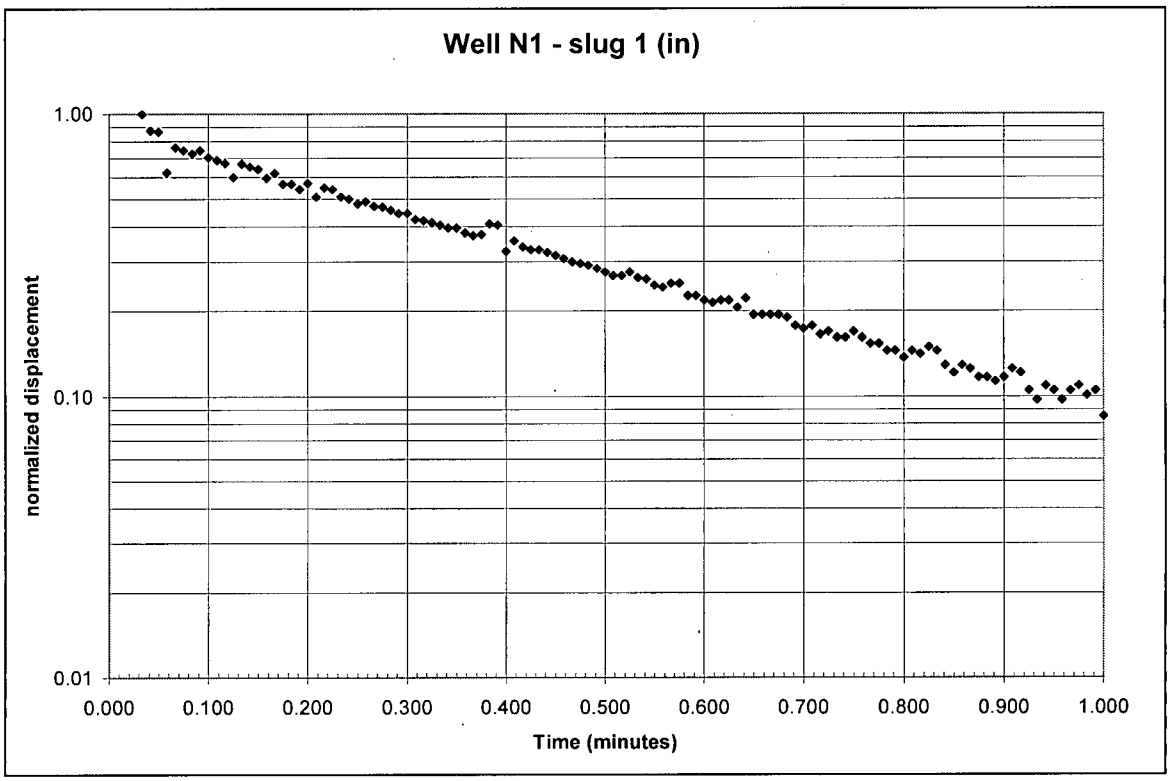

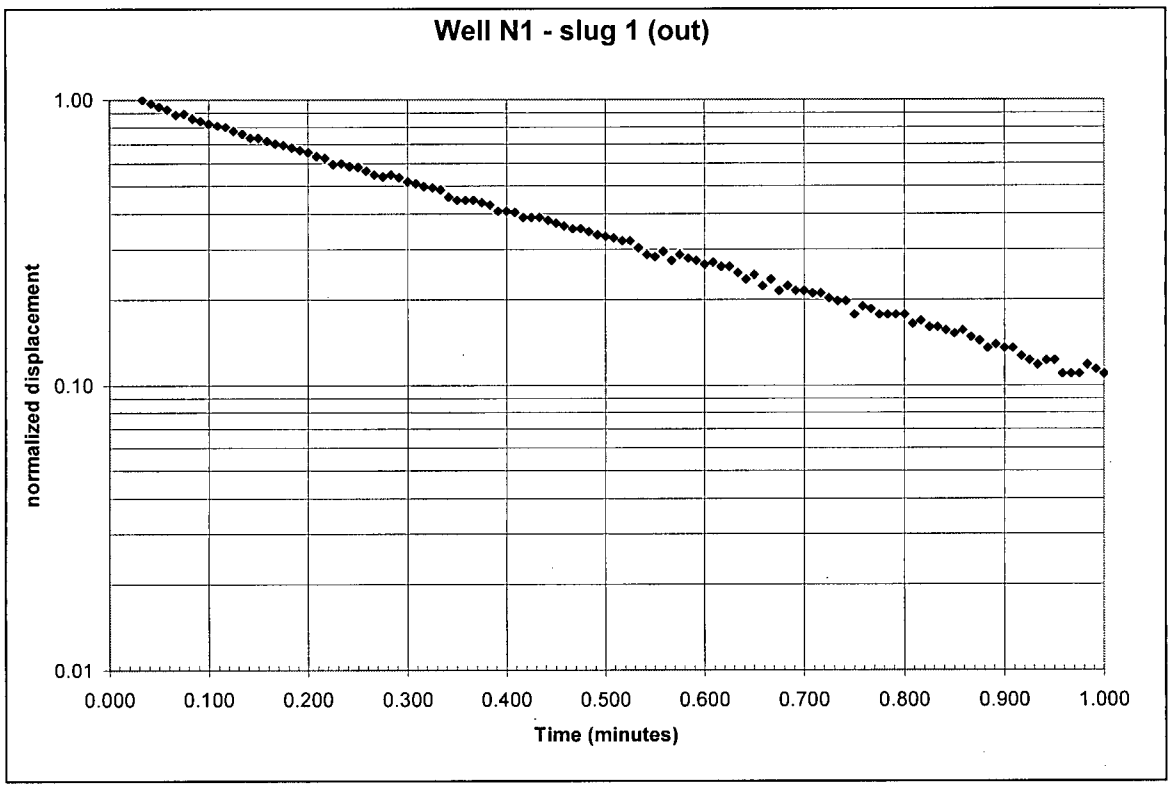

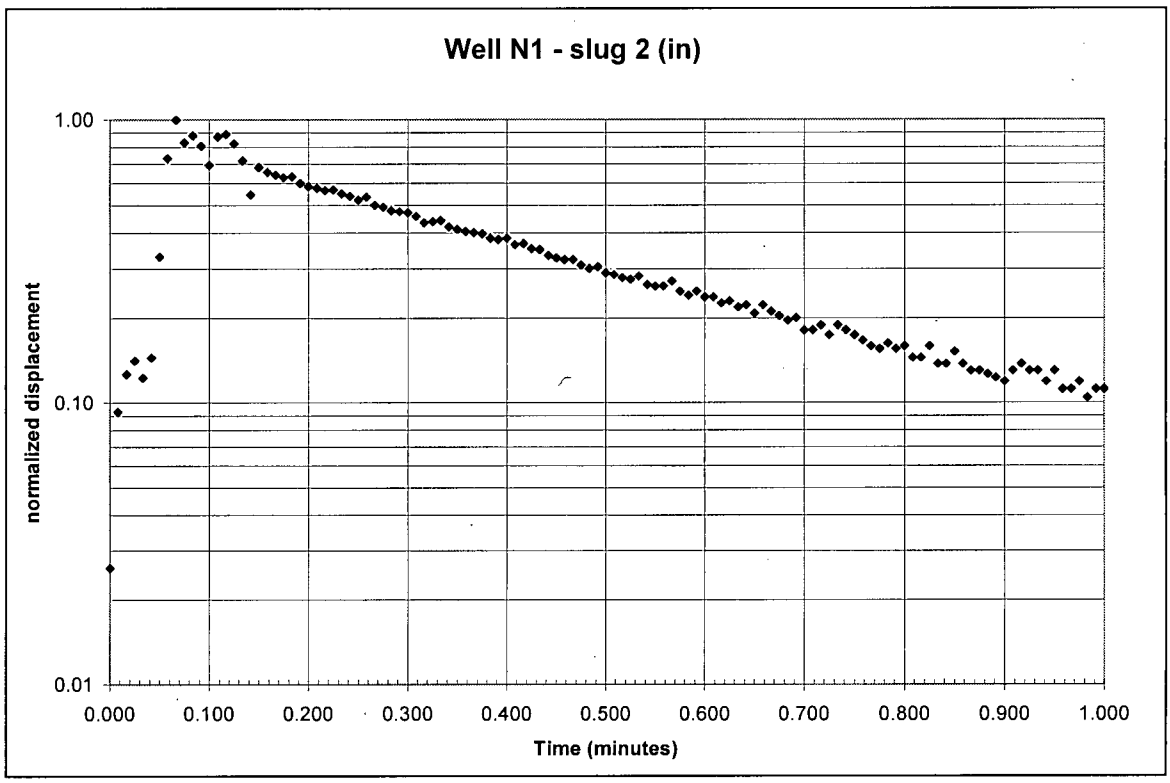
Well N1 - slug 2 (in)
normalized displacement
1.00
0.10
0.01
0.000
0.100
0.200
0.300
0.400
0.500
0.600
0.700
0.800
0.900
1.000
Time (minutes)

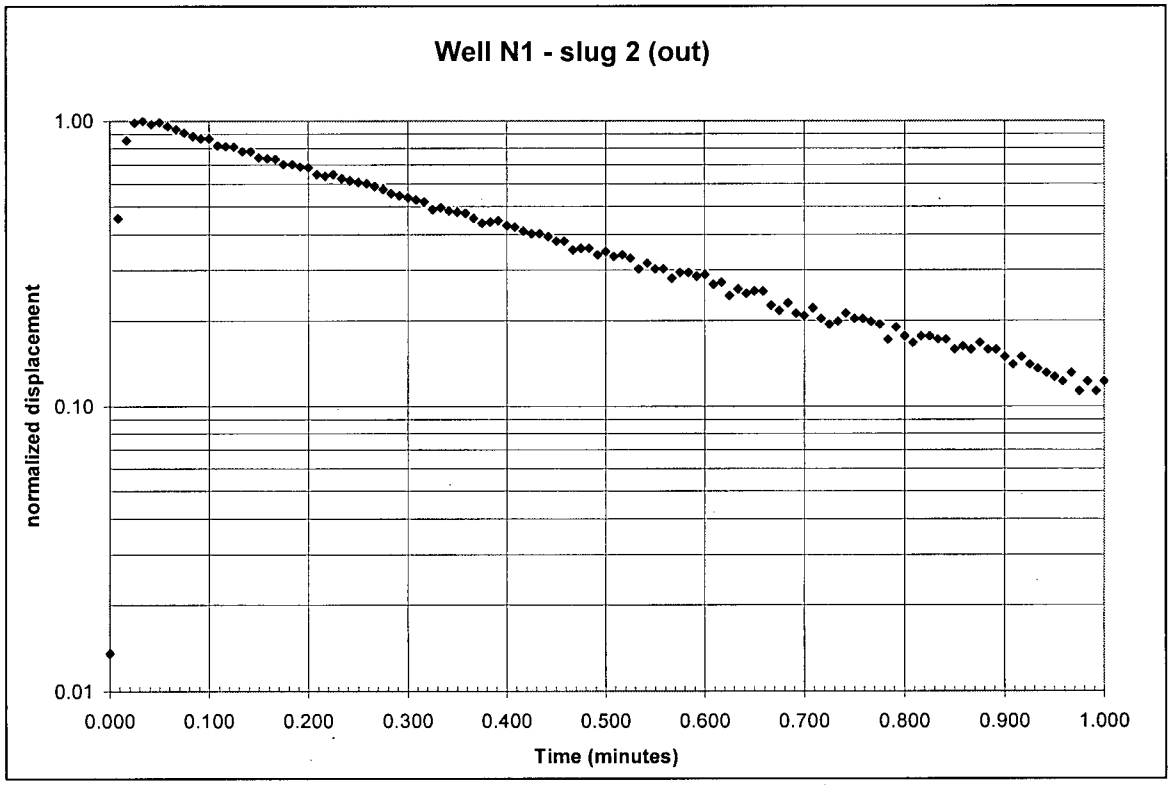
Well N1 - slug 2 (out)
normalized displacement
1.00
0.10
0.01
0.000
0.100
0.200
0.300
0.400
0.500
0.600
0.700
0.800
0.900
1.000
Time (minutes)

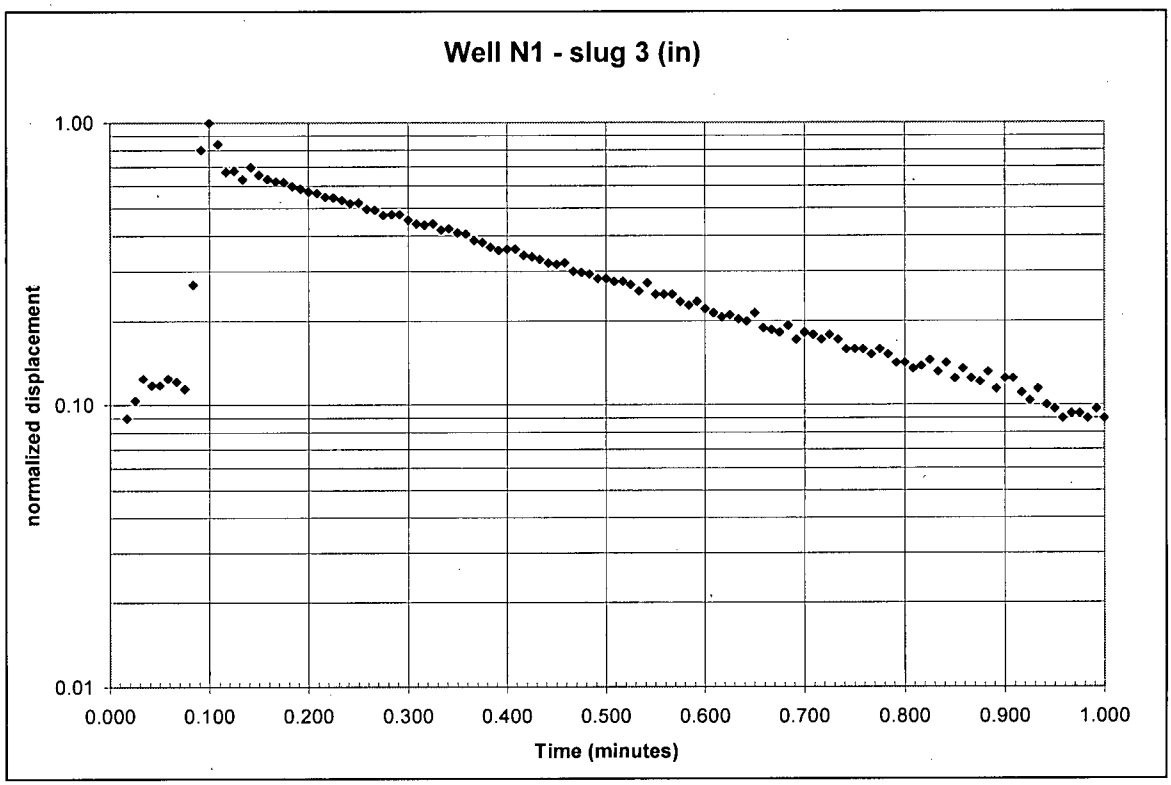
Well N1 - slug 3 (in)
normalized displacement
1.00
0.10
0.01
0.000
0.100
0.200
0.300
0.400
0.500
0.600
0.700
0.800
0.900
1.000
Time (minutes)

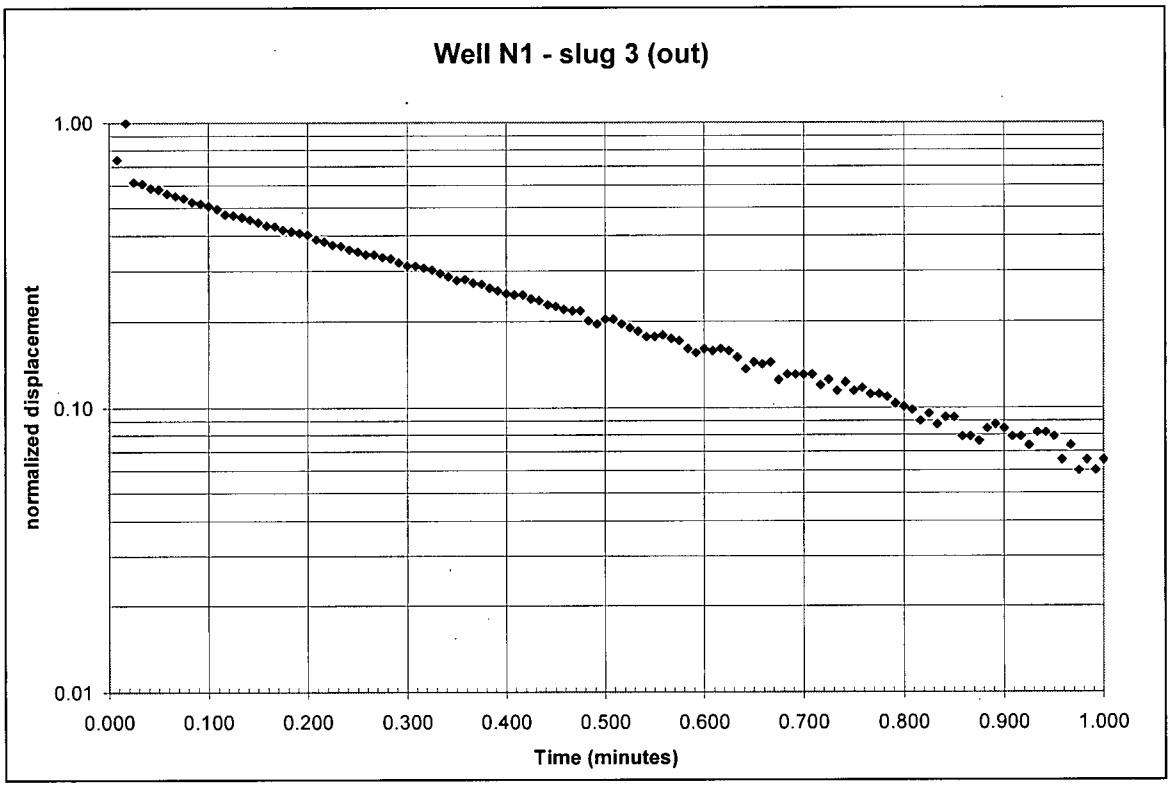
Well N1 - slug 3 (out)
normalized displacement
1.00
0.10
0.01
0.000
0.100
0.200
0.300
0.400
0.500
0.600
0.700
0.800
0.900
1.000
Time (minutes)

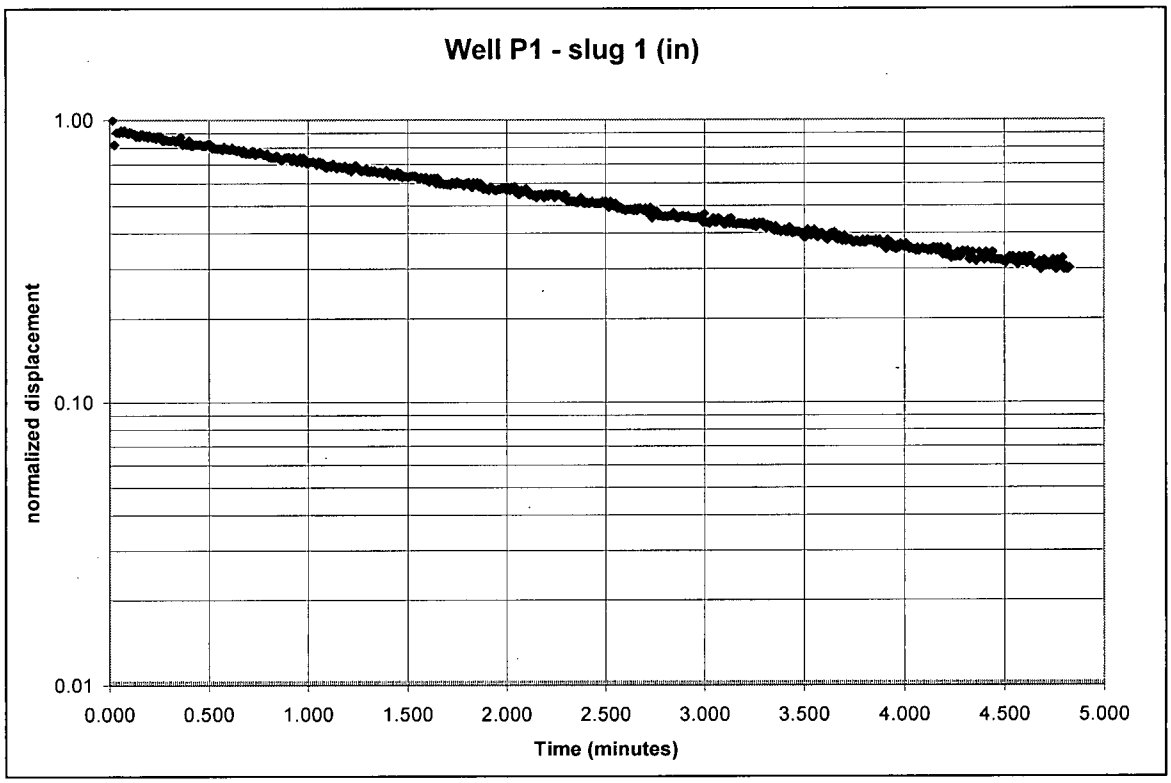
Well P1 - slug 1 (in)
normalized displacement
1.00
0.10
0.01
0.000
0.500
1.000
1.500
2.000
2.500
3.000
3.500
4.000
4.500
5.000
Time (minutes)

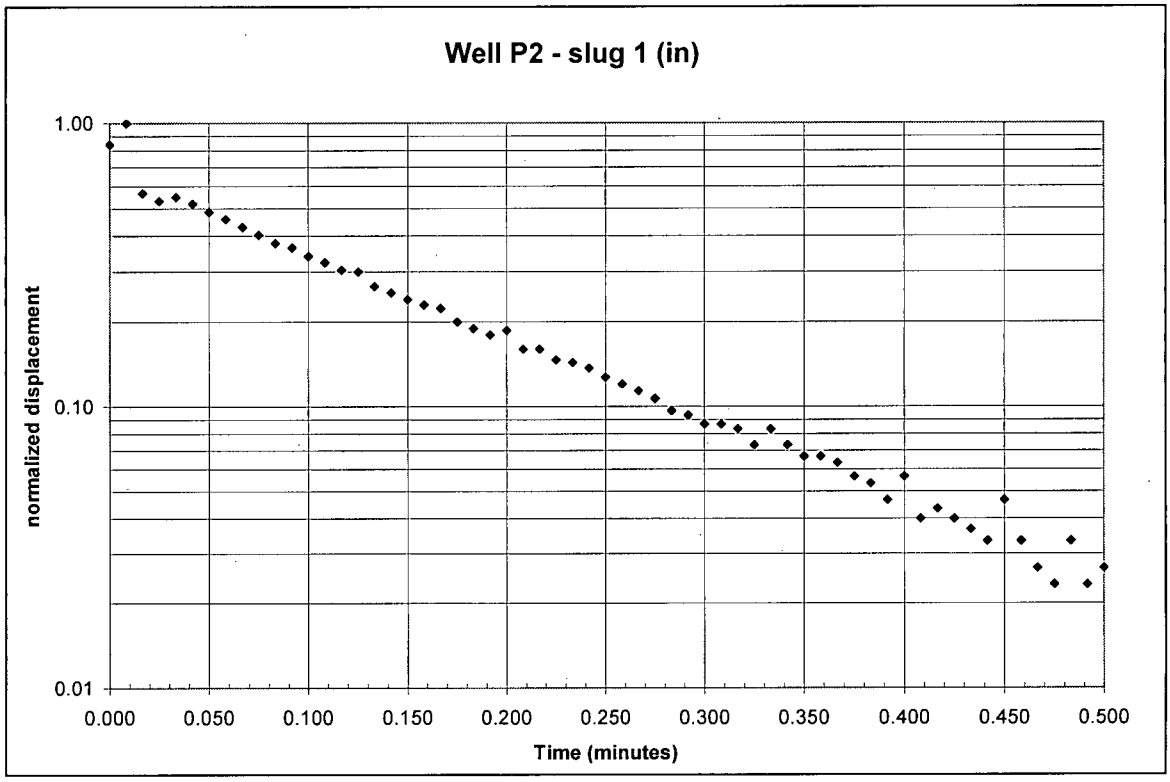
Well P2 - slug 1 (in)
normalized displacement
1.00
0.10
0.01
0.000
0.050
0.100
0.150
0.200
0.250
0.300
0.350
0.400
0.450
0.500
Time (minutes)

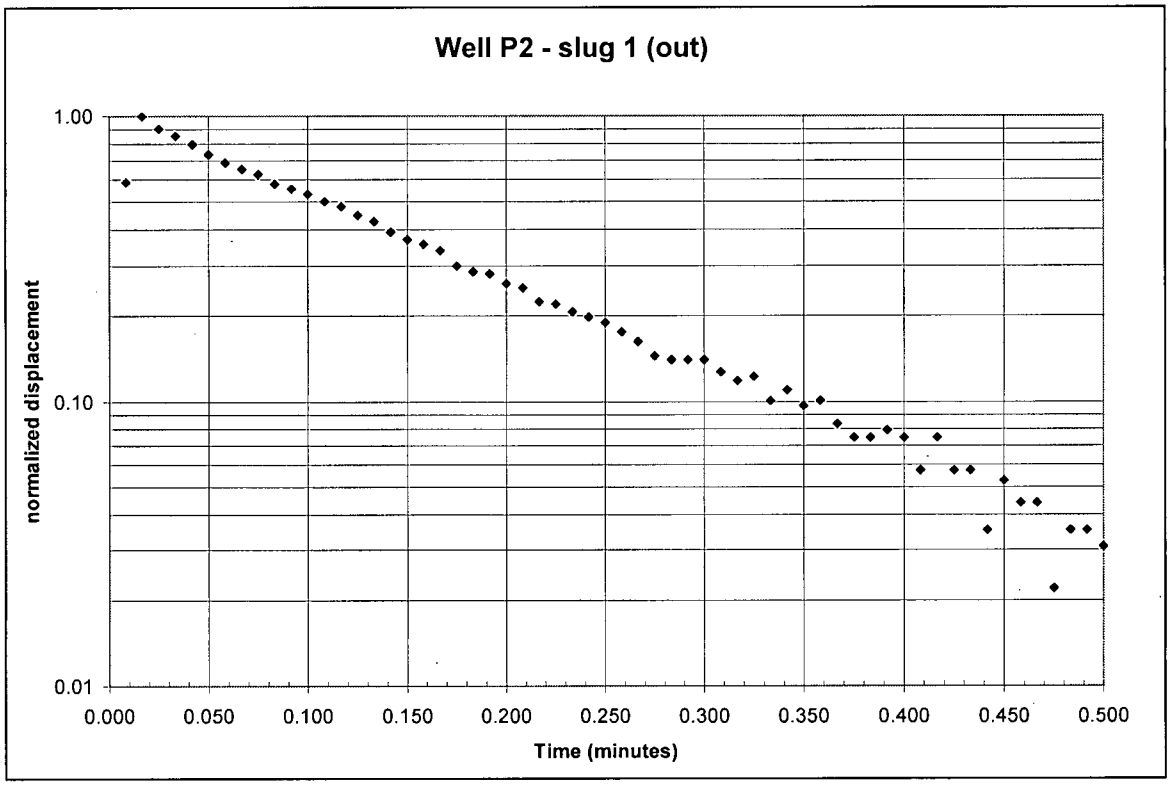
Well P2 - slug 1 (out)
normalized displacement
1.00
0.10
0.01
0.000
0.050
0.100
0.150
0.200
0.250
0.300
0.350
0.400
0.450
0.500
Time (minutes)

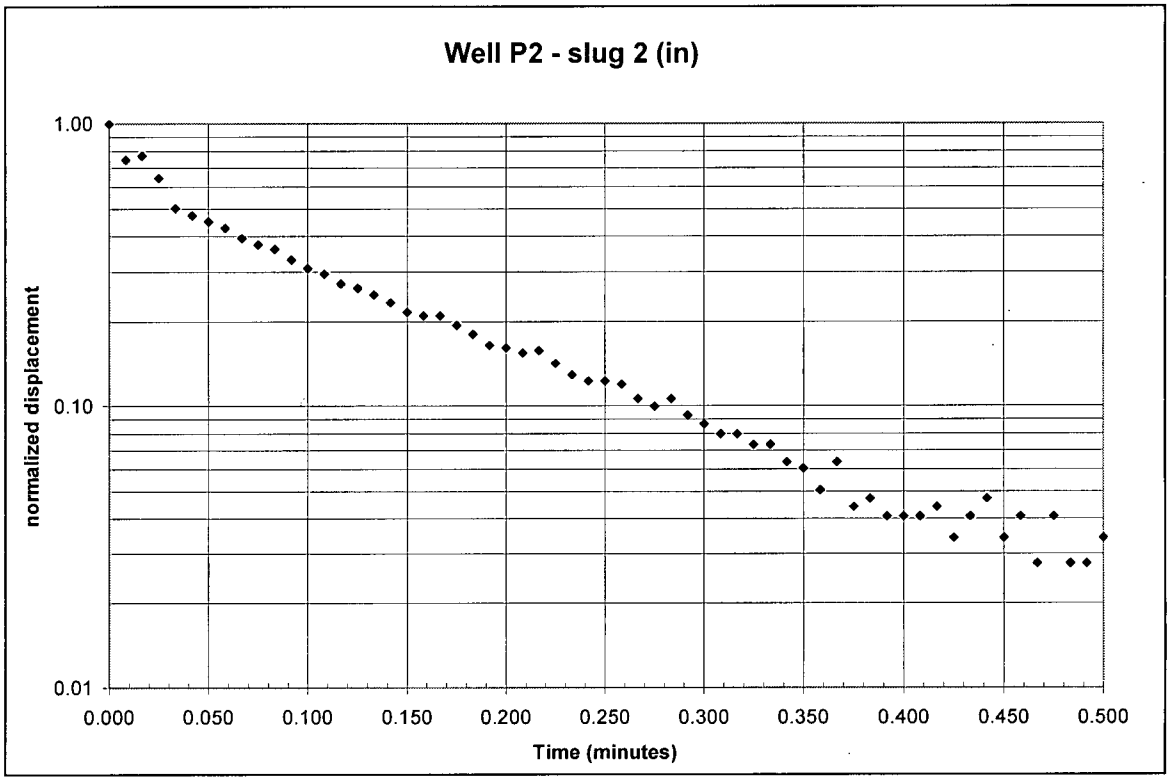
Well P2 - slug 2 (in)
normalized displacement
1.00
0.10
0.01
0.000
0.050
0.100
0.150
0.200
0.250
0.300
0.350
0.400
0.450
0.500
Time (minutes)

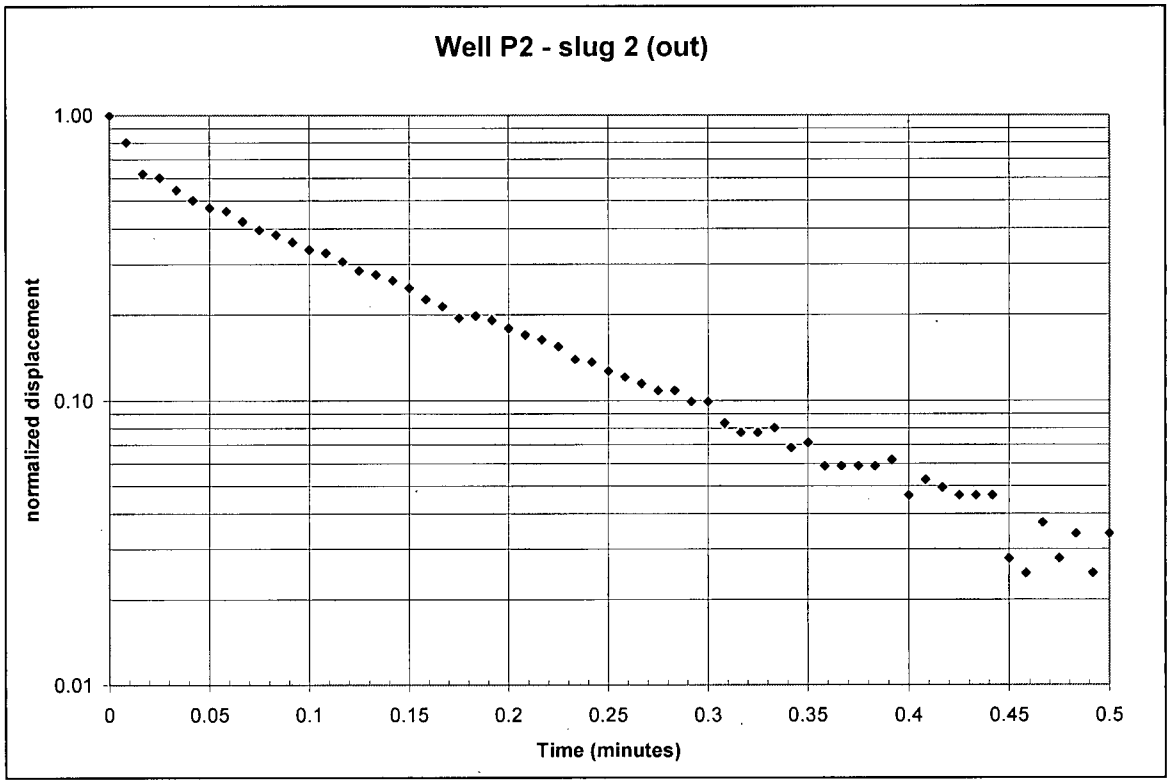
Well P2 - slug 2 (out)
normalized displacement
1.00
0.10
0.01
0
0.05
0.1
0.15
0.2
0.25
0.3
0.35
0.4
0.45
0.5
Time (minutes)

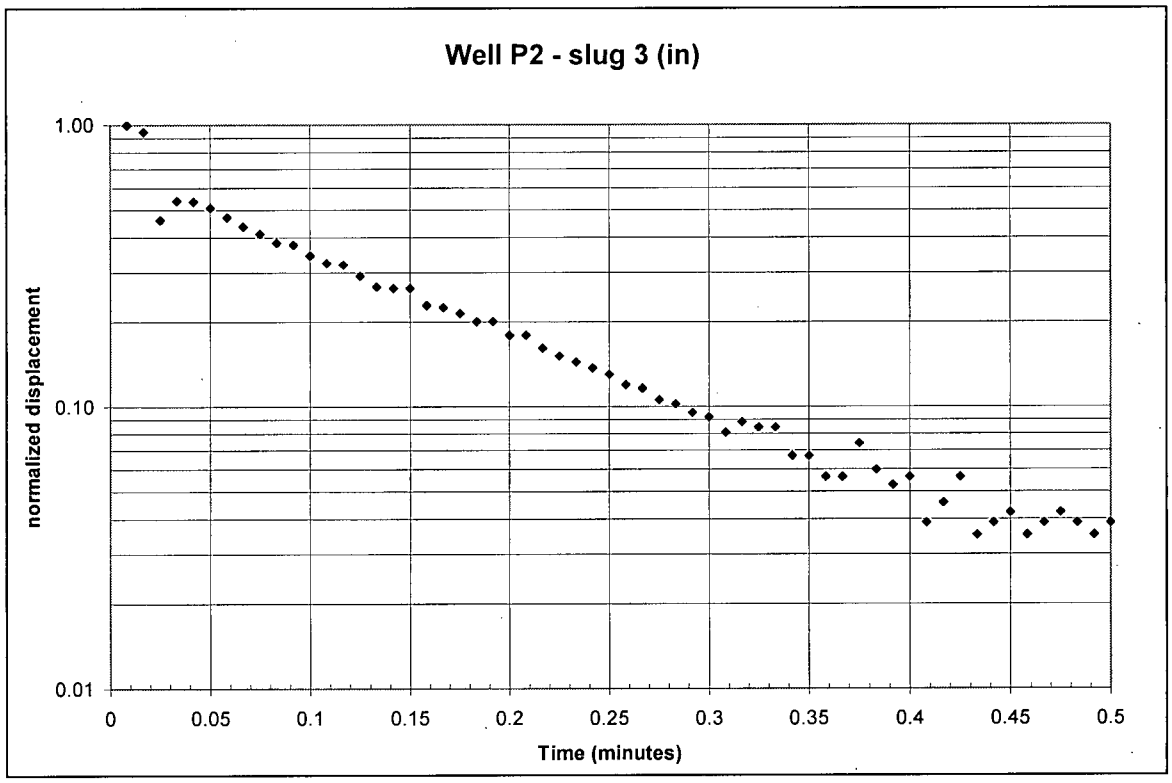
Well P2 - slug 3 (in)
normalized displacement
1.00
0.10
0.01
0
0.05
0.1
0.15
0.2
0.25
0.3
0.35
0.4
0.45
0.5
Time (minutes)

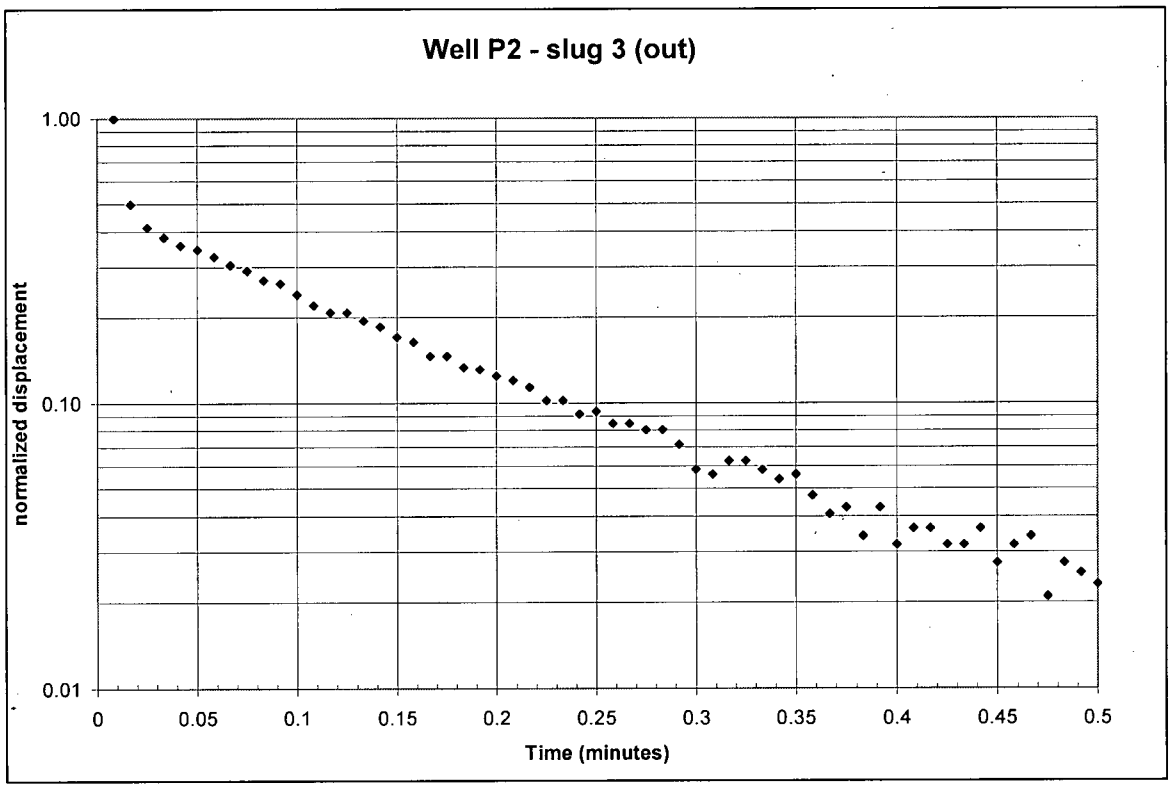
Well P2 - slug 3 (out)
normalized displacement
1.00
0.10
0.01
0
0.05
0.1
0.15
0.2
0.25
0.3
0.35
0.4
0.45
0.5
Time (minutes)

Appendix D – Salinity and Chloride Analyses

Salinity and Cl- analyses from the FSUML, August-September, 2002

	Analysts:	Jaye Cable, Andy Rhisosher	
	Methods:		
a	**salinity I**	refractometer	(performed by FSU, approximation used for dilutions)
b	**chloride**	ion chromatography	
c	**salinity II**	calculated from chloride	

Sample ID	Collection Date	Well or ID	a Salinity I (ppt)	b Cl- (mM)	c Salinity II (ppt)
1	8/17/2002	DPS site 1	31.0	500.81	32.1
2	8/17/2002	DPS site 1	31.2	476.39	30.5
3	8/25/2002	D-west	26.8	415.37	26.6
4	8/25/2002	D east	29.4	415.61	26.6
5	8/25/2002	C3	31.6	482.69	30.9
6	8/25/2002	A1	0.3	5.92	0.4
7	8/25/2002	A2	0.2	5.99	0.4
8	8/25/2002	C1	21.9	322.94	20.7
9	8/25/2002	B4	28.5	459.84	29.5
10	8/25/2002	B1	3.1	40.90	2.6
11	8/25/2002	B5	15.2	235.86	15.1
12	8/25/2002	BC1	22.9	383.20	24.5
13	8/25/2002	B6	19.6	291.27	18.7

Sample ID	Collection Date	Well or ID	a Salinity I (ppt)	b Cl- (mM)	c Salinity II (ppt)
15	8/26/2002	on 10'	0.2	5.98	0.4
16	8/26/2002	on 13'3 3/8"	0.2	5.32	0.3
17	8/27/2002	on 7.1m	0.3	5.51	0.4
18	8/28/2002	off 1-1	30.4	504.69	32.3
19	8/28/2002	off 1-2	27.6	402.74	25.8
20	8/28/2002	off 1-3	29.8	485.39	31.1
21	8/28/2002	off 1-4	29.5	435.67	27.9
22	8/29/2002	off 1-5	28.9	416.58	26.7
23	8/29/2002	off 1-6	20.3	301.16	19.3
24	8/29/2002	seawater	31.5	473.81	30.3
25	9/3/2002	BC2	19.1	283.30	18.1
26	9/3/2002	BC3	29.7	462.47	29.6
27	9/3/2002	BC4	31.4	455.45	29.2
28	9/3/2002	ML6	21.3	357.74	22.9
29	9/3/2002	ML5	22.1	312.93	20.0
30	9/3/2002	ML4	22.1	347.76	22.3
31	9/3/2002	ML3	25.1	387.56	24.8
32	9/3/2002	ML2	19.2	272.52	17.5
33	9/3/2002	ML1	15.0	221.67	14.2
34	9/4/2002	AB1	24.6	388.12	24.9
35	9/4/2002	AB2	19.4	276.88	17.7
36	9/4/2002	A3	0.2	6.10	0.4
37	9/4/2002	N2	0.1	5.75	0.4

Sample ID	Collection Date	Well or ID	a Salinity I (ppt)	b Cl- (mM)	c Salinity II (ppt)
38	9/4/2002	N1	0.1	5.24	0.3
39	9/4/2002	AB3	18.1	267.34	17.1
40	9/4/2002	P1	0.1	7.38	0.5
41	9/5/2002	DPS site 2	30.9	419.57	26.9
42	9/5/2002	DPS site 2	31.4	519.54	33.3
43	9/6/2002	ML1	15.2	206.76	13.2
44	9/6/2002	ML2	20.5	283.92	18.2
45	9/6/2002	ML3	25.6	387.08	24.8
46	9/6/2002	ML4	25.5	392.04	25.1
47	9/6/2002	ML5	25.6	428.61	27.5
48	9/6/2002	ML6	24.8	397.53	25.5
49	9/7/2002	ML1	15.8	241.65	15.5
50	9/7/2002	ML3	25.9	363.30	23.3
51	9/7/2002	ML4	25.3	408.51	26.2
52	9/7/2002	ML5	26.1	412.95	26.4
53	9/7/2002	ML6	25.3	397.49	25.5
54	9/7/2002	ML2	19.5	280.47	18.0
55*	9/1/2003	ML1	16.0	NA	NA
		ML2	NA	NA	NA
56*	9/1/2003	ML3	25.9	NA	NA
		ML4	NA	NA	NA
57*	9/1/2003	ML5	27.3	NA	NA
58*	9/1/2003	ML6	26.3	NA	NA

*sampled in 2003

References

Ataie-Ashtiani, B., R.E. Volker and D.A. Lockington, 1999. Tidal effects on sea water intrusion in unconfined aquifers. *J. Hydrology* 216, 17-31.

Burnett, W.C., M. Taniguchi and J.A. Oberdorfer, 2001. Measurement and significance of the direct discharge of groundwater into the coastal zone. *Journal of Sea Research* 46, 109-116.

Burnett, W.C., J. Chanton, J. Christoff, E. Kontar, S. Krupa, M. Lambert, W. Moore, D. O'Rourke, R. Paulsen, C. Smith, L. Smith, and M. Taniguchi, 2002. Assessing methodologies for measuring groundwater discharge to the ocean. *EOS* 83, 117-123.

Bokuniewicz, H., 1980. Groundwater Seepage into Great South Bay, New York. *Estuarine and Coastal Marine Science* 10, 437-444.

Cable, J.E., W.C. Burnett, J.P. Chanton and G.L. Weatherly, 1996. Estimating groundwater discharge into the northeastern Gulf of Mexico using radon-222. *Earth Planet. Sci. Let.* 144, 591-604.

Cable, J.E., W.C. Burnett and J.P. Chanton, 1997a. Magnitude and variations of groundwater seepage along a Florida marine shoreline. *Biogeochemistry* 38, 189-205.

Cable, J.E., W.C. Burnett, J.P. Chanton, D.R. Corbett and P.H. Cable, 1997b. Field Evaluation of Seepage Meters in the Coastal Marine Environment. *Estuarine, Coastal and Shelf Science* 45, 367-375.

Domenico, P.A. and F.W. Schwartz, 1998. Physical and Chemical Hydrogeology. John Wiley and Sons, New York.

Fang, W.W., M.G. Langseth, P.J. Schultheiss, 1993. Analysis and application of in situ pore pressure measurements in marine sediments. *Journal of Geophysical Research* 98 (B5), 7921-7938.

Findlatter, L.L., 2000. Analysis of Groundwater Flow in a Coastal Aquifer, Turkey Point, Florida. B.Sc. Honours Thesis, Dept. of Earth and Ocean Sciences, University of British Columbia.

Hvorslev, M.J., 1951. Time lag and soil permeability in ground water observations. U.S. Army Corps of Engr. Waterway Exp. Stat. Bull. 36, Vicksburg, MS.

Kelly, S. E. and L.C. Murdoch, 2002. Measuring the Hydraulic Conductivity of Shallow Submerged Sediments. *Ground Water* 41 (4), 431-439.

Kohout, F.A, 1966. Submarine springs: a neglected phenomenon of coastal hydrology. *Hydrology* 26, 391-413.

Kohout, F.A., 1960. Cyclic flow of salt water in the Biscayne Aquifer of southeastern Florida. *Jour. Geophys. Res.* 65, 2133-2141.

Langevin, C.D., 2003. Simulation of submarine ground water discharge to a marine estuary: Biscayne Bay, Florida. *Ground Water* 41 (6), 758-771.

Li, L., D. A. Barry, F. Stagnitti and J.-Y. Parlange, 1999. Submarine groundwater discharge and associated chemical input to a coastal sea. *Water Resources Research* 35 (11), 3253-3259.

Moore, W.S., 1996. Large groundwater inputs to coastal water revealed by ^{226}Ra enrichments. *Nature* 380, 612-614.

Moore, W.S. and T.M. Church, 1996. Reply to P.L. Younger, Submarine groundwater discharge. *Nature* 382, 121-122.

Moore, W.S., 2003. Sources and fluxes of submarine groundwater discharge delineated by radium isotopes. *Biogeochemistry* 66, 75-93.

Michael, H.A., J.S. Lubetsky and C.F. Harvey, 2003. Characterizing submarine groundwater discharge: A seepage meter study in Waquoit Bay, Massachusetts. *Geophysical Research Letters* 30 (6), 1297-1232.

Miller, J.A., 1986. Hydrogeologic Framework of the Floridan Aquifer System in Florida and Parts of Georgia, Alabama and South Carolina. USGS Prof. Paper 1403-B.

Paulsen, R.J., D. O'Rourke, C.F. Smith, and T. Wong, (in press). Influence of Tidal Loading and Saltwater Intrusion on Submarine Groundwater Discharge. *Ground Water* 42 (7).

Rasmussen, L.L., 1998. Groundwater Flow, Tidal Mixing and Haline Convection in Coastal Sediments. Unpublished M.Sc. Thesis, Florida State University, Dept. of Oceanography, 118 p.

Schmidt, W., 1984. Niogene stratigraphy and geologic history of the Apalachicola Embayment, Florida; Florida Geological Survey, Bulletin no. 58, 146 p.

SCOR (Working Group 112) website (April 2004): http://www.jhu.edu/~scor/wg112front.htm

Scott, T.M., 1992. A geologic overview of Florida. In G.L. Maddox, J.M. Lloyd and T.M. Scott (Eds.), Florida's Ground water quality monitoring program: background hydrogeochemistry. Florida Geological Survey Special Publication no. 32, pp. 4-20.

Smith, L. and W. Zawadzki, 2003. A hydrogeologic model of submarine groundwater discharge: Florida intercomparison experiment. *Biogeochemistry* 66, 95-110.

Taniguchi, M. and Y. Fukuo, 1993. Continuous Measurements of Ground-Water Seepage Using an Automatic Seepage Meter. *Ground Water* 31 (4), 675-679.

Taniguchi, M., W.C. Burnett, C.F. Smith, R.J. Paulsen, D. O'Rourke, S.L. Krupa and J.L. Christoff, 2003. Spatial and temporal distributions of submarine groundwater discharge rates obtained from various types of seepage meters at a site in the Northeastern Gulf of Mexico. *Biogeochemistry* 66, 35-53.

Therrien, R., E.A. Sudicky, and R.G. McLaren, 2003. FRAC3DVS: An Efficient Simulator for Three-dimensional, Saturated-Unsaturated Groundwater Flow and Density-dependent, Chain0Decay Solute Transport in Porous, Discreetly-Fracture Porous or Dual-porosity Formations. Unpublished User's Guide, Groundwater Simulations Group.

Uchiyama, Y., K. Nadaoka, P. Rolke, K. Adachi, and H. Yagi, 2000. Submarine groundwater discharge into the sea and associated nutrient transport in a sandy beach. *Water Resources Research* 36 (6), 1467-1479.

Yim, C.S., and M.F.N. Mohsen, 1992. Simulation of Tidal Effects on Contaminate Transport in Porous Media. *Ground Water* 30(1), 78-86.

Biographical Sketch

Joshua Lee Caulkins was born in Palo Alto, California, in 1976 and attended the University of California at Santa Cruz. He completed a Bachelor of Science in Earth Science from UCSC in 1998, receiving the Weber/Holt Award for Academic Excellence within the Earth Sciences upon his graduation. He spent one year doing graduate work in Geographic Information Science and Remote Sensing at Hunter College, City University of New York, and interned for a summer with the US Army Corps of Engineers, Coastal and Hydraulics Laboratory, Waterways Experiment Station in Vicksburg, Mississippi, using GIS and aerial photographs to model sediment transport in the Gulf of Mexico.

During the 2001-2002 academic year at UBC, Joshua was presented with the "Outstanding Teaching Assistant Award" within the Department of Earth and Ocean Sciences. Some of Joshua's non-academic time at UBC was dedicated to the Graduate Student Society as the Vice-President Academic and External, elected to that position by the graduate student body of 7,000 students for two years in a row.

Joshua is currently working on his Ph.D. in Geography at the University of British Columbia, focusing his studies on fluvial geomorphology.